Classifying Global Symmetries of 6D SCFTs

Peter R. Merkx^a

^a Department of Mathematics, U.C. Santa Barbara, Santa Barbara CA, 93106

E-mail: merkx@math.ucsb.edu

ABSTRACT: In this note we characterize the global symmetries for the conjecturally complete collection of all six dimensional superconformal field theories (6D SCFTs) and provide comprehensive checks of earlier 6D SCFT classification results via an alternative geometric approach yielding new restrictions eliminating certain theories. We reach our conclusions by directly constraining Weierstrass models for elliptically fibered Calabi-Yau (CY) threefolds and bypassing all anomaly cancellation machinery. This approach reduces the problem of classifying which 6D SCFT gauge and global symmetries are realizable in F-theory models before RG-flow to characterizing features of elliptic fibrations associated to these theories via analysis of polynomials determining their local models. We supply an algorithm with implementation producing from a given SCFT base an explicit listing of all compatible gauge enhancements with associated global symmetry maxima consistent with the geometric constraints we derive, thus making manifest the corresponding geometric ingredients for these symmetries including any possible Kodaira type realizations of each algebra summand. In mathematical terms, this amounts to determining all potentially viable non-compact CY threefold elliptic fibrations at finite distance in the moduli space with Weil-Petersson metric which meet certain requirements including the transverse pairwise intersection of singular locus components. We provide local analysis exhausting nearly all CY consistent transverse singular fiber collisions, global analysis concerning all viable gluings of these local models into larger configurations, and many novel constraints on such pairwise singular intersections and global fiber arrangements. We also investigate which transitions between 6D SCFTs can result from gauging of global symmetries and find that continuous degrees of freedom can be lost during such transitions.

Contents

1	Introduction				
2	The strategy				
	2.1	Weierstrass models and gauge algebras in F-theory	6		
	2.2	Global symmetries from F-theory geometry	7		
	2.3	Theories with one compact singular locus component	11		
	2.4	Algorithm summary	13		
	2.5	Flavor summand locality	15		
	2.6	Distinguished Calabi-Yau threefolds from global symmetry maxima	15		
3	Gauge algebras				
	3.1	Link enhancements	18		
	3.2	Comprehensive enhancement comparison	21		
	3.3	No trios of branching side-links, implementation scope	23		
4	Global symmetry classification summary via local contributions				
	4.1	23	24		
	4.2	(12)1, 81, 71, 61, 51	25		
	4.3	41	27		
	4.4	21	30		
	4.5	31	32		
	4.6	22	35		
5	Flavor symmetry structure via "atomic" decomposition				
	5.1	Interior links with node attachments	39		
	5.2	Side-links with a node attachment	42		
	5.3	Instanton-links with a node attachment	48		
6	Gauging global symmetries				
	6.1	Normal crossings constraints	52		
	6.2	Global to gauge symmetry promotion and 6D SCFT transitions	53		
7	Con	aclusions and outlook	54		
\mathbf{A}	Intersection contributions and forbidden pair intersections				
	A.1	Computing intersection contributions	59		
	A.2	Preliminaries	60		
	A.3	Type II curve intersections	60		
	A.4	Type III curve intersections	61		
	A.5	Type IV curve intersections	63		

	A.6 Type I_0^* curve intersections	64
	A.7 Type I_n^* curve intersections	76
	A.8 I_0,I_n^* curve intersections	78
	A.9 Compact I_0, I_n^* curve intersections	80
	A.10 Type I_n intersections with $A = B = 0$ curves	81
	A.11 I_0, I_0^* curve intersections	83
	Notes for using the computer algebra workbook	84
C	Tables of flavor symmetries for miscellaneous quivers	85
	C 1 001	
	C.1 $321m$:	85
	C.1 $321m$: C.2 31 :	85 86

1 Introduction

Six-dimensional superconformal field theories (6D SCFTs) are uniquely well-suited to shed light on the structure of the string landscape. Nearly two decades after the surprising appearance of the first arguments demonstrating their existence [1–3] resolved earlier proposals suggesting they might exist in principle but must be non-Lagrangian [4], renewed interest over the last several years [5–15] has enabled classification results for these theories [16, 17] relying heavily on tools from F-theory. Among the features of SCFTs these classifications leave implicit are their global symmetries.

Our primary focus here is to provide a characterization of these symmetries for possibly all 6D SCFTs, in particular those realizable in F-theory as classified in [16]. Global symmetries play a central role in recent lines of inquiry including investigations concerning renormalization group (RG) flows of 6D SCFTs [18, 19], but a systematic treatment has remained lacking. We outline the general structure of 6D SCFT global symmetries, provide summary rules to determine global symmetry maxima for each known 6D SCFT, and enable explicit listing of the maxima via implementation of an exhaustive search algorithm making manifest the potentially viable Kodaira type realizations of each gauge and global symmetry summand which may occur for a given SCFT base $B \cong \mathbb{C}^2/\Gamma$ determining a family of F-theory models where Γ is a discrete U(2) subgroup meeting stringent requirements detailed in [20]. In the process, we uncover new restrictions on the collection of permissible 6D SCFTs and carry out a check that our methods suffice to otherwise match the previously reported collection of [16] via manifestly geometric constraints without appeal to Coulomb branch anomaly cancellation machinery.

Global symmetries of theories with 1D Coulomb branch and those without non-abelian gauge algebra (for cases with B containing a single compact singular locus component) are treated in [21, 22], respectively. Here we extend that approach which involves determining

geometrically realizable SCFT global symmetries via the properties of non-compact Calabi-Yau threefold elliptic fibrations of the form $\pi: X \to B$ underlying F-theory 6D SCFT models. Flowing to a conformal fixed point after taking a limit in which all compact components of the singular locus are contracted yields a CFT whose geometrically realizable global symmetries are constrained by the permissible non-abelian algebras which can be carried on non-compact components of the singular locus of X via a correspondence of these algebras to global symmetries of the SCFT dating to early F-theory descriptions of the small $E_8 \times E_8$ instanton [23–25] also used recently in [15–17].

The geometrically realizable global symmetry maxima of F-theory 6D SCFT models for the cases treated in [21, 22] which have only a single compact singular locus component are subalgebras of the Coulomb branch global symmetry algebras permitted via field-theoretic gauge and mixed anomaly cancellation requirements underlying the gauge enhancement prescriptions of [16]. We find this is true more generally and appears to hold for all 6D SCFTs admitting an F-theory description.

While it has been argued that all continuous SCFT global symmetries must be gauged upon coupling to gravity [26], precise rules for determining these degrees of freedom for an arbitrary 6D SCFT and provision of gauging consistency conditions before and after such coupling have not been systematically treated in cases with Coulomb branch of dimension larger than one. While we will not discuss this global symmetry gauging mandated by coupling to gravity in any detail, we will briefly discuss gauging of global symmetries taking one SCFT to another. However, our primary focus in this note is simply to constrain the manifest geometrically realizable flavor symmetries of each F-theory 6D SCFT model. Note that the construction we study identifies these degrees of freedom in the UV though such models only give rise to a conformal theory after RG flow. This means that the actual global symmetries of an SCFT associated to each model may differ from those degrees of freedom we shall identify. As shown in [21, 22], these geometrically realizable global symmetries are (in some cases strictly) more constrained than those permitted on the Coulomb branch of the theory. Typically, the latter constrain the actual global symmetries of a CFT since these also act on the Coulomb branch of the theory, though in some cases additional field theoretic constraints can provide reductions beyond Coulomb branch gauge and mixed anomaly cancellation prescriptions, for example when we have $\mathfrak{su}(2)$ gauge algebra [27].

The approach we take reduces our central task to a mathematically well-defined problem which consists of providing a series of constraints on non-compact elliptically fibered Calabi-Yau threefolds we study by means of a singular elliptic fibration π determined by Weierstrass equation of the form

$$y^2 = x^3 + fx + q (1.1)$$

with auxiliary data detailed in Section 2.1 and f, g locally defined polynomials on a complex surface. More precisely, f, g are sections of $\mathcal{O}(-4K_B)$, $\mathcal{O}(-6K_B)$, respectively, with K_B the canonical bundle over the base B, as above. The constraints we obtain involve a careful analysis of local models for these elliptic fibrations. We treat sufficiently many cases that it is convenient to constrain the global Weierstrass models through implementation of

exhaustive computer search routines.

Note that we do not claim the existence of globally consistent F-theory models achieving the flavor symmetry maxima we report. While proofs to that end are often possible and even trivial in sufficiently many cases that one might expect only limited tightenings of these maxima may be obtained, doing so in full generality is delicate and will not be treated here.

Since restrictions on the geometry of Weierstrass models are seemingly necessary to reach the precise conclusions of [16], it is natural to ask whether a parsimonious approach giving a "purely geometric" characterization of all known constraints on 6D SCFT F-theory models is possible. In this note, we provide strong evidence towards answering this question in the affirmative.

Our methods extend those of [21] to the general case, thus resulting in a geometric classification of gauge and flavor symmetries realizable in F-theory models for 6D SCFTs classified in [16]. Since we proceed without appeal to field-theoretic tools based on Coulomb branch anomaly cancellation requirements involving hypermultiplet count pairing restrictions, this enables us to provide consistency checks on results derived via the latter approach where known. We rely instead on algebro-geometric analysis of elliptically fibered Calabi-Yau threefolds with our efforts focusing on local polynomial expansions of sections f, g occurring in (1.1).

To enable explicit listing of global symmetry maxima for each gauge enhancement of any fixed 6D SCFT base, we derive a series of constraints enabling our calculations to proceed via computer algebra system. These fall into three main categories. First, we determine which pairs of curves in B with generic fibers having specified Kodaira types are permitted to intersect without introducing singularities so severe that Calabi-Yau resolution of the fibration would be prevented. Second, we analyze local models for transverse singular curve collisions to determine the minimal "intersection contributions" (giving counts towards certain degrees of freedom along each curve) from every relevant permitted intersection. These both entail generalizing the analysis from [21, 22]. The final category concerns elimination of certain arrangements multiple singular locus components.

Together these tools enable us to constrain 6D SCFT gauge and global symmetry algebras independently of and more strongly than Coulomb branch gauge and mixed anomaly cancellation techniques detailed in [16, 21, 22]. Our approach is parsimonious in that constraints are obtained via manifestly geometric restrictions on elliptic fibrations in correspondence with 6D SCFTs rather than with a hybrid approach underlying [16] invoking both representation theoretic anomaly cancellation tools supplemented by such geometric restrictions.

Discrepancies we find for permitted gauge enhancements and bases with those of [16] are detailed in Section 3. Gauge enhancement prescriptions for certain constituents of SCFT bases, namely "links," obtained using the accompanying computer algebra routines are compared with outputs of routines from [16] after minor edits aimed to match prescriptions therein. Extending comparisons for links to those for general 6D SCFT bases yields novel restrictions in certain cases.

While the local analysis including intersection contribution data provided by [21, 22] plays a key role, our route is complicated by the following issues meriting significant ex-

tension of those treatments which address only theories with a model having singular locus with single compact curve Σ associated to a simple gauge algebra \mathfrak{g} . Determining which global symmetry algebras are realizable in such models can be treated via consideration of non-compact curve collections $\{\Sigma_i'\}$ with each Σ_i' transverse to Σ and carrying non-abelian simple Lie algebra \mathfrak{g}'_i . Relatively maximal algebras arising as $\bigoplus_i \mathfrak{g}'_i$ from a permissible configuration are identified as global symmetry maxima via a limit with Σ contracted. For such cases, analysis concerning non-compact curves collections with $\bigoplus_i \mathfrak{g}'_i$ potentially maximal suffices while configurations resulting in "small" $\oplus_i \mathfrak{g}'_i$ are irrelevant. To treat more general theories with multiple compact components $\{\Sigma_i\}$ in the singular locus giving rise to gauge algebra $\bigoplus_i \mathfrak{g}_i$, we consider collections of non-compact curves having transverse intersection with some Σ_i . While constraints on maximal algebra yielding configurations transverse to Σ_i derived in [21, 22] are helpful, the curves meeting Σ_i now include any compact neighbors $\Sigma_{i\neq i}$ which may carry "small" algebras corresponding to gauge summands comprising part of the data specifying a theory and hence may not be among the previously studied maximal configurations. This presents a significantly more involved combinatorial problem to find the maximal configurations meeting each fixed Σ_i given not only the Kodaira type along Σ_i but also those of any Σ_j meeting Σ_i with global considerations introducing various subtleties. Furthermore, intersection with a compact transverse curve often requires distinct local analysis from a non-compact counterpart and yields different intersection data.

The minimal orders of vanishing determining Kodaira types become insufficient to realize a permitted type assignment $\{T_i\}$ on each $\{\Sigma_i\}$ in the general case, e.g. (A.2). This leads us to develop local models for many transverse intersections of curve pairs with designated orders of vanishing nearly exhausting all permissible transverse singularity collisions for CY threefold fibrations. The algorithm we supply incorporates this analysis to yield a significant step towards explicit classification of such fibrations including a treatment of codimension-two singularities.

In addition to enabling explicit listing of gauge enhancements and their flavor symmetry maxima, we discuss the general structure of these symmetries and provide two complementary prescriptions involving rules dictating the flavor symmetry maxima that may occur for each 6D SCFT in terms of Kodaira types on curves determining a fixed gauge enhancement. The first consists of rules summarizing these maxima in terms of length two curve chains and constraints imposed additional neighboring curves. This summarizes results obtained with computer routines and organizes them into constraint equations and structured listings. Second, we detail these maxima for longer bases in terms of contributions arising from each of the building blocks in the "atomic" decomposition of 6D SCFT bases into "link" and "node" constituents from [16].

The rest of this note is organized as follows. In Section 2, we review several features of Weierstrass models in F-theory and previous 6D SCFTs global symmetry classification results for the small class of theories for which these have been treated systematically. We then detail an algorithm determining these symmetries for general 6D SCFTs based upon restrictions we derive in Appendix A and previous results of [21, 22]. We turn in Section 3 to a discussion of novel restrictions on 6D SCFT bases and their gauge enhancements providing slight refinements of the classification from [16] determined using our algorithm. We

then In Section 4 we summarize the geometrically realizable global symmetries of 6D SCFTs in terms of the permitted length two subquiver Kodaira type assignments for each valid base. In Section 5 we discuss the general structure of 6D SCFT global symmetries via summands arising from the "atomic" base decomposition constituents. The transitions between 6D SCFTs that can be obtained by occupying the degrees of freedom permitting global symmetry summands to instead allow further gauge summands (i.e., by "gauging global symmetries") are discussed in Section 6. Concluding remarks and an outline of applications and open problems appear in Section 7. Instructions for using the accompanying computer algebra workbook appear in Appendix B. Finally, tables summarizing global symmetries for several key cases helping to complete our analysis appear in Appendix C.

Acknowledgments

We extend our sincere thanks to Marco Bertolini for providing essential foundational ideas enabling this work and for significant ongoing input throughout its completion. We also thank David R. Morrison for proposing this project and providing helpful suggestions, Daryl Cooper, Denis Labutin, and Mihai Putinar for support and advice, and Tom Rudelius for useful discussions.

2 The strategy

Our approach generalizes that of [21] to cases with discriminant locus consisting of more than one compact curve. The first ingredient involves imposing the restrictions derived therein for single curve cases with associated non-abelian gauge algebra along with the remaining single curve cases without non-abelian gauge algebra treated in [22]. We next check a given global symmetry summand inducing configuration for consistency with the number of vanishings of f, g, and Δ required along each curve in a quiver. There are a handful of additional restrictions we shall impose including the elimination of a few configurations which are barred via the analysis presented in Appendix E.3 of [16] and a similar discussion we derive here in Appendix A.

Before moving to treat the local analysis and other tools we shall require, we begin in this section with a review of our general approach for determining global symmetry maxima within F-theory on purely geometric grounds (i.e., sans anomaly cancellation tools) and detail an algorithm and our accompanying implementation which allows us to reach conclusions through exhaustive search of configurations meeting known restrictions outlined here and those derived in Appendix A.

We shall make use of the maximal configurations for single curve theories determined in [21, 22] updated with tightenings in certain cases with non-abelian gauge algebra illustrated in Table 3 and in one case with trivial gauge algebra discussed in Section 2.3.2. In the remainder of Appendix A, we turn to a detailed local analysis on the number of vanishings required along each compact curve for all possible pairwise intersections of discriminant locus components which we shall encounter. In the process we also uncover various forbidden curve intersections. These restrictions are central to the approach we describe in this

section, but we postpone their discussion until we have outlined the task at hand since their details are somewhat involved.

2.1 Weierstrass models and gauge algebras in F-theory

The essential geometric ingredient for an F-theory formulation of an SCFT is a Weierstrass model determining a singular elliptic fibration given by $\pi: X \to B$ with fibers determined by a Weierstrass equation of the form (1.1) with $B \cong \mathbb{C}^2/\Gamma$, as above, in the case of 6D F-theory. The discriminant of this equation,

is a section of $\mathcal{O}(-12K_B)$ with its "discriminant locus,"

$$\{\Delta = 0\} , \qquad (2.2)$$

determining where the fibration is singular. The types of singularities that are permitted without being so severe as to prevent a Calabi-Yau resolution \widetilde{X} are given by the Kodaira classification of [28–30] with summary appearing in Table 1. "Non-minimal" fiber types indicated in the final row have resolution of singularities containing a curve which can be blown down. Blow-down of such a curve down leads to a new Weierstrass model with orders of vanishing of (f, g, Δ) along Σ reduced by (4, 6, 12). We hence discard such cases without loss of generality. Similarly, a two-dimensional Weierstrass model is minimal at P defined by $\{\sigma=0\}$ provided $\operatorname{ord}_{\sigma=0}(f)<4$, or $\operatorname{ord}_{\sigma=0}(g)<6$. To reiterate, we confine our study in this work to those models lacking non-minimal points. (From the Calabi-Yau condition, we could have blown up such points. Without loss of generality, we take such a model as our starting point.)

ord(f)	$\operatorname{ord}(g)$	$\operatorname{ord}(\Delta)$	type	singularity	non-abelian algebra
≥ 0	≥ 0	0	I_0	none	none
0	0	1	I_1	none	none
0	0	$n \ge 2$	I_n	A_{n-1}	$\mathfrak{su}(n) \text{ or } \mathfrak{sp}([n/2])$
≥ 1	1	2	II	none	none
1	≥ 2	3	III	A_1	$\mathfrak{su}(2)$
≥ 2	2	4	IV	A_2	$\mathfrak{su}(3)$ or $\mathfrak{su}(2)$
≥ 2	≥ 3	6	I_0^*	D_4	$\mathfrak{so}(8) \text{ or } \mathfrak{so}(7) \text{ or } \mathfrak{g}_2$
2	3	$n \ge 7$	I_{n-6}^*	D_{n-2}	$\mathfrak{so}(2n-4) \text{ or } \mathfrak{so}(2n-5)$
≥ 3	4	8	IV^*	\mathfrak{e}_6	$\mathfrak{e}_6 \text{ or } \mathfrak{f}_4$
3	≥ 5	9	III^*	\mathfrak{e}_7	\mathfrak{e}_7
≥ 4	5	10	II^*	\mathfrak{e}_8	\mathfrak{e}_8
≥ 4	≥ 6	≥ 12	non-minimal	-	-

Table 1. Singularity types with associated non-abelian algebras.

The precise gauge algebra which occurs in the cases of ambiguity is determined by inspection of the auxiliary polynomials appearing in Table 2 where Σ is a curve along the

singular locus $\{z=0\}$; larger gauge algebras result with more complete factorizations. A significant portion of our analysis concerns which splittings can take place in various intersection arrangements. Several results towards this end from [16, 21, 22] are crucial to our work.

type	equation of monodromy cover
$I_n^{s/ns}, n \ge 3$	$\psi^2 + (9g/2f) _{z=0}$
$IV^{s/ns}$	$\psi^2 - (g/z^2) _{z=0}$
$I_0^{*s/ss/ns}$	$ \psi^3 + (f/z^2) _{z=0} \cdot \psi + (g/z^3) _{z=0}$
$I_{2n-5}^{*s/ns}, n \ge 3$	$\psi^2 + \frac{1}{4}(\Delta/z^{2n+1})(2zf/9g)^3 _{z=0}$
$I_{2n-4}^{*s/ns}, n \ge 3$	$\psi^2 + (\Delta/z^{2n+2})(2zf/9g)^2 _{z=0}$
$IV^{*s/ns}$	$\psi^2 - (g/z^4) _{z=0}$

Table 2. Monodromy cover polynomials determining non-abelian gauge algebras.

The association of non-abelian algebras to Kodaira types indicated in Table 1 including non-simply laced cases dates to [31]. The essential idea is that the resolution of singularities \widetilde{X} for a given Kodaira type gives rise to a graph of curves we may naturally associate to a Dynkin diagram determining a Lie algebra \mathfrak{g} . This same \mathfrak{g} arises as the gauge algebra of a corresponding physical theory associated to an F-theory model compactified on a Calabi-Yau threefold \widetilde{X} with metric furnished via [32]. Cases in which non-simply laced algebras may occur further involve a cover of \widetilde{X} with properties determined by the auxiliary "monodromy cover" polynomials appearing in Table 2. These together with the local polynomial expansions for certain Kodaira types as detailed in Appendices A,B of [21] are the main objects involved in our discussion.

2.2 Global symmetries from F-theory geometry

The field-theoretic and geometrically realizable global symmetries of 6D SCFTs with an F-theory model having discriminant locus with a single compact component were studied in [21, 22] to treat 1D Coulomb branch cases and certain trivially gauged theories. This leaves us to focus on theories with models having more than one compact component after providing a few tightenings of earlier results detailed in Sections 2.3.

Two ingredients are essential in our derivations. We make heavy use of results from [21] giving expansions of f, g, and Δ that determine general forms for expansions giving local models of Kodaira type I_n^* and I_n curves largely dating from [9]. We also rely on Tables 41,42 taken (up to minor corrections) from [21] giving forbidden curve intersections and intersection contributions obtained from certain local models. Though we require significant generalizations derived in Appendix A, these local intersection models and contribution data play a key role. We also will use the maximal configurations derived in those works and several geometric restrictions on curve pair intersections derived in [16].

2.2.0.1 Setup and notation

Let us begin by reviewing aspects of our setup, notation and terminology largely based on [16, 21].

Global symmetries arise in F-theory via non-compact components of the discriminant locus. Coupling of the associated gauge group on each of these curves becomes zero after a rescaling, hence leading to a global symmetry [21]. Our main focus here involves extending the discussion of [21, 22] concerning symmetries constructed in this way from cases with discriminant locus containing a single compact curve (determining an SCFT with gauge algebra consisting of at most a single simple Lie algebra summand) to the general case of arbitrary 6D SCFTs as classified in [16], these typically having bases with multiple compact components of the discriminant locus.

Let us pause to discuss two limitations of our approach also noted in [21, 22]. First, the Tate's algorithm prescription of [9, 33] may not capture the most general possible forms for Kodaira types $I_{7 \le n \le 9}$. Since we shall rely on the Tate forms in these cases, it is possible that a limited class of configurations may be missed by our approach. Second, where local analysis permits non-compact curves to allow any monodromy designation, we report global symmetry maxima with those possibilities giving the largest algebras consistent with our analysis though additional restrictions could in principle be obtained in some cases. However, the maxima report always appear to be subalgebras of the Coulomb branch global symmetries which we generally expect to find as subalgebras of the actual global symmetry algebra for a given theory. This suggests that only limited further reductions from these maxima may be obtained. Note that multiple global symmetry maxima persist in many cases even when monodromy designations are unambiguous both in cases for fixed geometric realization of a given gauge algebra (e.g. $\mathfrak{su}(2)$ on a -1 curve realized by Kodaira type IV^{ns} with maxima appearing in Table 3) and in cases where we compare all geometries for fixed base realizing a given gauge assignment (e.g. $\mathfrak{su}(3)$ on a -1 curve with $\mathfrak{su}(10)$ and $\mathfrak{su}(3)^{\oplus 3}$ maxima read from Table 6.1 of [21]).

We now review a few details of the 6D SCFT classification of [16] given by detailing all possible connected trees of compact curves $\Sigma_i \subset \{\Delta = 0\} \subset \mathbb{C}^2$ having $\Sigma_i \cdot \Sigma_i = m_i$ over which the fibration is singular. This "atomic" decomposition into permitted subgraphs given by the values m_i , rules for their gluing and the gauge summands from each Σ_i dependent on nearby attachments leaves certain ambiguities in the Kodaira types which can realize a given gauge summand, e.g. types I_0 , I_1 , and II each yield trivial summand. One of our objectives here is to resolve these ambiguities and provide a geometric check of the classification.

Contraction of all Σ_i yields the orbifold base $B \cong \mathbb{C}^2/\Gamma$ with Γ a discrete U(2) subgroup determined by the values m_i or alternatively the values $\widetilde{m_i}$ obtained after iterated blowdown of all -1 curves to yield an "endpoint," these having been classified in [17] and restructured in [20]. Distinct curves Σ_j must have transverse intersections in at most a single point. The curves $\{\Sigma_i\}$ must be contractible at finite distance in the Calabi-Yau moduli space with Weil-Petersson metric dating in this context to [34, 35] which leads to a pair of conclusions via [36, 37]: i) $\Sigma_j \cong \mathbb{P}^1$ with negative self-intersection (that is, $\Sigma_i \cdot \Sigma_i < 0$), and ii) the graph consisting of the Σ_j must have positive definite adjacency

matrix given by

$$A_{ij} = -\Sigma_i \cdot \Sigma_j \ . \tag{2.3}$$

To simplify notation, we will often omit the minus signs giving curve self-intersections with the understanding that all self-intersections are negative (e.g., in place of the chain -3, -2, writing instead 3, 2). Any two digit self-intersections will be given with parentheses where ambiguous. For example, when writing 1, 12, 1 without commas, we shall write 1(12)1.

A key ingredient for our work is the general result of [16]: with few exceptions, every 6D SCFT base in F-theory is of the form

$$S_0 g_1 L_1 g_2 L_2 g_3 L_3 \cdots g_k L_k g_{k+1} \cdots g_{m-1}^{I \oplus s} L_{m-1} g_m S_m, \tag{2.4}$$

where $g_i \in \{4, 6, 7, 8, 9, (10), (11), (12)\}$ are "DE-type" nodes (referring to the gauge algebras supported on these curves), $I^{\oplus l}$ are subgraphs of the form 122....2 consisting of l curves called "instanton links", and S_i, L_i are "side links" and linear "interior links", respectively; attachment to DE-type nodes occurs via the exterior -1 curves when possible. Truncations of this general form are also permitted. Briefly, allowed bases are linear chains of curves with branching possible only near the ends. We refer to [16] for details of two exceptions to the above structure, the first allowing a limited class of bases with a single 4-valent curve that are linear away from this curve and the second allowing up to four instanton branches for certain bases with precisely five nodes.

We will now review and extend the setup, notation, and terminology introduced in [21]. We let the compact irreducible effective divisors of (2.3), namely $\Sigma_i \subseteq \{\Delta = 0\}$ lie at $\{z_i = 0\}$ and designate their self-intersection numbers via $m_i = -\Sigma_i \cdot \Sigma_i$. Let $P_{i,k}$ denote the intersections of Σ_i, Σ_k for $i \neq k$ when non-empty.

We shall consider non-compact collections of curves $\{\Sigma'_{i,j}\}_{j\in J_i}$ transversely intersecting Σ_i at $P'_{i,j}$ with $\Sigma'_{i,j}\cap\Sigma_k=\emptyset$ for $k\neq i$. Let $(a_i,b_i,d_i)=(a,b,d)_{\Sigma_i}$ indicate orders of vanishing of f,g and Δ along Σ_i and similarly define $(a'_{i,j},b'_{i,j},d'_{i,j})$ those for $\Sigma'_{i,j}$.

For Σ any of the curves Σ_i or $\Sigma'_{i,j}$ with orders $(a,b,d)=(a,b,d)_{\Sigma}$ we let

$$\widetilde{f}_{\Sigma} \equiv \frac{f}{z^a} , \qquad \qquad \widetilde{g}_{\Sigma} \equiv \frac{g}{z^b} , \qquad \qquad \widetilde{\Delta}_{\Sigma} \equiv \frac{\Delta}{z^d}, \qquad (2.5)$$

abbreviating these quantities as $\widetilde{f}, \widetilde{g}, \widetilde{\Delta}$ where unambiguous and noting they are sections of the line bundles

$$\widetilde{f} \leftrightarrow \mathcal{O}(-4K_B - a\Sigma) , \qquad \widetilde{g} \leftrightarrow \mathcal{O}(-6K_B - b\Sigma) , \qquad \widetilde{\Delta} \leftrightarrow \mathcal{O}(-12K_B - d\Sigma) .$$
 (2.6)

We will refer to $\tilde{\Delta}$ as the residual discriminant. When Σ is any of the compact divisors Σ_k , setting $m = m_k$ we have

$$K_B \cdot \Sigma = m - 2 \tag{2.7}$$

since $\Sigma \cong \mathbb{P}^1$ with genus g = 0; we define residual vanishings on Σ as the quantities

$$\tilde{a}_{\Sigma} = (-4K_B - a\Sigma) \cdot \Sigma = -4(m-2) + ma ,$$

$$\tilde{b}_{\Sigma} = (-6K_B - b\Sigma) \cdot \Sigma = -6(m-2) + mb ,$$

$$\tilde{d}_{\Sigma} = (-12K_B - d\Sigma) \cdot \Sigma = -12(m-2) + md ,$$
(2.8)

which count the number of zeros with multiplicity of the restrictions to Σ of \widetilde{f} , \widetilde{g} and $\widetilde{\Delta}$, respectively. To improve the naïve constraints on $\Sigma_i, \Sigma_{i,j}$ reading

$$(-4K_B - \sum_{i} a_i \Sigma_i - \sum_{j} a_{k,j} \Sigma'_{k,j}) \cdot \Sigma_k \ge 0 ,$$

$$(-6K_B - \sum_{i} b_i \Sigma_i - \sum_{j} b_{k,j} \Sigma'_{k,j}) \cdot \Sigma_k \ge 0 ,$$

$$(-12K_B - \sum_{i} d_i \Sigma_i - \sum_{j} d_{k,j} \Sigma'_{k,j}) \cdot \Sigma_k \ge 0 ,$$

$$(2.9)$$

we begin by defining for an intersection of two curves Σ, Σ' at P the intersection contributions from Σ' to Σ towards the residual vanishings given by the quantities

$$\tilde{a}_P \equiv \operatorname{ord}_P \tilde{f}\big|_{z=0}$$
, $\tilde{b}_P \equiv \operatorname{ord}_P \tilde{g}\big|_{z=0}$, $\tilde{d}_P \equiv \operatorname{ord}_P \tilde{\Delta}\big|_{z=0}$, (2.10)

abbreviating these as $(\tilde{a}_P, \tilde{b}_P, \tilde{d}_P)_{\Sigma}$. Note that strict inequalities in

$$\tilde{a}_P \ge a_{\Sigma'}$$
, $\tilde{b}_P \ge b_{\Sigma'}$, $\tilde{b}_P \ge b_{\Sigma'}$, $\operatorname{ord}_P f \ge a_{\Sigma} + a_{\Sigma'}$, $\operatorname{ord}_P g \ge b_{\Sigma} + b_{\Sigma'}$, $\operatorname{ord}_P \Delta \ge d_{\Sigma} + d_{\Sigma'}$, (2.11)

often follow from local analysis and that non-minimality at the intersection requires one of

$$\operatorname{ord}_{P} f < 4 , \qquad \operatorname{ord}_{P} g < 6 . \qquad (2.12)$$

Constraints tightening (2.9) using intersection contributions following from local analysis then read

$$\tilde{a}_{\Sigma} \geq \sum_{j} \tilde{a}_{P'_{k,j}} + \sum_{i \neq k} \tilde{a}_{P_{k,i}} = \sum_{i} \tilde{a}_{P_{i,\Sigma}} ,$$

$$\tilde{b}_{\Sigma} \geq \sum_{j} \tilde{b}_{P'_{k,j}} + \sum_{i \neq k} \tilde{b}_{P_{k,i}} = \sum_{i} \tilde{a}_{P_{i,\Sigma}} ,$$

$$\tilde{d}_{\Sigma} \geq \sum_{j} \tilde{d}_{P'_{k,j}} + \sum_{i \neq k} \tilde{a}_{P_{k,i}} = \sum_{i} \tilde{a}_{P_{i,\Sigma}} ,$$

$$(2.13)$$

where $P_{i,\Sigma}$ are relabellings of any intersection points between Σ and other components of the discriminant locus, namely $\{\Sigma_j\}_{j\neq i}$ and $\{\Sigma'_{k,j}\}_{j\in J}$. Further restrictions come from consistency checks for gluing these local models into globally well-defined configurations.

We shall employ the terminology of [21] referring to curves such that Σ at $\{z=0\}$ has

discriminant of the form

$$\frac{\Delta}{z^d} = \left(4\tilde{f}^3 + 27z^p\tilde{g}^2\right) , \qquad (2.14)$$

for some p>0 and $z \nmid \tilde{f}$ as having odd type and indicate the orders of vanishing as $(a,b+B,d)_{\Sigma}$, where $B=0,1,\cdots$. For such curves, the second term in the right hand side vanishes identically upon restriction to Σ and hence $\tilde{d}_P=3\tilde{a}_P$. When instead $(a+A,b,d)_{\Sigma}$, $A=0,1,\cdots$, the residual discriminant has the form

$$\frac{\Delta}{z^d} = \left(4z^p \tilde{f}^3 + 27\tilde{g}^2\right) \tag{2.15}$$

for some p > 0, and $z \nmid \widetilde{g}$ making $\widetilde{d}_P = 2\widetilde{b}_P$, we refer to such curves as *even* type. The remaining cases with Kodaira types I_n and I_n^* are termed *hybrid* types, these having both $\widetilde{f}|_{z=0}$ and $\widetilde{g}|_{z=0}$ involved in contributions to vanishings of the residual discriminant.

Note that the analysis of [21] for single curve theories addressed the general cases having any permitted $A \ge 0$ and $B \ge 0$ via the observation that maximal global symmetry algebras arise for a given Kodaira type when A = B = 0. Theories having multiple compact components of Δ however often require some Σ_i have A > 0 or B > 0 to realize a maximal configuration making our analysis somewhat more demanding. For example, consider the gauge enhancement with type assignment given by

$$\begin{array}{ccc}
3 & 1 & [\mathfrak{g}_{GS}] \\
(IV^s,\mathfrak{su}(3)) & (I_0,-) & \\
& (A,B,0) & \\
\end{array} \tag{2.16}$$

Observe that the maximal global symmetry algebra $[\mathfrak{g}_{GS}]$ which can arise is \mathfrak{e}_6 realized by a type IV*s fiber meeting the -1 curve. This requires $A \geq 1$ in (2.16) by (2.9). Hence, to search for consistent geometric assignments yielding maximal algebras, it becomes relevant to consider non-zero A, B. In fact, non-zero A, B values are often required by a gauge enhancement before any global symmetry considerations as noted above, e.g. the configuration of (A.2). Together, it is hence natural to study nearly all A, B local intersection models in development of a brute force algorithmic approach to finding maximal configurations.

2.3 Theories with one compact singular locus component

We now review details of global symmetry algebra maxima realizable in F-theory for single curve theories. Our approach to treat arbitrary 6D SCFT bases found in F-theory constructions via our algorithm requires also the data consisting of the maximal transverse configurations for single curve theories as detailed in [21, 22]. Many of these configurations do not lead maximal algebras for single curve theories but do constrain the transverse configurations we encounter in trying to do determine these maxima for more general bases.

2.3.1 Non-trivially gauged theories

Global symmetries realizable in F-theory for those cases where a single compact curve in the base carries non-abelian gauge algebra first appeared in [21]. We shall use these restrictions

with a few new tightenings for type III and IV curves as indicated with a '†' symbol in Tables 3. In cases with non-abelian gauge algebra, the Coulomb branch global symmetry predictions from field theory are remarkably close to the constraints we find from F-theory geometry, the latter being more restrictive in some cases.¹

type along Σ	algebra on Σ	$-\Sigma^2$	max. global symmetry algebra(s)	
		2	$\mathfrak{so}(7)$	
III	$\mathfrak{su}(2)$	1	$\mathfrak{so}(7)\oplus\mathfrak{so}(7)\oplus\mathfrak{su}(2)$	
111	\$u(2)		$\mathfrak{so}(7) \oplus \mathfrak{sp}(3)$ (†)	
			$\mathfrak{sp}(5)$ (†)	
	$\mathfrak{su}(2)$	2	\mathfrak{g}_2 (†)	
			$\mathfrak{g}_2\oplus\mathfrak{g}_2\oplus\mathfrak{su}(3)$ (†)	
		1	$\mathfrak{g}_2\oplus\mathfrak{sp}(2)$ (†)	
			$\mathfrak{sp}(3)$ (†)	
IV		3 -		
		2	$\mathfrak{su}(3) \oplus \mathfrak{su}(3)$	
		2	$\mathfrak{sp}(2)$	
	$\mathfrak{su}(3)$		$\mathfrak{su}(3)^{\oplus 4}$	
		$\mathfrak{su}(3)^{\oplus 2} \oplus \mathfrak{sp}(2)$	$\mathfrak{su}(3)^{\oplus 2} \oplus \mathfrak{sp}(2)$	
			$\mathfrak{su}(3) \oplus \mathfrak{sp}(3)$	
			$\mathfrak{sp}(4)$	

Table 3. Global symmetries of gauged F-theory models on Kodaira type III and IV curves.

2.3.2 Gaugeless theories

The global symmetries and maximal transverse configurations which may arise in F-theory models lacking non-abelian gauge algebra (i.e., where the discriminant locus contains only a single trivially gauged compact curve) first appeared in [22] as Tables 3,5,7, thus completing a characterization of the geometrically realizable global symmetries for single curve theories. We shall use the fact that a further tightening is possible for an I_1 curve; the flavor symmetry maximum coming from an I_n^* transverse fiber with n=4 can be constrained slightly by observing that such a fiber must have monodromy, yielding a reduction for one of the maxima from $\mathfrak{so}(16)$ to $\mathfrak{so}(15)$. We shall also use the maximal configurations and tabulations of intersection contributions (appearing in [22] as Tables 4,6) in these gaugeless cases. Generalizations of this data to cases with A, B > 0, are treated in the Appendix A. Arguments yielding these results appearing in [22] use the same approach we take here and in [21]. We extend this analysis in part for treatment of arbitrary bases since gaugeless compact components of the discriminant locus often can appear in longer bases only if A, B > 0. We detail the relevant intersection contributions and forbidden intersections for

 $^{^1}$ As noted in [21], results of [27] constrain field theory global symmetries beyond Coulomb branch gauge anomaly cancellation requirements in some cases including one with $\mathfrak{su}(2)$ gauge algebra in which the reduction resolves a mismatch with geometrically realizable global symmetries to bring agreement with predictions from F-theory. Whether yet unknown further constraints on field theory might allow precise matching in all cases remains an intriguing question.

such curves. This extension plays a key role in our algorithm determining global symmetry maxima consistent with the other restrictions derived in Appendix A.

A few comments in the case of a single type I_0 curve Σ may be helpful. The maximal configurations from [38] are those permitted as collections of singular points along Σ , but we impose stronger requirement that these arise from a transverse curve configuration. As with many other cases we study here, these maximal configurations may place distinct restrictions on the singularity type of the compact curves they intersect. As an example, among the maximal gauged curve configurations above for a type I_0 are $[III^*,III]$ and $[IV^{*s},IV^s]$, from which the algebras $\mathfrak{e}_7 \oplus \mathfrak{su}(2)$ and $\mathfrak{e}_6 \oplus \mathfrak{su}(3)$ arise. These require B > 0 and A > 0, respectively where $(a, b, d)_{\Sigma} = (A, B, 0)$. Since A, B cannot simultaneously be non-zero in type I₀, a given fixed compact component of the discriminant locus with designated orders of vanishing permits only one of these transverse curve collections. In this sense, they can only arise in distinct geometries. This phenomenon is one motivation for tracking the geometric data captured by the orders of f, g, Δ in our work. In our example, we have a larger algebra in which these are both subalgebras, namely \mathfrak{e}_8 . We might hastily conclude the geometrically realizable global symmetry algebra for all models with a single I₀ curve is then always \mathfrak{e}_8 . However, when B>0, intersection with any e_8 bearing curve is nonminimal. Our approach intends to enable a broader determination of whether the distinct global symmetries we find may arise from distinct SCFTs with their data specified by the geometry of the fibration at a level of precision beyond specification of the gauge algebra. For this reason and to confirm preliminary existence checks for geometric realizations of each gauge enhancement and their global symmetry maxima inducing configurations, we further track the orders of f, g, Δ along each of the compact and non-compact components of the discriminant locus.

2.4 Algorithm summary

In this section we describe an algorithm we have implemented via series of computer algebra system routines. These routines are intended to allow adaptation for other purposes, though the primary focus in their development is the computation of 6D SCFT global symmetries. There are three main groupings of methods. The first computes 6D SCFT gauge enhancements from geometric considerations. The second handles semisimple Lie algebra inclusion rules. The final grouping determines curve configurations leading to geometrically realizable global symmetry maxima. Several subroutines dual a purpose role in the first and third groupings. The reason for this is that many of the restrictions on which Kodaira types may be paired in curve collisions often hold even when one of the curves is non-compact.

A summary of the algorithm determining gauge enhancements and global symmetries for each enhancement on a quiver given by the values m_i follows. ² Certain subroutines are more elaborate than indicated to allow efficiency boosts and result formatting including

²Bases permitting infinitely many enhancements complicate our summary and we shall separate the statements for such quivers. The core algorithm applies identically for such "rogue bases." Since our implementation includes an argument effectively giving an upper bound on the algebra rank permitted for any gauge summand to yield a finite time algorithm through bypassing the infinity of enhancements permitted on a rogue base, awkward summary statements extending those we provide follow in the obvious way with this caveat introduced by such a user determined rank bound.

'sewing' results by combining shorter quivers together to treat longer quivers, storage of partial results during computation, writing data to file for later use and presentation in text, and enabling parallel computation. Since these are non-essential to the underlying algorithm, we will not further discuss these aspects here, instead providing the precise work-flow via inclusion of our implementation with arXiv submission of this note.

Given a quiver Q specified via the values m_i , the first leg of the algorithm finds all compatible gauge algebra assignments on Q while tracking the Kodaira types T_i yielding gauge algebras $\bigoplus_i \mathfrak{g}_i$. For each of these type assignments $\mathcal{T} \sim \{T_i\}$, the second leg determines all geometrically realizable global symmetry maxima for \mathcal{T} .

This process begins by assigning all possible orders of vanishing $(a, b, d)_{\Sigma_i}$ on each Σ_i in Q compatible with naive non-minimality constraints (2.9) up to user specified maximum values $A_{\max,T}$, $B_{\max,T}$ to be allowed for each Kodaira type T. Each order assignment $\{(a, b, d)_{\Sigma_i}\}$ is then paired with every naïvely permitted monodromy assignment appearing in Table 1. Intersection contributions are computed for each T_i in each assignment \mathcal{T} to check (2.13) with failing assignments discarded. Any remaining \mathcal{T} are checked against restrictions on pairwise intersections of compact curves. Each length three subquiver is then checked against restrictions on maximal configurations involving such triplets. If Q is a branching quiver, a final check against restrictions on transverse trio configurations mostly derived in [21, 22] is applied. The resulting list of permitted \mathcal{T} determines the gauge enhancements we allow for the given quiver.

The second leg of the algorithm constrains any geometrically realizable global symmetries by finding transverse configurations $\{\Sigma'_{i,j}\}$ permitted for each assignment \mathcal{T} . This beings by assigning for each fixed \mathcal{T} every transverse collection $\{\Sigma'_{i,j}\}$ of non-trivially gauged non-compact curves, again in two phases with the second involving decoration by a monodromy assignment with constraints on configurations provided by (2.9),(2.13), respectively. Each collection is then checked against restrictions on pair intersections, transverse duets and triplet degenerations, and certain larger maximal configurations slightly generalizing those determined in [21]. The remaining transverse configurations $\{\mathcal{T}' \sim \{\Sigma'_{i,j}\}\}_{\mathcal{T}' \in J_{\mathcal{T}}}$ determine all possible geometrically realizable global symmetry summands for fixed \mathcal{T} .

Each configuration \mathcal{T}' for a fixed \mathcal{T} is then explicitly associated to a global symmetry algebra summand $\mathfrak{g}_{GS,\mathcal{T}'} \cong \oplus_{i,j} \mathfrak{g}_{i,j}$. Any relatively maximal algebras among $\{\mathfrak{g}_{GS,\mathcal{T}'}\}_{\mathcal{T}'\in J_{\mathcal{T}}}$ are determined via an implementation of semisimple Lie algebra inclusion rules and analysis of maximal semisimple Lie subalgebras from [39]. These are the global symmetry algebras we permit for the enhancement \mathcal{T} . Any \mathcal{T}' with strictly smaller associated algebras are discarded and the resulting list returned to give the explicit geometric realizations of any global symmetry maxima for \mathcal{T} . In making the maxima comparisons, we put all \mathcal{T} having differing A_i, B_i assignments on the same footing provided the Kodaira types are matching.

A repackaged version of the program provided in conjunction with [16] is included along with methods allowing direct comparisons of enhancements described in the literature and those we compute via other methods enabling tracking of geometric data not previously available. We generally find agreement for the enhancements permitted on links with those of [16] and consequentially also for most 6D SCFTs with a handful of exceptions eliminated via geometric constraints on F-theory bases as detailed in Section 3. The input Q for our

implementation is not confined to links; only the finitely many 4-valent bases are barred.

2.5 Flavor summand locality

We now pause to provide an example illustrating one result of our analysis. Briefly, global symmetry contributions are local in quiver position for fixed Kodaira type but not for fixed gauge algebra. Each assignment \mathcal{T}_{α} for $\alpha \sim 2215$ with $\mathfrak{g}_{\text{gauge}} \cong \mathfrak{su}(2) \oplus \mathfrak{e}_6$ appears in Table 4, where n_0 denotes the trivial algebra, flavor summands appear below the curves on which they arise, and the right-most column contains the flavor symmetry maxima for a given type assignment. While we can realize a \mathfrak{g}_2 global symmetry summand from the left-most -2 curve and an $\mathfrak{su}(3)$ summand from the -1 curve, these options are mutually exclusive, i.e., all global symmetry algebras for an $\mathfrak{su}(2) \oplus \mathfrak{e}_6$ gauge theory realizable in F-theory via this quiver are strictly smaller than $\mathfrak{su}(3) \oplus \mathfrak{g}_2$.

2	2	1	5	GS Total:
$(III,\mathfrak{su}(2))$	(II,n_0)	(I_0,n_0)	$(\mathrm{IV}^{*s}, \mathfrak{e}_6)$	
A_1	0	A_1	0	A_1^2
$(IV^{ns},\mathfrak{su}(2))$	(II,n_0)	(I_0,n_0)	$(\mathrm{IV}^{*s}, \mathfrak{e}_6)$	
\mathfrak{g}_2	0	A_1	0	$A_1 \oplus \mathfrak{g}_2$
$(I_2,\mathfrak{su}(2))$	(I_1,n_0)	(I_0,n_0)	$(\mathrm{IV}^{*s},\mathfrak{e}_6)$	
A_2	0	A_2	0	A_2^2
$(\mathfrak{su}(2))$	(n_0)	(n_0)	(\mathfrak{e}_6)	
A_2	0	A_2	0	A_2^2
\mathfrak{g}_2	0	A_1	0	$A_1 \oplus \mathfrak{g}_2$
(II,n_0)	$(III,\mathfrak{su}(2))$	(I_0,n_0)	$(\mathrm{IV}^{*s},\mathfrak{e}_6)$	
0	A_1	0	0	A_1
(II,n_0)	$(IV^{ns},\mathfrak{su}(2))$	(I_0,n_0)	$(\mathrm{IV}^{*s}, \mathfrak{e}_6)$	
0	\mathfrak{g}_2	0	0	\mathfrak{g}_2
(I_1,n_0)	$(I_2,\mathfrak{su}(2))$	(I_0,n_0)	$(\mathrm{IV}^{*s},\mathfrak{e}_6)$	
0	A_2	0	0	A_2
(n_0)	$(\mathfrak{su}(2))$	(n_0)	(\mathfrak{e}_6)	
0	\mathfrak{g}_2	0	0	\mathfrak{g}_2

Table 4. All global symmetry maxima for 2215 with gauge algebra $\mathfrak{su}(2) \oplus \mathfrak{e}_6$ along with each possible Kodaira type assignment to the quiver realizing this gauge algebra.

For a quiver α , we thus fix a Kodaira type assignment \mathcal{T}_{α} before addressing which global symmetries are geometrically realizable. We can then compare results among all \mathcal{T}_{α} having shared gauge algebra, as above. Somewhat surprisingly, while various constraints are "non-local" in curve position including the permitted orders $(a, b, d)_{\Sigma_i}$ (as illustrated in Table 19), the $\mathfrak{g}_{\text{global}}$ maxima for fixed \mathcal{T}_{α} instead appear to always include every relatively maximal product of any permitted curve contributions. In contrast, this ceases to hold when varying \mathcal{T}_{α} for $\mathfrak{g}_{\text{gauge}}$ fixed as illustrated by the above example.

2.6 Distinguished Calabi-Yau threefolds from global symmetry maxima

In this section we introduce a distinguished class of elliptically fibered CY threefolds determined by global symmetry maxima of 6D SCFTs. We examine the role of these symmetries in the field-theory to geometry "dictionary" and show that a nearly bijective correspondence results when including these symmetries among the data specifying an SCFT.

Briefly, the idea is to consider which singular elliptically fibered CY threefolds $\pi: X \to B$ give F-theory models for a 6D SCFT having data ($\mathfrak{g}_{\text{gauge}}, \mathfrak{g}_{\text{global}}, \Gamma$), where $\mathfrak{g}_{\text{gauge}}$ and $\mathfrak{g}_{\text{global}}$ are gauge and global symmetry Lie algebras, respectively, and Γ discrete U(2) subgroup gauge fields. As discussed in [16], Γ determines a unique quiver $\{m_i\}$ that is the minimal blowup of the endpoint associated to Γ permitting gauge enhancement given by $\mathfrak{g}_{\text{gauge}}$. Such quivers do not exhaust those for F-theory models with matching gauge content, i.e., dropping $\mathfrak{g}_{\text{global}}$ from the SCFT data leaves the geometry severely underspecified. Models compatible with ($\mathfrak{g}_{\text{gauge}}, \Gamma$) often allow many choices for $\{m_i\}$, \mathcal{T} with geometrically realizable global symmetry algebras $\{\mathfrak{g}_{\text{global}}\}$ so different that their common merger at a conformal fixed point upon renormalization would be highly surprising. When instead tentatively regarding $\mathfrak{g}_{\text{global}}$ as an essential ingredient in specifying a CFT, matching models become so constrained that we find a nearly bijective map from 6D SCFTs to corresponding CY threefolds. The distinguished collection of all threefolds determined via this correspondence from the 6D SCFT landscape appears to be a natural candidate for further study.

We now turn to an example before further discussing this correspondence more generally. Consider the collection of theories having $\mathfrak{g}_{gauge} \cong \mathfrak{e}_6$. The compatible bases include: 1,2,21,3,31,131,4,41,141,5,51,151,512,1512. The number of curves in the base is not fixed by \mathfrak{g}_{gauge} , nor by also specifying Γ . We can say more upon fixing \mathfrak{g}_{global} . We consider the case that $\mathfrak{g}_{global} \cong \mathfrak{su}(3)$ and note that any compatible base has at least two curves since each single curve theory with $\mathfrak{g}_{gauge} \cong \mathfrak{e}_6$ gauge algebra has \mathfrak{g}_{global} trivial via Table 6.2 of [21]. We can eliminate the bases 131,141,151,1512 since each has all $\mathfrak{g}_{gauge} \cong \mathfrak{e}_6$ compatible enhancements with \mathfrak{g}_{global} being too large.

We should now specify Γ to distinguish between the bases 51,512, and others. Consider the $\mathfrak{g}_{gauge} \cong \mathfrak{e}_6$ compatible \mathcal{T} on 51,512. These appear in Tables 5 and 6. Upon fixing either base, \mathcal{T} is determined by a choice of \mathfrak{g}_{global} . Now we observe that the field theory data Γ distinguishes between the remaining $\mathfrak{g}_{global} \cong \mathfrak{su}(3)$ compatible bases and hence in conjunction with \mathfrak{g}_{global} specifies the geometry uniquely up to quiver and Kodaira type assignment.

5	1	GS Total:
$(\mathrm{IV}^{*s}, \mathfrak{e}_6)$	(I_0,n_0)	
0	A_2	A_2
$(\mathrm{III}^*,\mathfrak{e}_7)$	(I_0,n_0)	
0	A_1	A_1
$(IV^{*ns},\mathfrak{f}_4)$	(I_0,n_0)	
0	A_2	A_2
$(IV^{*ns},\mathfrak{f}_4)$	$({\rm II},\!{\rm n}_0)$	
0	\mathfrak{g}_2	\mathfrak{g}_2
$(IV^{*ns},\mathfrak{f}_4)$	(I_1,n_0)	
0	A_2	A_2
(\mathfrak{f}_4)	(n_0)	
0	\mathfrak{g}_2	\mathfrak{g}_2

Table 5. All gauge and global symmetry options for 51 with each possible Kodaira type specification realizing a given gauge theory.

Table 6. All global symmetry maxima for 512 with gauge algebra \mathfrak{e}_6 and each Kodaira type assignment realizing this algebra.

This example suggests that it is natural to consider a field-theory/geometry "dictionary" relating elliptic fibrations compatible with a choice of field theory data $(\Gamma, \mathfrak{g}_{gauge}, \mathfrak{g}_{global})$. Here \mathfrak{g}_{global} constrains which blowups of the aforementioned minimal $(\mathfrak{g}_{gauge}, \Gamma)$ compatible base should be considered, for example by requiring blowup of a base with a single -4 curve to 51 when $\mathfrak{g}_{gauge} \cong \mathfrak{f}_4$ and \mathfrak{g}_{global} is non-trivial, or with another Γ , from -3 to 512. Such a dictionary formulation thus gives a natural route from field-theory to the bulk of geometries in correspondence with 6D SCFTs, with the role of \mathfrak{g}_{global} essential in accessing the better part of this geometric landscape. The fibration with minimally blown-up base can be viewed as a degenerate case in which we have omitted any \mathfrak{g}_{global} specification.

Let us return to our $\mathfrak{g}_{\text{gauge}} \cong \mathfrak{e}_6$ example, instead now fixing Γ_{-3} corresponding to the endpoint -3. Since $\mathfrak{g}_{\text{gauge}}$ has a single summand and all curves Σ having $m_{\Sigma} \geq 3$ carry non-trivial \mathfrak{g}_{Σ} , there can only be one $m \geq 3$ curve in any compatible base. All curves must have $1 \leq m \leq 6$ since $m_{\Sigma} \geq 7$ requires Σ minimally support $\mathfrak{g}_{\Sigma} \cong \mathfrak{e}_{\geq 7}$. For the base -3, we have $\mathfrak{g}_{\text{global}} = 0$, and this is the only such base. The remaining bases with shared endpoint which can match $\mathfrak{g}_{\text{gauge}}$ have

$$\alpha \in \{41, 151, 512, 1612, 161\}$$
.

For 41, we have a unique $\mathfrak{g}_{global} \cong \mathfrak{su}(3)$. From the data above for 51, we can deduce that when α given by 151, the unique $\mathfrak{g}_{global} \cong \mathfrak{su}(3)^{\oplus 2}$. For the only trivalent option, this becomes $\mathfrak{su}(3)^{\oplus 3}$ (noting Table 7). For 1612, options for \mathfrak{g}_{global} match those from 512 after appending an $\mathfrak{su}(3)$ summand coming from the outer -1 curve. To simplify the correspondence, let us consider only the geometries leading to the maximal \mathfrak{g}_{global} on each quiver. This gives for 512, $\mathfrak{g}_{global} \cong \mathfrak{su}(2) \oplus \mathfrak{su}(3)$ and for 1612, $\mathfrak{g}_{global} \cong \mathfrak{su}(2) \oplus \mathfrak{su}(3)^{\oplus 2}$. To summarize, α and \mathcal{T} are determined uniquely in each case by \mathfrak{g}_{global} .

Observe that "special" CY threefold fibrations are singled out by this "dictionary," namely those which have singular curve collections carrying one of the \mathfrak{g}_{global} maxima for a 6D SCFT. Denoting this collection of varieties $\mathcal{M}_{\mathfrak{g}_{global}}$, our example summary amounts to concluding that inverting the map

$$\mathcal{M}_{\mathfrak{g}_{\mathrm{global}}}|_{(\mathfrak{g}_{\mathrm{gauge}}\cong\mathfrak{e}_{6},\Gamma_{-3})}\mapsto (\mathfrak{e}_{6},\mathfrak{g}_{\mathrm{global}},\Gamma_{-3})$$

from bases with enhancements specified up to Kodaira type to their relatively maximal global symmetries gives an injective map from \mathfrak{g}_{global} to $\mathcal{M}_{\mathfrak{g}_{global}}$. Generalizing this statement to all 6D SCFTs is non-trivial due to subtleties including the presence of multiple relative maxima for \mathfrak{g}_{global} . Note that there is an analog of this distinguished class of threefolds in the moduli space of compact Calabi-Yau threefolds upon consideration of a compact base giving an F-theory model coupled to gravity wherein the global symmetries we describe are promoted to gauge symmetries via assignment of values m_i to non-compact \mathfrak{g}_{global} carrying curves when possible while our transversality requirements are relaxed.

The distinguished threefolds $\mathcal{M}_{\mathfrak{g}_{\text{global}}}$ in contact with F-theory models are remarkably sparse among CY threefold elliptic fibrations. Consider a fibration with base containing a single compact curve Σ and $T_{\Sigma} \sim I_0$. The unique degenerate fiber collection along Σ corresponding to the unique flavor symmetry maximum for such models, namely $\mathfrak{g}_{\text{global}} \cong \mathfrak{e}_8$ arising from a transverse curve Σ' with $T_{\Sigma'} \sim II^*$, corresponds to the a distinguished geometry among the many others appearing as entries of "Persson's list" from [38]. Enhancing Σ to reach $T_{\Sigma} \sim I_n^{ns}$ for n odd makes the number of transverse configurations grow exponentially in n while only $\frac{n+3}{2}$ geometries are in correspondence with the $\mathfrak{g}_{\text{global}}$ maxima of Tables (6.1-2) of [21]. This sparsity is not limited to single curve bases. For example, there are infinitely many minimally enhanced bases with outer links permitting an $\mathfrak{e}_8 \oplus \mathfrak{e}_8$ global symmetry. For each, we have a variety with that flavor symmetry arising in the singular limit which is distinguished from the remaining varieties inducing any of the 6757 proper $\mathfrak{g}_{\text{global}}$ subalgebra isomorphism classes.

$$\begin{array}{cccc} 6 & 1 & \text{GS Total} \\ (\text{IV}^{*s}, \mathfrak{e}_6) & (\text{I}_0, \text{n}_0) & \\ 0 & A_2 & A_2 \\ (\text{III}^*, \mathfrak{e}_7) & (\text{I}_0, \text{n}_0) & \\ 0 & A_1 & A_1 \end{array}$$

Table 7. All gauge and global symmetry options for 61 with each possible Kodaira type specification realizing a given gauge theory.

3 Gauge algebras

In this section we discuss gauge algebra assignments for each base permitted via [16] though forbidden via the geometric constraint algorithm outlined in Section 2. We also outline our method for comprehensive comparison of gauge enhancements permitted via [16] versus our algorithm. The latter are strictly more constrained with a minority of cases excluded.

3.1 Link enhancements

We now inspect the link gauge assignments compatible with some explicit Kodaira type specification meeting our geometric constraint algorithm. We compare our prescriptions for links with those determined in [16] and then extend to a comparison for general 6D SCFT bases via the node attachment restrictions of [16].

3.1.1 Consequences of $\mathfrak{so}(13)$ global symmetry constraints

An $\mathfrak{so}(13)$ gauge summand can only be carried on a curve of negative self-intersection m=2 or m=4. The F-theory global symmetry from [21] for such a curve, $\mathfrak{sp}(5)$, is independent of m, while the Coulomb branch global symmetry is given by $\mathfrak{sp}(9+\Sigma^2)$. These agree for m=4, but the discrepancy for m=2 leads to gauge enhancements for a family of bases which are more constrained than those characterized in [16]. In particular, gauge enhancements for quivers which are truncations of $21414\cdots$ containing the link 21 beginning $\mathfrak{so}(13)$, $\mathfrak{sp}(6 \leq l \leq 7)$, \cdots are eliminated.

3.1.2 Further link enhancement restrictions

We have carried out a comprehensive comparison between the link gauge enhancements permitted by our approach versus those prescribed in [16]. The few discrepancies between these prescriptions are discussed in this section. Our comparisons are drawn after adjustments to the gauge enhancement prescription algorithm implementation accompanying [16] aimed to make these fully consistent with the gauge algebra constraints of [16] and identification of $\mathfrak{su}(2)$ and $\mathfrak{sp}(1)$. We find agreement for all link enhancements except those appearing in Table 8 or contained in the family detailed in Section 3.1.1. We now briefly discuss geometric elimination of the former.

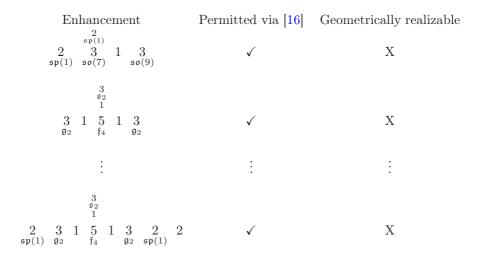


Table 8. Discrepancies with gauge enhancements prescribed via [16].

 $^{^{3}}$ These edits resolve mismatches with prescriptions of [16] for the bases 13, 213, and 2 31 (affecting results for longer quivers) resolved by adjustments bringing listings for these into agreement with underlying gauging rules. Details of edits appear in the workbook accompanying the arXiv submission of this note in the subroutines for those quivers.

3.1.2.1 No \mathfrak{g}_2 trifecta branching from \mathfrak{f}_4

Certain enhancements permitted via [16] contain the configuration

on a sub-quiver. This can be excluded via the following geometric considerations.

For a gaugeless curve to support an $\mathfrak{f}_4,\mathfrak{g}_2$ neighbor pair, it must be a type II curve. This leaves only

as an assignment of Kodaira types potentially realizing this enhancement. However, this too is ruled out since $\tilde{d}_{\Sigma} = \deg(\tilde{\Delta}_{\Sigma}) = 4$ along a -5 curve Σ with \mathfrak{f}_4 algebra while each type II contributes two vanishings of $\tilde{\Delta}_{\Sigma}$.

This in turn eliminates each enhancement from [16] containing the above gauge assignment, these being the five truncations of

obtained by removing any choice of -2 curves.

3.1.2.2 Eliminating a 2313 enhancement

Enhancing the quiver 2313 to yield the enhancement

$$\begin{array}{cccc}
 & 2 & & \\
2 & 3_{\Sigma'} & 1_{\Sigma} & 3 & \\
\mathfrak{sp}(1) & \mathfrak{so}(7) & & \mathfrak{so}(9)
\end{array} \tag{3.4}$$

appears to be permitted by [16] gauging requirements and is among the companion work-book enhancement listings. However, geometric considerations eliminate this enhancement.

We proceed by inspecting which Kodaira types might be permitted to realize the relevant gauge algebra assignments. The -2 intersections with an $\mathfrak{so}(7)$ algebra carrying -3 curve requires these have Kodaira type III. This implies that of the 6 residuals in $\tilde{\Delta}_{\Sigma'}$ available along the -3 curve, we have used three for each -2 curve intersection. This leaves no residual vanishings for the -1 curve to carry a Kodaira type other than I_0 . However, a type I_0 assignment is not permissible since 6+7 vanishings of $\tilde{\Delta}_{\Sigma}$ are required along this curve to support intersections with the neighboring curves which must have Kodaira types

 I_0^{*ss} and I_1^{*ns} (as we can read from their algebra content) making their \tilde{d}_{Σ} contributions to the -1 curve at least 6 and 7, respectively.

3.1.3 Summary of link comparisons

After compensating for the aforementioned issues, we find agreement with the gauge enhancement structure on all links with that of [16]. In other words, there is some Kodaira type assignment and chosen orders of f, g, Δ along each curve of the link that meets all geometric constraints known to us and realizes each link enhancement dictated via the auxiliary computer algebra workbook listings of [16] after the minor aforementioned edits with the above eliminated enhancement exceptions.

3.2 Comprehensive enhancement comparison

We now compare enhancements for bases with nodes we obtain with previous results. After accounting for a few technical exceptions, the enhancements we permit match those of [16]. We begin with a summary of comparisons for single node attachments to a link and then turn to discuss attaching a pair of nodes to an interior link.

3.2.1 \mathfrak{e}_6 , \mathfrak{e}_7 and \mathfrak{e}_8 attachments

Enhancements of bases formed by left attachment of an \mathfrak{e}_7 or \mathfrak{e}_8 node to a link of the form $L \sim 1223\cdots$ yield matches as do instanton links (taking the form $122\cdots$) with \mathfrak{e}_8 node attachment. Explicit comparisons for the latter are made awkward by differences in the handling of infinite link enhancement families but can be treated by confining listings of [16] to those with empty gauge summand on the two leftmost curves and the rightmost matching a corresponding term from our listings.

We also find agreement for left \mathfrak{e}_6 and \mathfrak{e}_7 attachments to links of the form $123\cdots$, $1223\cdots$, and $122\cdots$. Comparisons for the latter can be made with a procedure analogous to \mathfrak{e}_8 instanton link case, here instead via restriction to link enhancements obeying the gauging condition of [16] making the leftmost -2 curve empty, $\mathfrak{sp}(1)$, or $\mathfrak{su}(3)$ (with the latter only for \mathfrak{e}_6 attachment).

Excluding the links 123 and 122315131 discussed in Section 3.2.4, explicit comparisons yield agreement for the remaining branching links meeting $\mathfrak{e}_{\geq 6}$ curves, thus confirming all link attachment prescriptions of [16] for a single compact curve carrying an $\mathfrak{e}_{\geq 6}$ algebra with exceptions noted above.

3.2.2 Attachments to an interior link

Gauging rules of [16] for interior links with node attachments match those following from our approach in all cases except for exclusion of a forbidden node pair to 122315131 discussed shortly. Matching for cases with attachment of a -6 or -4 curve to the link 1315131 and all allowed attachments to 131513221 or 13151321 can be confirmed by comparison of these gauging rules with our listings for each quiver of this form. Agreement for enhancements of node attachments to the links 12231, 12321, and 1231 follows from link enhancement agreement and inspection that our prescriptions respect those attachment gauging rules as

does that for 131, though checks for the latter are involved as specification of enhancements permitted by [16] require supplementing attachment rules with convexity conditions.

These checks can be extended to confirm that all bases with interior links and no side-links having up to two nodes except bases of the form $(1)4141\cdots$ yield matches.⁴ In fact, after matches confirmed in the following subsections, we can conclude that with the aforementioned exceptions for noble branching link discrepancies, $\mathfrak{so}(13)$ caveats, certain pairings for 122315131, and bases with node attachment to 123, we find agreement for all gauge enhancements. This follows from checks on multi-node bases revealing no further eliminations. Whether stronger geometric restrictions on short quivers can be derived to more significantly reduce the 6D SCFT landscape via our algorithm remains an intriguing question for future work.

3.2.3 Enhancements on quivers of the form (2)(1)414...

Excluding the restriction discussed in Section 3.1.1 above, our method yields matching enhancements for quivers of the form $(2)(1)414\cdots$ with those prescribed via [16]. Carrying out this check is delicate as each such quiver permits infinitely many enhancements. However, these obey a simple set of rules determined in [16] which match the restrictions on length three sub-quiver gauge algebra assignments dictated by geometric global symmetry restrictions excluding the aforementioned $\mathfrak{so}(13)$ caveat.

To explicitly confirm matching away from those special cases detailed in Section 3.1.1 using our algorithm, we begin by fixing a quiver in this family and choosing an upper bound on gauge summand rank. Listing all compatible enhancements and discarding those having summands matching the rank bound allows confirmation via inspection that remaining enhancements obey the corresponding gauging conditions of [16]. Checks through large rank and quiver length reveals the claimed matching.

3.2.4 Novel links and link attachment restrictions

The links $1\overline{5}13215$ and $31\overline{5}1315$ appear to be allowed, though absent from the listings of [16]. These blow-down consistently and permit multiple valid gauge assignments including options with \mathfrak{f}_4 on the rightmost -5 curve. It thus appears that each is a properly a noble link rather than its truncation (of the outer -5 curve) being an alkali link permitting only right \mathfrak{e}_6 or \mathfrak{e}_7 attachment.

Among the links listings of [16] is 321_{Σ} with indicated attachments for (only) $\mathfrak{e}_6, \mathfrak{e}_7$, though neither appears to be permitted. The \mathfrak{e}_6 algebra is not possible, since this requires attachment to a curve with $m \leq 6$ which then cannot satisfy the adjacency matrix condition. For \mathfrak{e}_7 algebra, we have $m \leq 7$ similarly barred, leaving m = 8 as the only potentially

⁴This accounts for two exceptions we have noted elsewhere. The first concerns 12231513221, which does not permit $(\mathfrak{e}_6,\mathfrak{e}_6)$ attachments as a consequence of blowdowns induced on neighboring nodes, namely (5,5). The second concerns attachment of a -4 curve to 122315131 curve with $\mathfrak{so}(N)$ with $8 \le N \le 12$, which appears to be permitted.

consistent option. However, this is also barred as after one blow-down we reach

$$\frac{2}{317}$$
, (3.5)

which is inconsistent with the normal crossings condition. We conclude this link is not permitted any attachments (making it a noble link), though an \mathfrak{e}_6 global symmetry can arise from Σ .

3.2.5 Link and attachments summary

Novel links and link attachment prescriptions (comparing with [16]) appear in Table 9.

321
$$\overset{1}{1513215}$$
 31 $\overset{1}{51315}$ 12231513221 122315131 no attachments \checkmark \checkmark $(\mathfrak{e}_{\geq 6+k_l};\mathfrak{e}_{\geq 6+k_r})$ $(\mathfrak{e}_{\geq 6};\mathfrak{f}_4,\mathfrak{e}_{\geq 6} \text{ or } \mathfrak{so}(N))$

Table 9. Summary of novel links and link attachment prescriptions versus those [16]. Here ' \checkmark ' indicates a link that appears to be allowed though not listed in [16].

3.3 No trios of branching side-links, implementation scope

Our implementation of the algorithm outlined in Section 2.4 does not treat 4-valent bases. The only bases not treated directly are the single instanton link decorations

$$S_L \underset{L \oplus n}{\mathfrak{g}} S_R \tag{3.6}$$

of single node bases which are treated directly, these being of the form

$$S_L \mathfrak{g}^{S_U} S_R$$
 (3.7)

Our implementation also does not treat branching from any vertical branches, but this does not impose any limitations. While a priori the classification of [16] allows for a pair of branching side-links S_L , S_U meeting a node which then joins the backbone giving

$$S_L \stackrel{S_U}{\mathfrak{g}} L_R \cdots ,$$
 (3.8)

this situation is never encountered in practice. To check this, we confirm that -12 is the only possible node allowing a pairs of branching side links and an interior link L_R . In this case, we can only have L_R be interior link -1 and no attachments to this link are possible. In fact, there is only one such base and it can be rewritten in the form

$$S_L(12)S_R$$
, (3.9)

where S_L is given by 1513221 and S_R is the reverse of this link.

4 Global symmetry classification summary via local contributions

Since flavor symmetries for bases with a single compact singular locus component were characterized in [21, 22], we are left to contend with bases containing at least two compact curves. In this section, we detail analogous results capturing the general case obtained via the algorithm of Section 2.4 by dictating the flavor summand maxima arising from each segment of a base with specified enhancement.

Though curves Σ_i in a base may have any of the values $1 \leq m_{\Sigma_i} \leq 8$ or $m_{\Sigma_i} = 12$, length two chains are highly constrained with the only options being $\alpha \in \{1k \text{ for } k > 1, 22, 23\}$. We shall use this fact to characterize flavor summands arising from each curve of every viable short subquiver decorated with a Kodaira type assignment. This yields a classification of 6D SCFT flavor symmetries via decomposition of an arbitrary base into short chains for which we prescribe summands with a combination of configuration listings and short constraint equations which in many cases tighten the permissible symmetries beyond those permitted by the free multiplet counts for the cases detailed in [16].

A fact we shall use frequently is that any curve carrying gauge algebra $\mathfrak{f}_4, \mathfrak{e}_6, \mathfrak{e}_7$, or \mathfrak{e}_8 does not support any non-abelian global symmetry summand. As elsewhere in this note, bracketed terms indicate global symmetry summands. Note that for a curve Σ with $7 \leq m_{\Sigma} \geq 8$, only the assignment III* $\leftrightarrow \mathfrak{e}_7$ is permitted; for $6 \leq m_{\Sigma} \geq 8$, type IV^{ns} $\leftrightarrow \mathfrak{f}_4$ is barred while $\mathfrak{e}_{6\leq k\leq 7}$ types are permitted; for $m_{\Sigma} \leq 4$, each of \mathfrak{f}_4 and $\mathfrak{e}_{6\leq k\leq 7}$ assignments are valid; finally, \mathfrak{e}_8 assignment requires $m_{\Sigma} = 12$. We shall use these facts to treat multiple quivers simultaneously and refer to them as "the permitted gauging rules."

It will be convenient to introduce notation $[\mathfrak{g}_{\alpha}]$ for flavor symmetry summands arising from a subquiver $\alpha \subset \beta$ (e.g. $23 \subset 232$) upon fixing a type assignment on β given by \mathcal{T}_{β} , taking $\beta = \alpha$ when no containing quiver is apparent from context. For example, since the type assignment $\mathcal{T} \sim \mathcal{T}_{23} \sim \text{III}, I_0^{*ss}$ to 23 allows an $\mathfrak{su}(2)$ flavor summand from the -3 curve via (4.1), we shall write $[\mathfrak{g}_{23},\mathcal{T}] \cong \mathfrak{su}(2)$ or simply $[\mathfrak{g}_{23}] \cong \mathfrak{su}(2)$ when context makes \mathcal{T} unambiguous. We will similarly refer to flavor summands arising from a given curve Σ by $[\mathfrak{g}_{\Sigma}]$ when context makes the containing type assignment clear, e.g. in 23_{Σ} with $\mathcal{T}_{\Sigma} \sim I_0^{*ss}$, we have $[\mathfrak{g}_{\Sigma}] \cong \mathfrak{su}(2)$.

4.1 23

The only permissible Kodaira type assignments for the bare quiver 23 are

$$\begin{array}{cccc}
2 & 3_{\Sigma} \\
& & & \\
& & & \\
& & & \\
& & & \\
& & & \\
& & & \\
& & & \\
& & & \\
& & & \\
& & & \\
& & & \\
& & & \\
& & & \\
& & & \\
& & \\
& & & \\
& & \\
& & \\
& & \\
& & \\
& & \\
& & \\
& & \\
& & \\
& & \\
& & \\
& & \\
& & \\
& & \\
& & \\
& & \\
& & \\
& & \\
& & \\
& & \\
& & \\
& & \\
& & \\
& & \\
& & \\
& & \\
& & \\
& & \\
& & \\
& & \\
& & \\
& & \\
& & \\
& & \\
& & \\
& & \\
& & \\
& & \\
& & \\
& & \\
& & \\
& & \\
& & \\
& & \\
& & \\
& & \\
& & \\
& & \\
& & \\
& & \\
& & \\
& & \\
& & \\
& & \\
& & \\
& & \\
& & \\
& & \\
& & \\
& & \\
& & \\
& & \\
& & \\
& & \\
& & \\
& & \\
& & \\
& & \\
& & \\
& & \\
& & \\
& & \\
& & \\
& & \\
& & \\
& & \\
& & \\
& & \\
& & \\
& & \\
& & \\
& & \\
& & \\
& & \\
& & \\
& & \\
& & \\
& & \\
& & \\
& & \\
& & \\
& & \\
& & \\
& & \\
& & \\
& & \\
& & \\
& & \\
& & \\
& & \\
& & \\
& & \\
& & \\
& & \\
& & \\
& & \\
& & \\
& & \\
& & \\
& & \\
& & \\
& & \\
& & \\
& & \\
& & \\
& & \\
& & \\
& & \\
& & \\
& & \\
& & \\
& & \\
& & \\
& & \\
& & \\
& & \\
& & \\
& & \\
& & \\
& & \\
& & \\
& & \\
& & \\
& & \\
& & \\
& & \\
& & \\
& & \\
& & \\
& & \\
& & \\
& & \\
& & \\
& & \\
& & \\
& & \\
& & \\
& & \\
& & \\
& & \\
& & \\
& & \\
& & \\
& & \\
& & \\
& & \\
& & \\
& & \\
& & \\
& & \\
& & \\
& & \\
& & \\
& & \\
& & \\
& & \\
& & \\
& & \\
& & \\
& & \\
& & \\
& & \\
& & \\
& & \\
& & \\
& & \\
& & \\
& & \\
& & \\
& & \\
& & \\
& & \\
& & \\
& & \\
& & \\
& & \\
& & \\
& & \\
& & \\
& & \\
& & \\
& & \\
& & \\
& & \\
& & \\
& & \\
& & \\
& & \\
& & \\
& & \\
& & \\
& & \\
& & \\
& & \\
& & \\
& & \\
& & \\
& & \\
& & \\
& & \\
& & \\
& & \\
& & \\
& & \\
& & \\
& & \\
& & \\
& & \\
& & \\
& & \\
& & \\
& & \\
& & \\
& & \\
& & \\
& & \\
& & \\
& & \\
& & \\
& & \\
& & \\
& & \\
& & \\
& & \\
& & \\
& & \\
& & \\
& & \\
& & \\
& & \\
& & \\
& & \\
& & \\
& & \\
& & \\
& & \\
& & \\
& & \\
& & \\
& & \\
& & \\
& & \\
& & \\
& & \\
& & \\
& & \\
& & \\
& & \\
& & \\
& & \\
& & \\
& & \\
& & \\
& & \\
& & \\
& & \\
& & \\
& & \\
& & \\
& & \\
& & \\
& & \\
& & \\
& & \\
& & \\
& & \\
& & \\
& & \\
& & \\
& & \\
& & \\
& & \\
& & \\
& & \\
& & \\
& & \\
& & \\
& & \\
& & \\
& & \\
& & \\
& & \\
& & \\
& & \\
& & \\
& & \\
& & \\
& & \\
& & \\
& & \\
& & \\
& & \\
& & \\
& & \\
& & \\
& & \\
& & \\
& & \\
& & \\
& & \\
& & \\
& & \\
& & \\
& & \\
& & \\
& & \\
& & \\
&$$

noting that the indicated $[\mathfrak{g}_{\Sigma}]$ may be further constrained by the presence of an additional neighboring curve Σ' which must have $1 \leq m_{\Sigma'} \leq 2$. Resulting reductions of $[\mathfrak{g}_{\Sigma}]$ are

dictated by the Kodaira type $T_{\Sigma'}$ on Σ' . When $m_{\Sigma'}=2$, a unique assignment

$$\begin{array}{cccc} 2 & 3 & 2 \\ \underset{\mathfrak{su}(2)}{\text{III}} & \underset{\mathfrak{so}(7)}{\overset{*}{\text{II}}} & \underset{\mathfrak{su}(2)}{\text{III}} \\ \end{array}$$

results and $[\mathfrak{g}_{232}]$ is trivial. When $m_{\Sigma'}=1$, $[\mathfrak{g}_{23}]$ is trivial provided $T_{\Sigma'}$ is non-trivially gauged or type II. When $T_{\Sigma'}\in\{\mathrm{I}_0,\mathrm{I}_1\}$, $[\mathfrak{g}_{\Sigma}]\cong\mathfrak{su}(2)$ persists.

4.2 (12)1, 81, 71, 61, 51

Since the unique gauge assignment for (12)1 has no flavor summand arising from either curve and a unique Kodaira type assignment given by

$$\begin{array}{ccc}
12 & 1 \\
II^* & I_0 \\
 & \underline{} \\
\end{array} ,$$
(4.3)

neighboring curves are irrelevant to prescribe contributions from this curve pair.

The permitted configurations for the bare bases m1 with $5 \le m \le 8$ are

$$\begin{array}{lll}
5 \leq m \leq 8 & 1 \\
& \text{III}^* & I_0 & [\mathfrak{su}(2)] \\
& \text{IV}^{*ns}/\text{IV}^{*s} & I_0 & [\mathfrak{su}(3)] \\
& \text{IV}^{*ns} & I_1 & [\mathfrak{su}(3)] \\
& \text{IV}^{*ns} & \text{II} & [\mathfrak{g}_2] & .
\end{array} \tag{4.4}$$

Note that the permitted gauging rules constrain the allowed values of m in various cases. This condition will be implicit in the further listings with indeterminate m in this section. Since flavor summands which can arise from the curve pairs m1 in longer quivers depend on Kodaira types of right neighboring curves, we next detail the effect of these attachments while observing the irrelevance of any left attachment.

Via [16], the only forms for links which can attach to an \mathfrak{e}_6 node are

$$123 \cdots$$
, $1223 \cdots$, or $12(2)(2) \cdots$. (4.5)

We proceed through the type assignments for these links compatible with the presence of node with $7 \le m \le 8$ and detail flavor summands arising from the subquiver m1 for each. All remaining links allow only $m \le 6$ attachment, these being of the form $13 \cdots$. Briefly, a -m curve carrying \mathfrak{f}_4 or \mathfrak{e}_6 gauge have an $\mathfrak{su}(N \le 3)$ maximum for $[\mathfrak{g}_{\Sigma}]$ in $m1_{\Sigma} \cdots$ with N dependent on other curves attached Σ ; for $m1 \cdots$ with $m \ge 7$, this is reduced to $\mathfrak{su}(2)$. Note that $T_{\Sigma} \sim I_0$ is required for $m \ge 7$ as intersection with III* is otherwise non-minimal.

• $123\cdots$: Attaching a -7 or -8 curve Σ to a link of this form requires the -2 curve

have $\mathfrak{su}(2)$ gauge summand from Kodaira type III. When $7 \leq m \leq 8$, $[\mathfrak{g}_{m1}]$ is trivial. The only difference when attaching a curve with $5 \leq m \leq 6$ is that we can realize this $\mathfrak{su}(2)$ gauge summand via IV^{ns} . All configurations are among

• $1223\cdots$: Link attachments of this form to a curve Σ with $5 \leq m_{\Sigma} \leq 8$ require $[\mathfrak{g}_{m1}]$ for Σ enhanced to \mathfrak{e}_7 as is required when $m_{\Sigma} \geq 7$. Otherwise an $\mathfrak{su}(2)$ flavor summand can occur. All potentially viable configurations are

$$5 \le m \le 8 \qquad 1 \qquad 2 \qquad 2 \qquad 3$$

$$III^* \qquad I_0 \qquad II \qquad IV^{ns} \qquad I_0^{*ns}$$

$$IV^{*s}/IV^{*ns} \qquad I_0 \qquad II \qquad IV^{ns} \qquad I_0^{*ns} \qquad .$$

$$[\mathfrak{su}(2)] \qquad IV^{ns} \qquad I_0^{*ns} \qquad .$$

$$[\mathfrak{su}(2)] \qquad IV^{ns} \qquad I_0^{*ns} \qquad .$$

• $12_{\Sigma}(2)(2)\cdots$: When Σ has non-trivial gauge summand, $[\mathfrak{g}_{m1}]$ is trivial as required by [22, 38]. For gaugeless Σ , instead $[\mathfrak{g}_{m1}]$ are constrained by T_{Σ} according to

All configurations for the bases m12 with $m \geq 5$ appear in Table 46. Note that attachment of additional -2 curves does not ensure further constraints except when their types require T_{Σ} be raised beyond I_1 .

• $1_{\Sigma}3\cdots$: Attaching links of this form to Σ' requires $m_{\Sigma'} \leq 6$ and $[\mathfrak{g}_{m1}]$ being trivial. This follows since the unique assignment to 613 is $IV^{*s}I_0IV^s$, which leaves no further residual vanishings of $\tilde{\Delta}_{\Sigma}$ along Σ ; The only possible assignments for m13 with $5 \leq 1$

 $m \leq 6$ are

Note that the above treatment also captures each possible linking to a curve with $m \leq 4$ enhanced to one \mathfrak{f}_4 , $\mathfrak{e}_{6 \leq k \leq 7}$ provided we substitute m=5 in the above discussion with the appropriate value of m and consider only links consistent with the number of blowdowns permitted by m as detailed in [16] Appendix D. (For m=4, links of each form discussed are permitted.)

4.3 41

Our discussion here more involved since -4 node permits gauged -1 neighbors. We first discuss the highly constrained configurations for certain bases with subquiver $4_{\Sigma}1_{\Sigma'}$. As there are infinitely many enhancements of the base 41, determining $[\mathfrak{g}_{41}]$ presents certain difficulties. However, there is little freedom for the Kodaira types of curves permitted intersect a -4 curve while maintaining non-minimality. The only infinite family of enhancements have the form $\mathfrak{so}(N), \mathfrak{sp}(N')$ and flavor summands for these enhancements can be characterized by a few simple conditions with the rest easily handled by inspection.

Non-trivial $[\mathfrak{g}_{\Sigma}]$ may arise depending on the neighboring Kodaira type $T_{\Sigma'}$ provided $T_{\Sigma} \leftrightarrow \mathfrak{so}(N)$. The only compatible gauged types are I_n^{ns} curves carrying $\mathfrak{sp}(N')$ algebras. A constraint on $[\mathfrak{g}_{\Sigma}]$ accounting for any neighboring curves can be derived via simple tallying conditions for contributions towards the residual vanishings \tilde{d}_{Σ} . Simple conditions capturing this constraint treat all but finitely many cases which we resolve first by working through the permitted attaching links and discussion of the bare base 41. We confine ourselves to $T_{\Sigma} \leftrightarrow \mathfrak{so}(N)$ since \mathfrak{f}_4 and $\mathfrak{e}_{\geq 6}$ assignments are captured in Section 4.2.

The only permitted right attachments to a -4 curve are among

We proceed through these possibilities, in each turning to consider simultaneous left attachments after discussing the bare cases, i.e., those without a left attachment to Σ .

• 4132: This base has a single type assignment given by

$$\begin{array}{cccc} & & & 2 \\ 4 & 1 & 3 & 2 \\ (I_0^{*s},\mathfrak{so}(8)) & (I_0,n_0) & (I_0^{*ss},\mathfrak{so}(7)) & (III,\mathfrak{su}(2)) \end{array}$$

with trivial flavor symmetry from all curves, thus making left attachments irrelevant.

• $412_{\Sigma_2}3\cdots$: Here $[\mathfrak{g}_{41}]$ is trivial except for gaugeless Σ' , as we can read from (4.2) and Table 3. This is also trivial when \mathfrak{g}_{Σ} is \mathfrak{f}_4 or $\mathfrak{e}_{\geq 6}$, and again when $\mathfrak{g}_{\Sigma} \cong \mathfrak{so}(8)$ and $T_{\Sigma'} \sim \text{II}$; we can confirm the latter using the maximal configurations for type II and I_0^{*s} curves from [22] and [21], respectively.

The remaining gaugeless types, I_0 and I_1 arise in few configurations. For $\mathfrak{g}_{\Sigma} \cong \mathfrak{so}(8)$, these have a -1 curve summand $[\mathfrak{g}_{\Sigma'}] \cong \mathfrak{su}(3)$ when $T_{\Sigma_2} \sim \text{III}$ and $[\mathfrak{g}_{\Sigma'}]$ otherwise trivial when $T_{\Sigma_2} \sim \text{IV}^{ns}$. In the remaining cases $T_{\Sigma} \leftrightarrow \mathfrak{so}(N)$ for $9 \leq N \leq 12$ with $[\mathfrak{g}_{\Sigma'}]$ is trivial for $11 \leq N \leq 12$. When $9 \leq N \leq 10$, $[\mathfrak{g}_{\Sigma'}]$ is trivial for $T_{\Sigma_2} \sim \text{IV}^{ns}$ otherwise has maximum for $T_{\Sigma_2} \sim \text{III}$ given by $\mathfrak{su}(2)$. Finally, the -4 curve summand $[\mathfrak{g}_{\Sigma}] \cong \mathfrak{sp}(N-8)$ except for the unique assignment to the quiver 4123 featuring a type I_1 curve along Σ' when is reduced to $[\mathfrak{g}_{\Sigma}] \cong \mathfrak{sp}(1)$.

• 413····: Since the quiver 413 permits a (large but) finite number of enhancements, all configurations with flavor symmetry maxima indicated can be listed directly with the accompanying workbook.⁵ The key features of every such configuration can be captured as follows.

When \mathfrak{g}_{Σ} is any of \mathfrak{f}_4 , \mathfrak{e}_6 , or \mathfrak{e}_7 algebra, $[\mathfrak{g}_{41}]$ is trivial. Remaining cases involve an $\mathfrak{so}(N)$ algebra on Σ with $8 \leq N \leq 24$, with $[\mathfrak{g}_{\Sigma}]$ obeying the following constraints. For N=9, it is trivial unless $T_{\Sigma'} \sim I_0$ when $[\mathfrak{g}_{\Sigma}] \cong \mathfrak{su}(2)$. For $N \geq 10$ and $T_{\Sigma'} \sim I_0$ we have $[\mathfrak{g}_{\Sigma}] \cong \mathfrak{sp}(2)$ and $[\mathfrak{g}_{\Sigma'}]$ is trivial. Otherwise, we have (in agreement with convexity conditions) $T_{\Sigma'} \leftrightarrow \mathfrak{sp}(M)$ for $M \geq 1$ and $[\mathfrak{g}_{\Sigma}] \cong \mathfrak{sp}(M')$ with $M+M' \leq \lfloor N/2 \rfloor -1$. Attachment of further -1 curves Σ_L, Σ_U meeting Σ give $[\mathfrak{g}_{\Sigma}]$ obeying $M+M'+M_L+M_U \leq \lfloor N/2 \rfloor -1$ where $\mathfrak{g}_{\Sigma_L}, \mathfrak{g}_{\Sigma_U}$ are given by $\mathfrak{sp}(M_L), \mathfrak{sp}(M_U)$, respectively. Tracking the Kodaira types along the -1 curves gives a stronger constraint depending on the types realizing neighboring gauge summands (particularly when N is even) via (2.13) using the raised intersection contributions given in Table 34. To simplify its statement, we consider the configuration

$$\begin{array}{ccc}
1_{\Sigma_1} \\
1_{\Sigma_2} & 4_{\Sigma} & 1_{\Sigma_3} \\
 & [\Sigma_4]
\end{array} \tag{4.11}$$

with types $T_{\Sigma_i} \sim \mathrm{I}_{n_i}^{n_s}$ and $T_{\Sigma} \sim \mathrm{I}_n^* \leftrightarrow \mathfrak{so}(N)$. Configurations are then constrained by $\tilde{d}_{\Sigma} = 4n$ via

$$4n \ge \left(\sum_{i} n_{i}\right) + \delta_{N,\text{even}}\left(\sum_{i} \delta_{n_{i},\text{odd}}\right). \tag{4.12}$$

This extends to restrictions on sub-configurations obtained by omission of terms corresponding to any removed outer curves (e.g. to also constrain 141).

⁵To provide a listing including all enhancements, the parameter restricting N in $\mathfrak{so}(N)$ gauge summands, namely 'maxNForInstar' should be set to allow $N \geq 24$ (i.e., by setting the value as at least 8 to allow $I_{n\leq 8}^*$) and the global symmetry I_n fiber maximum chosen accordingly via consultation of Table (6.1) of [21].

Here $[\mathfrak{g}_{\Sigma'}]$ can also be non-trivial. When $\mathfrak{g}_{\Sigma} \cong \mathfrak{so}(N_L)$ with $N_L \leq 9$, this summand is trivial with a single exception for $T_{\Sigma'} \sim I_3^{ns}$ and $N_L = 9$ allows $[\mathfrak{g}_{\Sigma'}] \cong \mathfrak{su}(2)$. If the -3 curve Σ_R has $\mathfrak{g}_{\Sigma_R} \cong \mathfrak{g}_2$, then $[\mathfrak{g}_{\Sigma'}]$ is trivial except again when $T_{\Sigma'} \sim I_3^{ns}$ and $N_L = 9$ allows $[\mathfrak{g}_{\Sigma'}] \cong \mathfrak{su}(2)$. The remaining enhancements appear as

$$(\mathbf{I}_{n_L}^*, \mathfrak{so}(N_L)) \quad (\mathbf{I}_n^{n_S}, \mathfrak{sp}(M)) \quad (\mathbf{I}_{n_R}^*, \mathfrak{so}(N_R))$$

$$(4.13)$$

with $10 \leq N_L \leq 24$ and $7 \leq N_R \leq 12$; note that $\lfloor n/2 \rfloor = M$ and that $7 + n_L + \delta_{N_L,even} = N_L$, where the Kronecker symbol is nonzero for even values of N_L . Values of N_R and n_R are related similarly. These cases have $[\mathfrak{g}_{\Sigma'}]$ trivial or of the form $\mathfrak{su}(N_T)$ with N_T constrained via a generalization of conditions from [16] obtained by type tracking which reads

$$4M + 2\delta_{n,2M+1} \ge N_L + N_R + 2N_T - 14 + (2\delta_{n,2M+1} - 1)(\delta_{N_L,\text{even}} + \delta_{N_R,\text{even}}).$$
(4.14)

• $414\cdots$: Quivers of this form support infinitely many enhancements, but enhancement of either -4 node to \mathfrak{f}_4 or $\mathfrak{e}_{\geq 6}$ is forbidden. Constraints here mirror those for 413. Again $[\mathfrak{g}_{\Sigma'}]$ obeys with (4.14). The summand $[\mathfrak{g}_{\Sigma'}]$ is essentially captured by gauging condition of [16] (which can be viewed as counting roots $\tilde{\Delta}_{\Sigma}$ needed for $I_{n_i}^{n_s}$ junctions requiring n_i vanishings). In the presence of a left neighboring -1 curve Σ_L (giving $\cdots 1_{\Sigma_L} 41 \cdots$) noting assignments to 141 are of the form $\mathfrak{sp}(M_1), \mathfrak{so}(N), \mathfrak{sp}(M_2)$ while $[\mathfrak{g}_{\Sigma}] \cong \mathfrak{sp}(M_3)$ with M_3 constrained by

$$N \ge M_1 + M_2 + M_3 + 8, (4.15)$$

with the corresponding term dropped for Σ_L absent. Similarly, the flavor summands which may appear from the -4 curve at the T-junction in 141 are constrained by

$$N \ge M_0 + M_1 + M_2 + M_3 + 8, (4.16)$$

where $\mathfrak{sp}(M_0)$ gives the gauge algebra along the upper -1 curve.

The gauging restriction on M of [16] for $\mathfrak{so}(N_L)$, $\mathfrak{sp}(M)$, $\mathfrak{so}(N_R)$ enhancements reading

$$4M \ge N_L + N_R - 16$$

naturally generalizes to constrain $[\mathfrak{g}'_{\Sigma}] \cong \mathfrak{su}(M')$ in $41_{\Sigma'}4$ via (4.14), noting that Kodaira type specification beyond the precision needed to determine the gauge content is essential.

• $412_{\Sigma_2}\cdots$: The discussion for 413 captures all details here except in cases with Σ_2 gaugeless or carrying $\mathfrak{su}(n)$. The $[\mathfrak{g}_{41}]$ restriction for $\mathfrak{so},\mathfrak{sp},\mathfrak{so}$ enhancements is again given by (4.14). We shall treat the remaining cases in three groups. The first features gaugeless Σ', Σ_2 . The second feature type III or IV. Both are quickly characterized

explicitly using the accompanying workbook by selecting small bounds for I_n and I_n^* fibers. The final group contains infinitely many enhancements with $\mathfrak{so}, \mathfrak{sp}, \mathfrak{su}$ gauge summands arising from $I_{n_L}^*, I_{n_M}^{n_s}, I_{n_R}^s$ assignments.

The latter are again governed by extension of [16] conditions on 412 gauging. We shall account for a triple of curves meeting Σ' with fibers of the types

Here $\mathfrak{g}_L \cong \mathfrak{sp}(N'_L)$ where N_L obeys the same restriction leading to condition (4.16) with the appropriate terms dropped in the absence neighboring curves, namely

$$N_L \ge N_L' + |n_M/2| + 8. (4.18)$$

The summand $\mathfrak{g}_R \cong \mathfrak{su}(N_R')$ must satisfy

$$2n_R \ge n_M + N_R'. \tag{4.19}$$

Finally, $[\mathfrak{g}_{M'}]$ maxima may be realized by a type $I_{m'}^*$ fiber giving $[\mathfrak{g}_{M'}] \cong \mathfrak{so}(M')$ with one of M' = 2m' + 8 or M' = 2m' + 7 and M' required to satisfy constraints on \tilde{d} along the -1 curve reading

$$n_M \ge n_R + m' + n_L + \delta_{n_M, \text{odd}}(\delta_{N_L, \text{even}} + \delta_{M', \text{even}}),$$
 (4.20)

or by a second type of potentially relatively maximal flavor summand with one of the forms $\mathfrak{su}(M')$ or $\bigoplus_{M'_k} \mathfrak{su}(M'_k)$ obeying $\tilde{d}_{\Sigma'}$ constraints (generalizing the maximal configurations for an I_n^{ns} fiber appearing in [21] to include multiple \mathfrak{su} curves and a single \mathfrak{so} curve) which reads

$$\sum_{k} M'_{k} \le 4 + n_{M} - n_{L} - \delta_{n_{M}, \text{odd}} (1 + \delta_{N_{L}, \text{even}}) - n_{R} . \tag{4.21}$$

One can check this implies that in all cases where m' is permitted to be non-negative and $n_M > 2$, the $\mathfrak{so}(M')$ summand is always the unique maximal global contribution from the -1 curve and when (4.20) requires m' < 0, instead the second type of summand gives the maximal contribution and does so when k = 1. When $n_M \leq 2$, a IV^s intersection is also permitted, which makes the analysis more involved and leads to multiple relative maxima for $[\mathfrak{g}_{\Sigma'}]$ under certain conditions, in particular when $n_M = 2$, $N_L = 9$ and $n_R = 1$ where these are $\mathfrak{so}(8)$ and $\mathfrak{su}(2) \oplus \mathfrak{su}(3)$ (the latter arising from I_2, IV^s).

4.4 21

Our treatment here is simplified by the fact that left attachments to $2_{\Sigma}1_{\Sigma'}$ can only begin with a -2 or -3 curve. Attachments to Σ' can result in many enhancements, in particular

when the curve attached is a -4, -3 or -2 curve. We shall proceed by determining the $[\mathfrak{g}_{21}]$ in cases without left attachment before returning to treat their presence. Observe that we have already treated 21m via Table 46 when $5 \le m \le 8$ or m = 12. We begin by reviewing these cases.

- $21(12)\cdots$: Here $[\mathfrak{g}_{21}]$ is trivial since Σ' must have type I_0 . Left attachments are hence irrelevant.
- 218 · · · or 217 · · · : An $\mathfrak{su}(2)$ flavor summand can arise from each of Σ, Σ' simultaneously provided $T_{\Sigma'} \sim I_1$ and $T_{\Sigma'} \sim I_0$. As we can read from Table 46 (providing identical data via replacement in the \mathfrak{e}_7 cases of the -6 curve with a -8 or -7 curve), for $[\mathfrak{g}_{21}] \cong \mathfrak{su}(2)$ with $\mathcal{T}_{21} \sim I_0, I_0$ or $\mathcal{T}_{21} \sim II, I_0$. Otherwise $[\mathfrak{g}_{21}]$ is trivial.
- $21m_{\Sigma_R} \cdots$ with $5 \leq m \leq 6$: All configurations for these quivers appear in Table 46. In all cases the rank of $[\mathfrak{g}_{21}]$ is bounded by 5. Enhancement of Σ_R to \mathfrak{e}_7 is covered by the above treatment for 217. When $\Sigma_R \leftrightarrow \mathfrak{e}_6$, non-trivial $[\mathfrak{g}_{\Sigma}]$ may arise depending on \mathcal{T}_{21} beyond the precision for gauge specification and $[\mathfrak{g}_{\Sigma}]$ may be trivial, $\mathfrak{su}(2)$, or $\mathfrak{su}(3)$. When m=5 and $\mathfrak{g}_{\Sigma_R} \leftrightarrow \mathfrak{f}_4$ specification of $[\mathfrak{g}_{21}]$ is sufficiently involved that we defer to Table 46 noting the bound $[\mathfrak{g}_{\Sigma}] \subset \mathfrak{sp}(4)$.
- $214_{\Sigma_R} \cdots$: Left attachments here can only yield (3)2214 or 3214. The highly constrained configurations on these quivers are treated in our Section 5.2 discussion for side-links. Right attaching links and further nodes do not affect the structure of $[\mathfrak{g}_{21}]$. The presence of Σ_R places strong restrictions on permitted enhancements since $\mathfrak{g}_{\Sigma_R} \cong \mathfrak{so}(N_R)$ requires $T_{\Sigma'}$ be gaugeless or type $I_{N_M}^{ns}$. The discussion of $[\mathfrak{g}_{\Sigma}]$ and $[\mathfrak{g}_{\Sigma'}]$ complements that for 412 and only involves conditions introduced there together a restriction on $[\mathfrak{g}_{\Sigma}]$ given by (4.22).
- The bare quiver 21: Infinitely many enhancements of the form \mathfrak{su} , \mathfrak{su} and \mathfrak{su} , \mathfrak{sp} realized by types $I_{n_L}^s$, $I_{n_R}^s$ and $I_{n_L}^s$, $I_{n_R}^{n_s}$, respectively, are permitted here. The main ingredient determining $[\mathfrak{g}_{21}]$ is the discussion for I_n fibers appearing [21]. There are finitely many remaining enhancements, though numerous. These are readily listed explicitly via the accompanying workbook (via rank bounds on I_n and I_n^* similar to those we detailed to 413.). We hence abbreviate their discussion here accordingly.

Let us first detail $[\mathfrak{g}_{\Sigma}]$ for the aforementioned infinite families. In \mathfrak{su} , \mathfrak{su} enhancements with $I_{n_L}^s, I_{n_R}^s$ realization, $[\mathfrak{g}_{\Sigma}]$ is of the form $\mathfrak{su}(n_M)$ where

$$2n_L > n_R + n_M. \tag{4.22}$$

This constraint also governs the contributions from the -2 curve in $\mathfrak{su}, \mathfrak{sp}$ enhancements realized by $I_{n_L}^s, I_{n_R}^{n_s}$.

Prescribing $[\mathfrak{g}_{\Sigma'}]$ is slightly more involved. Most relevant details appear in our treatment for 412. Consider the cases with such $\mathfrak{su},\mathfrak{su}$ enhancements. When $n_R \geq 3$, intersection with an $\mathfrak{so}(M)$ fiber is barred via non-minimality requirements. Resulting maxima are given by $\mathfrak{su}(n_{M'})$ terms with $8 + n_R + \delta_{6,n_R} \geq n_L + n_{M'}$. When

 $n_R \leq 2$ the $\mathfrak{su}(M')$ contributions are governed by the same conditions as the cases with $\mathfrak{su}, \mathfrak{sp}$ enhancements. The latter allow two possible forms for $[\mathfrak{g}_{\Sigma}]$ consisting of $\mathfrak{so}(M')$ and $\mathfrak{su}(M')$ summands. The former is maximal when permitted with M' > 8. These appear from a type $I_{m'}^*$ fiber having M' = 6 + 2m' or M' = 5 + 2m' (depending on monodromy) and must obey

$$4 + n_R \ge n_L + m' + \delta_{n_R, \text{odd}} (1 + \delta_{M', \text{even}}).$$

The $\mathfrak{su}(M')$ summands which may appear from a type $I_{M'}^s$ fiber are slightly more constrained than in the $\mathfrak{su},\mathfrak{su}$ enhancement cases. These obey

$$12 + n_R \ge n_L + M' + 4 + 2\delta_{n_R, \text{odd}}.$$

This leaves us to contend with finitely many remaining \mathcal{T}_{21} involving at least one of the types II, III, IV, or $I_{n\leq 4}^*$. When the latter occurs as T_{Σ} to give an enhancement of the form $\mathfrak{so},\mathfrak{sp}$ with gauge summands realized by types $I_{n_L}^*,I_{n_R}^{ns}, [\mathfrak{g}_{\Sigma'}]$ is governed by the maximal configurations discussed in [21] concerning type I_n^{ns} curves; these consist of $\mathfrak{so}(M'>8)$ flavor summands when permitted and otherwise involve only $\mathfrak{su}(N\leq 4)$ terms. We omit further discussion for the finitely many remaining \mathcal{T}_{21} since complete listings are quickly obtained via the accompanying workbook.

Let us now also briefly discuss consequences of left attachment to 21. All such attachments are via a -2 or -3 curve. The former leads to a short instanton link with further right attachments discussed in Section 5.3. Instead attaching a -3 curve is highly constraining as it gives a 32 subquiver; further right node attachments is discussed in 5.2. This leaves discussions for the quiver 321 and right attachments giving 3215, and 3213. The latter are detailed in Table 44 while 321 is discussed in Section 5.2.2.4 with all configurations captured via Table 14.

4.5 31

Left attachment of Σ_L to $3_{\Sigma}1_{\Sigma'}$ requires $1 \leq m_{\Sigma_L} \leq 2$. Right attachment of Σ_R is permitted for $2 \leq m_{\Sigma_R} \leq 6$. There are many enhancements of quiver involving such attachments and these often feature a rich global symmetry algebra structure making this perhaps the most non-trivial case. We begin by discussing $[\mathfrak{g}_{\Sigma}]$ in each of these contexts.

4.5.1 The -3 curve contributions

- · · · 231 · · · : Left attachment with $m_{\Sigma_L} = 2$ is highly constraining, as we can read from Table (4.1). Here $[\mathfrak{g}_{\Sigma}]$ is at most $\mathfrak{su}(2)$, with non-triviality requiring $\mathfrak{g}_{\Sigma} \cong \mathfrak{so}(7)$ rather than \mathfrak{g}_2 , the $T_{\Sigma'} \in \{I_0, I_1\}$, and $T_{\Sigma_L} \sim \text{III}$ rather than IV^{ns} .
- · · · 315 · · · and · · · 316 · · · : Right attachment with $5 \leq m_{\Sigma_L} \leq 6$ also places tight restrictions on the gauge and flavor summands from Σ . We can read from Table (4.9) that an $\mathfrak{su}(2)$ flavor summand $[\mathfrak{g}_{\Sigma}]$ may arise, but only if $m_{\Sigma_R} = 5$ and Σ_R is unenhanced (with \mathfrak{f}_4 algebra) while $\mathfrak{g}_{\Sigma} \cong \mathfrak{g}_2$. Any gauged left attachment again makes $[\mathfrak{g}_{\Sigma}]$ trivial.

- The bare base 31: This base permits a wide variety of enhancements and flavor symmetries detailed fully in Table 45. The structure of $[\mathfrak{g}_{\Sigma}]$ permits a condensed description. These summands are of the form $\mathfrak{sp}(N)$ for $N \leq 5$ except when \mathfrak{g}_{Σ} is given by $\mathfrak{so}(8)$ in which case $[\mathfrak{g}_{\Sigma}] \cong \mathfrak{sp}(1)^{\oplus n}$ for $n \leq 3$, where n is determined by $T_{\Sigma'}$. The value n=3 only occurs when $T_{\Sigma'} \sim I_0$; n=2 can arise when $T_{\Sigma'} \sim I_{1\leq k\leq 2}$; we have n=1 for $T_{\Sigma'} \sim I_{3}^{ns}$. For $\mathfrak{g}_{\Sigma} \in \{\mathfrak{su}(3), \mathfrak{f}_4, \mathfrak{e}_6, \mathfrak{e}_7\}$, instead $[\mathfrak{g}_{\Sigma}]$ is trivial. For $\mathfrak{g}_{\Sigma} \cong \mathfrak{g}_2$, we have $[\mathfrak{g}_{\Sigma}] \subset \mathfrak{sp}(1)$ with non-triviality precisely when Σ' is gaugeless. The remaining cases have $\mathfrak{g}_{\Sigma} \cong \mathfrak{so}(M)$ with $[\mathfrak{g}_{\Sigma}] \cong \mathfrak{so}(N)$ where N is determined by $\mathfrak{g}_{\Sigma'} \cong \mathfrak{sp}(N')$; for M=7, we have $N+N'\leq 2$; otherwise 1 and 1 is constrained by 1 and 1 is constrained by 1 and 1 is
- $\cdots 314_{\Sigma_R} \cdots$: The Σ_R attachment still allows enhancement Σ' which makes a full treatment somewhat involved. However, quivers containing 314 permit finitely many enhancements. Hence, all configurations are readily detailed via the accompanying workbook. Sub-enhancements along 31 are the subset of those for 31 allowing Σ_R and consequently $[\mathfrak{g}_{\Sigma}]$ can be read from Table 45 by confining to compatible enhancements conveniently detailed in [16]. These $[\mathfrak{g}_{\Sigma}]$ are bounded by $\mathfrak{sp}(1)$ for $\mathfrak{g}_{\Sigma} \cong \mathfrak{so}(9)$, by $\mathfrak{sp}(2)$ for those with $\mathfrak{g}_{\Sigma} \cong \mathfrak{so}(10 \leq N \leq 11)$, and by $\mathfrak{sp}(3)$ for $\mathfrak{g}_{\Sigma} \cong \mathfrak{so}(12)$, as follows by confining to the subset obeying convexity requirements on Σ' with minimally enhanced Σ_R neighbor having $\mathfrak{g}_{\Sigma_R} \cong \mathfrak{so}(8)$.
- $\cdots 313_{\Sigma_R} \cdots$: Details here are identical to the previous base except for freedoms introduced when we reduce \mathfrak{g}_{Σ_R} below $\mathfrak{so}(8)$. This reduction allows $[\mathfrak{g}_{\Sigma}] \subset \mathfrak{sp}(3)$ when $\mathfrak{g}_{\Sigma} \cong \mathfrak{so}(10 \leq N \leq 11)$ and $[\mathfrak{g}_{\Sigma}] \subset \mathfrak{sp}(4)$ for $\mathfrak{g}_{\Sigma} \cong \mathfrak{so}(12)$ with proper inclusions mandated by the condition for $\mathfrak{g}_{\Sigma} \cong \mathfrak{so}(N)$ having $[\mathfrak{g}_{\Sigma}] \cong \mathfrak{sp}(M)$ and $\mathfrak{g}_{\Sigma'} \cong \mathfrak{sp}(M')$ neighbors requiring $M + M' \leq N 7$. Details for all (of the finitely many) configurations are readily available via the accompanying workbook. Note that left attachment of $\Sigma_L \leftrightarrow \mathfrak{sp}(M_L)$ with $m_{\Sigma_L} = 1$ reduces $[\mathfrak{g}_{\Sigma}]$ according to $N 7 \geq M + M' + M_L$ with further reductions possible for even N dependent on the types realizing $\mathfrak{sp}(M')$, $\mathfrak{sp}(M_L)$ through introduction of Kronecker symbols for I_n^{ns} realizations having n odd via 4.24.
- 312 : The noble link $3_{\Sigma}1_{\Sigma'}2$ permits a large but finite number of enhancements. We can treat the bare quiver by listing all possible configurations via the accompanying workbook. Since this is a "noble link" and enhancements of containing links are strongly limiting, we shall content ourselves with explicit configuration listings for these links without loss of depth in our discussion for longer bases. Attachments on the right must begin with a -3 curve while those on the left attachments must begin with a -2 curve Σ_L . Contributions from $[\mathfrak{g}_{\Sigma}]$ are easily determined from T_{Σ_L} using subquiver 23 constraints of (4.1) while noting that reduction to trivial $[\mathfrak{g}_{\Sigma}]$ results for $T_{\Sigma'}$ \sim II or $T_{\Sigma'}$ gauged.
- · · · 131 · · · : Many of the large but finite number of enhancements on $1_{\Sigma_L} 3_{\Sigma} 1_{\Sigma'}$ feature multiple flavor symmetry maxima. Outer attachments Σ_a and Σ_b require $m_{\Sigma_i} \geq 3$ and $m_{\Sigma_a} = m_{\Sigma_b} = 3$ is forbidden (to blow-down consistently). As a result, features of

 $[\mathfrak{g}_{31}]$ for enhancements of 131 occurring in longer bases are captured by discussion in Section 5 while most 131 configurations are irrelevant except in discussion of the bare quivers 131 and 3131 for which we content ourselves with the availability of explicit workbook listings as in the previous case.

The largest family of enhancements for this base is of the form

$$\begin{bmatrix} 1_{\Sigma_1} \\ 1_{\Sigma_2} & 3_{\Sigma} & 1_{\Sigma_3} \end{bmatrix} \tag{4.23}$$

with types $T_{\Sigma_i} \sim I_{n_i}^{n_s}$ and $T_{\Sigma} \sim I_n^* \leftrightarrow \mathfrak{so}(N)$. The analog of (4.12) for these cases is relies on (6.73),(6.77) of [21] to obtain sharpening beyond bounds imposed by $\tilde{d}_{\Sigma} = 6 + 3n$, this being replaced instead by

$$\tilde{d}'_{\Sigma} \equiv \tilde{d}_{\Sigma} - (2 + \delta_{n,\text{odd}}) = 4 + 3n - \delta_{n,\text{odd}}.$$

to yield

$$4 + 3n - \delta_{n,\text{odd}} \ge \left(\sum_{i} n_{i}\right) + \delta_{N,\text{even}}\left(\sum_{i} \delta_{n_{i},\text{odd}}\right). \tag{4.24}$$

Analogous restrictions hold on sub-configurations obtained by omission of terms corresponding to removed outer curves (e.g. to also constrain 31).

4.5.2 The -1 curve contributions

We now discuss flavor summands from $31_{\Sigma'}$ arising via Σ' . We proceed through these cases for right attachments Σ_R which constrain these, starting with the largest values for m_{Σ_R} .

- $315\cdots$ and $316\cdots$: Here $[\mathfrak{g}_{\Sigma'}]$ is trivial for each enhancement.
- $314_{\Sigma_R} \cdots$: Non-trivial $[\mathfrak{g}_{\Sigma'}]$ requires $\mathfrak{g}_{\Sigma_R} \cong \mathfrak{so}(N_R)$. Compatible assignments appear as $\mathfrak{so}(N_L)\mathfrak{sp}(M)\mathfrak{so}(N_R)$ with $[\mathfrak{g}_{\Sigma'}] \cong \mathfrak{su}(N_T)$ having N_T constrained via T_{Σ_R} (beyond the precision to specify $\mathfrak{g}_{\Sigma_R}, \mathfrak{g}_{\Sigma_R}$) via (4.14).
- $313_{\Sigma_R} \cdots$: As for 314, enhancements of the form $\mathfrak{so}(N_L) \mathfrak{sp}(M) \mathfrak{so}(N_R)$, all have $[\mathfrak{g}_{\Sigma'}]$ obeying (4.14). The remaining enhancements have trivial $[\mathfrak{g}_{\Sigma'}]$ with the exceptions

and those obtained by reversing roles of Σ, Σ' .

• 312, 3123, 131, 31: Each of these cases permits finitely many enhancements and we can proceed by listing all possible configurations via the accompanying workbook. Since there are very few arrangements for 23, the configurations for 3123 are rather limited. Strong restrictions from context in longer bases limits the relevance of a discussion for the bare quivers 312 and 131, thus we leave details to explicit listings without loss of general structural insight.

4.6 22

We first discuss the infinite family of classical enhancements and conclude with the few remaining cases featuring non- $\mathfrak{su}(N)$ algebras. The only essential restriction for the classical enhancements of bases of the form $\cdots 222 \cdots$ is a condition which extends naturally to constrain flavor symmetries for such configurations. The extended condition reads

$$2N_M \ge N_L + N_T + N_R \tag{4.26}$$

for a subquiver of the form

$$\begin{array}{ccc} \mathfrak{su}(N_L) & \mathfrak{su}(N_M) & \mathfrak{su}(N_R) \\ 2 & 2 & 2 \\ & [\mathfrak{su}(N_T)] \end{array},$$

where the flavor symmetry contribution from the middle curve is indicated with brackets. Note that in the absence of a neighboring curve, the condition is that obtained by dropping the corresponding term N_j . In the case of a T-junction, an additional term appears and gives flavor contribution from the -2 curve at the junction of

$$\begin{array}{ccc} & & \mathfrak{su}(N_U) \\ 2 & & 2 \\ \mathfrak{su}(N_L) & \mathfrak{su}(N_M) & \mathfrak{su}(N_R) \\ 2 & 2 & 2 \\ & [\mathfrak{su}(N_T)] \end{array}$$

obeying

$$2N_M \ge N_L + N_T + N_R + N_U \ . \tag{4.27}$$

The remaining enhancements of the above quivers feature fiber types other than I_n .

These appear below along with global symmetry summands indicated.

2 2 (continued) : II II
$$\frac{\text{III/IV}^{ns} \quad \text{IV}^s}{\text{ISu}(3)]}$$

$$\frac{\text{IV}^s \quad \text{IV}^s}{\text{ISu}(3)]} \frac{\text{IV}^s}{\text{ISu}(3)]}$$

$$\frac{\text{III/IV}^{ns} \quad \text{I}^{*ns}_0}{\text{ISp}(3)]}$$

$$\frac{\text{III}}{\text{III}} \frac{\text{I}^{*ss}_0}{\text{ISp}(3) \oplus \mathfrak{sp}(1)]}$$

5 Flavor symmetry structure via "atomic" decomposition

Here we discuss the structure of 6D SCFT global symmetries with help from the "atomic" base decomposition (2.4) of [16]. Briefly, flavor symmetries only arise from curves near the tail ends of a base with the largest rank summands coming from side-links and short subquivers containing the few permissible -4 curves when either is present. The only exceptions are also the only bases for which decomposition summand and total rank bounds are absent, these having the form $(1)2\cdots 2$ or $(1)414\cdots 4(1)$. The latter are readily treated separately via the methods Section 4 using simple constraint equations.

This decomposition allows us to characterize flavor summands for each theory by way of contributions from each term in (2.4) upon fixing an enhancement, i.e., via summands $[\mathfrak{h}_{i,j}]$ in

giving total flavor symmetry $\mathfrak{g}_{GS}\cong \oplus_{i,j}\mathfrak{h}_{i,j}$, with $\mathfrak{h}_{i,j}$ depending on the enhancement. To

achieve this, we simply detail contributions from each link with node attachment(s) which can appear in a base. Let us begin with an abbreviated summary of this approach and its results.

For linear bases, global symmetry summands arise only near the tail ends of multi-node bases with the exception of those for which the only nodes are -4 curves. This follows from our discussions in Sections 5.1.1,5.1 together with the permitted chains of nodes classified in Appendices B,C of [16] obeying the algebra inclusions of (5.48) from [16] requiring that gauge summands \mathfrak{g}_i from the nodes g_i obey

$$\mathfrak{g}_1 \subset \mathfrak{g}_2 \subset \cdots \subset \mathfrak{g}_m \supset \cdots \supset \mathfrak{g}_k$$
 (5.2)

This containment property implies that subquivers with -4 curves only occur towards the periphery of a base. The classification of node chains places severe limits the number of such nodes. (In the presence of any other node type, at most eight can occur; in nearly all node chain families, far fewer are permitted.) This means that determining flavor symmetries arising for a typical base is achievable in practice via classification of contributions from: (i) interior-link node pairings (Section 5.1), (ii) side-links attachments (Section 5.2), and (iii) instanton-link attachments (Section 5.3).

Flavor summands for theories with a linear base have all rank r_i contributions from curves Σ_i such that $r_i > 1$ arising in subquivers where the only nodes (if any) are -4 curves on the base periphery (via (5.2)) when any $\mathfrak{e}_{\geq 6}$ gauge summands are present. The total contributions arising from an interior link L_i joining nodes having gauge summands \mathfrak{g}_L and \mathfrak{g}_R are severely constrained. In fact, we have

$$\mathfrak{g}_{L} \qquad \mathfrak{g}_{R} \qquad [\mathfrak{h}_{i,r}] \subset \\
\mathfrak{e}_{\geq 7} \qquad \mathfrak{e}_{\geq 7} \qquad 0 \\
\mathfrak{f}_{4}/\mathfrak{e}_{6} \qquad \mathfrak{f}_{4}/\mathfrak{e}_{\geq 6} \qquad \mathfrak{su}(2) \\
\mathfrak{so}(N_{L}) \qquad \mathfrak{f}_{4}/\mathfrak{e}_{\geq 6} \qquad \mathfrak{su}(2) \\
\mathfrak{so}(N_{L}) \qquad \mathfrak{so}(N_{R}) \qquad \mathfrak{su}(2)^{\oplus 3} \text{ or } \mathfrak{sp}(2) \quad \text{for } L_{i} \not\sim 1 ,$$
(5.3)

with precise specification depending on the enhancement as detailed shortly and summarized in (5.3), (5.7) and (5.9)–(5.11). Flavor summands from g_i are trivial for $g_i \neq 4$ and $\mathfrak{g}_i \ncong \mathfrak{so}(N)$; for $g_i = 4$ we have $[\mathfrak{h}_{i,l}] \subset \mathfrak{sp}(4)$ unless $L_i = L_{i-1} = 1$ where $\mathfrak{sp}(M) \cong [\mathfrak{h}_{i,l}]$, M > 4 summands can appear, as detailed Section 5.1.1. The tight constraints on the number of D-nodes in node chains featuring any E-nodes as classified in Appendices B,C of [16] together with our interior chain, side-link and interior-link node attachment contribution treatments readily yield bounds on the flavor symmetries arising for all enhancements of each base not permitting infinitely many enhancements (i.e., excluding (2)(1)414··· and (1)222··· and their branching variants), in most cases determining them precisely with little effort up to treating side-link summands.

Note that explicit listing via the accompanying workbook is also computationally feasible in practice except with very large numbers of nodes for which supplementing outer subquiver results using interior link contributions summands detailed here suffices as a practical route. Enhancement listings even for long quivers are typically computationally inexpensive. Side-link flavor summand maxima detailed here or readily computed in isolation with designated node attachment allow extending to the general case. (In fact, all enhancements and these maxima for every side-link with node attachment can be quickly listed.) Side-link enhancement matching on overlaps with nodes allows lookup enabling a practical method for arbitrary base treatment even for arbitrarily large bases. Assisted by the long and short base classifications of [16] Appendix C, global symmetries for all 6D SCFTs classified therein are thus readily determined. The number of side-links which can attach to certain bases is somewhat large, so for expository purposes we shall stop short of providing explicit listings for each short and long base, instead contenting ourselves with having provided a route making their explicit computation feasible.

5.1 Interior links with node attachments

Since the structure of any 6D SCFT base consists of a linear quiver with decoration possible only near the ends, a key ingredient in a general characterization of SCFT flavor symmetries is a treatment for linear bases consisting of an interior link with a pair of outer node attachments. In the following subsections we determine global symmetry contributions for such subquivers.

5.1.1 Interior of linear base flavor contribution summary

We shall proceed by treating each interior link with a pair of outer node attachments. The left-right symmetrization of rules below applies, i.e., rules for node pairs follow upon reversing the link orientation. We tacitly exclude the single -1 curve link as the only permitted node attachments are -4 curves yield the $414\cdots$ quivers already treated in Section 4. Our statements here hold for cases with a node bounding each side of an interior link, which shall also remain implicit. We shall refer to the flavor symmetry contribution from the left and right portion of each quiver by $[\mathfrak{g}_L]$ and $[\mathfrak{g}_R]$, respectively.

 \bullet Attachment of a node n to the interior link

```
\alpha \in \{12231513221, 1223151321, 122315131, 12231\}
```

forming $n\alpha \sim n_{\Sigma} 1_{\Sigma'} \cdots$ for $n \geq 7$ or $\mathfrak{g}_{\Sigma} \cong \mathfrak{e}_{\geq 7}$ requires $[\mathfrak{g}_L]$ is trivial, while an unenhanced n = 6 node has $[\mathfrak{g}_L] \cong [\mathfrak{g}_{\Sigma'}] \cong \mathfrak{su}(2)$.

• Right attachment of a curve with $m \geq 6$ to

```
\alpha \in \{1223151321, 122315131, 13151321, 1315131, 12321, 12231, 1321, 131\}
```

leaves $[\mathfrak{g}_R]$ trivial.

• Left attachment of Σ with $m_{\Sigma} = 4$ to an interior link α when \mathfrak{g}_{Σ} is among $\mathfrak{f}_4, \mathfrak{e}_{\geq 6}$ yields trivial $[\mathfrak{g}_L]$ with two exceptions: (i) an \mathfrak{f}_4 attachment to α of the form $13_{\Sigma}1\cdots$

with assignment

allowing $[\mathfrak{g}_{\Sigma}] \cong \mathfrak{su}(2)$, (ii) $\alpha \sim 1$, i.e., for 41 when $[\mathfrak{g}_{4_{\Sigma}1}] \subset \mathfrak{g}_2$ with precise specifications in (4.4).

• Left attachment of a -4 curve Σ with $\mathfrak{so}(N \geq 9)$ gauge assignment to an interior link of the form $1_{\Sigma_L} 3_{\Sigma_M} 1_{\Sigma_R} \cdots$ requires $[\mathfrak{g}_{\Sigma_L}] = [\mathfrak{g}_{\Sigma_M}] = 0$ with the exceptions: (i) non-trivial $[\mathfrak{g}_L]$ as indicated for the sub-enhancements

noting that all $T_{\Sigma_M} \not\sim I_3^{ns}$ which realize $\mathfrak{g}_{\Sigma_M} \cong \mathfrak{su}(2)$ (e.g. I_2) have $[\mathfrak{g}_{\Sigma_L}]$ trivial, and (ii) classical enhancements of 41314 which we cover separately. These are simply governed by (4.12), (4.14), (4.24).

Contributions from Σ when $T_{\Sigma_L} \sim I_0$ are $[\mathfrak{g}_{\Sigma}] \cong \mathfrak{sp}(M)$, where M = N-8. For N = 8, we have $[\mathfrak{g}_{\Sigma_M}]$ trivial unless Σ_L, Σ_R are gaugeless and $[\mathfrak{g}_{\Sigma_M}] \cong \mathfrak{su}(2)$ may occur for $\mathfrak{g}_{\Sigma} \cong \mathfrak{g}_2$. For $\mathfrak{g}_{\Sigma_L} \cong \mathfrak{sp}(M')$, maxima $[\mathfrak{g}_{\Sigma}] \cong \mathfrak{sp}(M)$ obey

$$M + M' \le N - 8. \tag{5.4}$$

For $T_{\Sigma_L} \sim I_{n'}^{ns}$ with n' odd and N even, (4.12)) gives the stronger constraint

$$M + M' < N - 9. (5.5)$$

• For $Q \sim \cdots 14141 \cdots$, $[\mathfrak{g}_Q]$ obeys (4.12),(4.14) and weaker simplified constraints (4.10) and (4.14) as discussed in Section 4.

We shall employ the notation from Section 5.2.1 of [16] for interior links via tracking induced blow-down counts to condense our summaries. For example, in place of an interior -1 link, we write \oplus . Recall this notation for the remaining interior links reads

By substituting node gauge summands while suppressing their self-intersections, the above abbreviates to refine (5.3) as

where D indicates any permitted $\mathfrak{so}(N \geq 8)$ node, D^+ an $\mathfrak{so}(N \geq 8)$ or \mathfrak{f}_4 node, and E_n^+ an E_n or \mathfrak{f}_4 node. We now extend the above shorthand to treat link enhancements by labeling forced T_i (or \mathfrak{g}_i when unambiguous) while unlabeled positions remain a priori unconstrained. We denote minimally (non-minimally) enhanced links via an ' \sim ' (' $\not\sim$ ') symbol. For example,

We have the following abbreviated summary.

$$\begin{array}{c} \stackrel{3,3}{\bigcirc} \leftrightarrow 1315131 \quad \text{E-to-E pairings:} \qquad \qquad \left[\mathfrak{h}_{i,r}\right] \qquad \qquad \left[\mathfrak{h}_{i,t}\right] \\ E_6^+ \mathop{\bigcirc}_{\mathfrak{C}_6}^{3,3} E_6 \qquad \qquad 0 \qquad \qquad 0 \\ \mathfrak{so}(8)/\mathfrak{f}_4 \mathop{\bigcirc}_{\mathfrak{So}}^{3,3} \mathfrak{so}(8)/\mathfrak{f}_4 \qquad \qquad 0 \qquad \qquad 0 \\ \mathfrak{so}(8)/\mathfrak{f}_4 \mathop{\mathfrak{g}_2-}_{\mathfrak{So}} \mathcal{E}_6 \qquad \qquad \mathfrak{su}(2) \qquad \qquad 0 \\ \mathfrak{so}(8)/\mathfrak{f}_4 \mathop{\mathfrak{g}_2-}_{\mathfrak{So}} \mathcal{E}_6 \qquad \qquad \mathfrak{su}(2) \qquad \qquad 0 \\ \mathfrak{so}(8)/\mathfrak{f}_4 \mathop{\mathfrak{g}_2-}_{\mathfrak{So}} \mathcal{So}(8)/\mathfrak{f}_4 \qquad \qquad \mathfrak{su}(2)^{\oplus 2} \qquad \qquad 0 \\ \end{array}$$

The remaining D-to-D node pairings via \bigcirc are more easily characterized using decomposition about the -5 curve as detailed above.

The remaining $\overset{2,2}{\oplus}$ D-to-D node pairings are characterized by (4.12),(4.14),(4.24) with complete listings available via the auxiliary workbook.

5.2 Side-links with a node attachment

We shall break our discussion of these cases into two parts. The first concerns determining flavor symmetry contributions arising on the inner side-link curves and the second those appearing from outermost curves. We shall tacitly exclude instanton-links from being considered as side-links, instead addressing these in Section 5.3. We also separate our discussion of two particular cases: 413 (discussed in Section 4) and 4131. Each permits finitely many enhancements and is readily treated via direct listings supplied by the accompanying workbook. We hence treat the remaining cases with statements requiring modification when applied to instanton-links and side-links 13 and 131 attached to -4 curves.

5.2.1 Contributions from non-outermost curves of side-links

For each curve Σ in a non-instanton side-link with node attachment, $[\mathfrak{g}_{\Sigma}]$ is highly limited except when Σ is "outermost curve," i.e., one having a single compact neighbor. Even these typically have $[\mathfrak{g}_{\Sigma}]$ trivial unless $m_{\Sigma} = 1$. Non-outermost curve contributions typically obey

 $[\mathfrak{g}_{\Sigma}] \subset \mathfrak{su}(2)$ and are always among $\mathfrak{su}(2)^{\oplus k \leq 3}$, $\mathfrak{su}(N \leq 4)$, or $\mathfrak{sp}(2)$ when non-trivial (upon the aforementioned tacit exclusion of 13 and 131 from our discussion).

We now detail all non-trivial non-outermost curve flavor symmetry contributions. Note that having excluded instanton-links from our discussion rules out non-trivial $[\mathfrak{g}_{\Sigma'}]$ for example from $m_{\Sigma}1_{\Sigma'}$ when $\mathfrak{g}_{\Sigma} \cong \mathfrak{e}_{>7}$.

- E^+ linking curve contributions: In $m_{\Sigma} 1_{\Sigma'} r_{\Sigma_R} \cdots$ with $\mathfrak{g} \cong \mathfrak{e}_{k \geq 6}$, $[\mathfrak{g}_{\Sigma'}]$ is trivial unless k = 6 and Σ_R is gaugeless when $[\mathfrak{g}_{\Sigma'}] \cong \mathfrak{su}(2)$ can arise. When instead $\mathfrak{g}_{\Sigma} \cong \mathfrak{f}_4$, we have $[\mathfrak{g}_{\Sigma'}] \cong \mathfrak{su}(N \leq 3)$ with N = 3 requiring $T_{\Sigma_R} \sim I_{l \leq 1}$; For $T_{\Sigma_R} \sim II$, $N \leq 2$. For Σ_R gauged, $[\mathfrak{g}_{\Sigma'}]$ is trivial. In particular, this allows non-trivial $[\mathfrak{g}_L]$ in $E_{k \geq 6}^+ \alpha$ only when $\alpha \sim 1223 \cdots$.
- Interior \mathfrak{g}_2 curve contributions: The subquiver $13_{\Sigma'}1$ occurs in many links and permits $\mathcal{T}_{131} \sim \text{II}, I_0^{*ns}, \text{II}$ in many contexts. These curves may support $[\mathfrak{g}_{\Sigma'}] \cong \mathfrak{su}(2)$. This accounts for many of the non-trivial contributions in longer bases.
- D-node linking curve contributions: Since we are not treating the cases 41, 412 and 413 here and instead focusing on longer side-links, $[\mathfrak{g}_{\Sigma'}]$ in $\alpha \sim 41_{\Sigma'} \cdots$ for the remaining cases is limited to one of: (i) For $[\mathfrak{g}_{\Sigma'}] \cong \mathfrak{su}(2)$, we must have $\mathcal{T} \sim I_1^{*ns}, I_3^{ns}, I_0^{*ns} \cdots$ or $\mathcal{T} \sim I_1^{*s}/I_1^{*ns}, I_0$,III (relevant in links beginning as 413 and 412, respectively), (ii) $[\mathfrak{g}_{\Sigma'}] \cong \mathfrak{su}(3)$ for $\mathcal{T} \sim I_0^{*s}, I_0$,III (applicable in $412 \cdots$).

5.2.2 Outermost curve contributions

To treat the outer curves of a side-link, it will be helpful to separate our discussion of such curves with m=1. The remaining cases contribute small summands and are easily characterized.

5.2.2.1 Outer curves with $m \geq 2$

- $\cdots 23_{\Sigma}$: Side-links of this form with $\mathcal{T}_{23} \sim \text{III}, I_0^{*ss}$ permit $[\mathfrak{g}_{\Sigma}] \cong \mathfrak{su}(2)$.
- $\cdots 13_{\Sigma}$: Here instead $\mathcal{T}_{13} \sim \text{II}, I_0^{*ns}$ permits $[\mathfrak{g}_{\Sigma}] \cong \mathfrak{su}(2)$. This is supported on many links ending as $\cdots 513$.
- $\cdots 5_{\Sigma}1_{\Sigma'}2$: Since Σ' must be gaugeless and left attachments require $\mathfrak{g}_{\Sigma} \cong \mathfrak{f}_4$, the \mathfrak{f}_4 compatible enhancements of 512 appearing in Table 46 determine $[\mathfrak{g}_{512}]$ for the side-links of interest.

5.2.2.2 Outer curves with m=1

We begin by treating the outermost -1 curves bordering a -5 curve. With two exceptions we shall discuss shortly for the links

these are the only outer -1 curves which can arise off the linear portion of a link, instead bordering a -5 curve T-junction. Such curves can give rise to $\mathfrak{su}(3)$ or \mathfrak{g}_2 flavor summands, the latter requiring Kodaira type II along the -1 curve. At most two type II curves are permitted to meet a -5 curve as discussed in Section 3.1.2.1. Since links with a -5 curve bearing a T-junction often require type II curves on each side of the junction (e.g. those with linear portion having truncation of the form 2315132), only an $\mathfrak{su}(3)$ contribution is typically possible from the outermost -1 curves branching from the linear portion of a link away from its ends. When the T-junction is in the outermost (penultimate) position, however, a \mathfrak{g}_2 summand may appear from (typically at most one of) these outermost -1 curves. All possible configurations such inner and outer T-junctions appear in Table 10.

Interior T-junctions				
Extension T innetions	· · · 1	$ \begin{bmatrix} \mathfrak{su}(3)] \\ 1 \\ I_0 \\ 5 \\ IV^{ns} \end{bmatrix} $	1	
Exterior T-junctions		[(0)]		
	· · · 1	$ \begin{array}{c} [\mathfrak{su}(3)] \\ 1 \\ I_0 \\ 5 \\ IV^{ns} \end{array} $	1 II	$[\mathfrak{g}_2]$
	···1	$\begin{bmatrix}\mathfrak{su}(3)]\\1\\I_0/I_1\\5\\IV^{ns}\end{bmatrix}$	${1\atop I_0/I_1}$	$[\mathfrak{su}(3)]$
	$\cdots _{\mathrm{I}_{0}}^{1}$	$\begin{bmatrix} \mathfrak{g}_2 \\ 1 \\ \text{II} \\ 5 \\ \text{IV}^{ns} \end{bmatrix}$	1 II	$[\mathfrak{g}_2]$

Table 10. −5 curve T-junction flavor symmetry contributions from links.

The remaining outermost -1 curve contributions from side-links with a node attachment arise in $\cdots 21$ and $\cdots 31$.

5.2.2.3 Outermost -1 curves in $\cdots 31$

We begin with treating the two special cases noted above in which such a -1 curve can appear over a -3 curve T-junction.

• $2\overline{3}21$: This link L permits \mathfrak{e}_6 and \mathfrak{e}_7 node attachments. Both result in the same \mathcal{T}_L with the only non-trivial flavor summand arising from the outer -1 curve. The same essential details persist for \mathfrak{f}_4 attachments. All configurations are among

• $2_{\Sigma_L} 3_{\Sigma_M} 1_{\Sigma_R}$: The only node Σ which may attach to this link α has $m_{\Sigma} = 4$, as required for blow-down consistency. Further attachment to Σ is similarly barred making our discussion irrelevant for longer bases. We condense it accordingly while providing enough detail to illustrate a few subtleties. Gauge enhancements of α are highly constrained by the subquiver 23 allowing only $\mathfrak{su}(2)$, $\mathfrak{so}(7)$ and $\mathfrak{su}(2)$, \mathfrak{g}_2 enhancements of (4.1) from which we read that $T_{\Sigma_L} \in \{\text{III}, \text{IV}^{ns}\}$, the latter possible only in select \mathfrak{g}_2 cases.

Enhancing to $\mathfrak{g}_{\Sigma} \cong \mathfrak{f}_4$ requires $\mathfrak{g}_{\Sigma_M} \cong \mathfrak{g}_2$ and $T_{\Sigma_U} \sim I_0$ since $T_{\Sigma_R} \sim II$; this yields $[\mathfrak{g}_{\Sigma_U}] \cong \mathfrak{so}(8)$. In the remaining cases, $\mathfrak{g}_{\Sigma} \cong \mathfrak{so}(N \leq 13)$. For N=8, the maximum $[\mathfrak{g}_{\Sigma_U}] \cong \mathfrak{so}(8)$ requires $T_{\Sigma_R} \sim I_0$. When $\mathfrak{g}_{\Sigma_M} \cong \mathfrak{g}_2$, the maximum $[\mathfrak{g}_{\Sigma_U}] \cong \mathfrak{f}_4$ requires $T_{\Sigma_U} \sim II$; this is reduced to $[\mathfrak{g}_{\Sigma_U}] \cong \mathfrak{su}(4)$ when $T_{\Sigma_U} \sim I_1$, in turn demanding $T_{\Sigma_L} \sim IV^{ns}$ and $T_{14} \sim I_0, I_0^{*s}$. For N>8, we have $\mathfrak{g}_{\Sigma_M} \cong \mathfrak{so}(7)$; the above completes all \mathfrak{g}_2 cases with those remaining having $T_{\Sigma_L} \sim III$. This in turn requires $T_{\Sigma_R} \sim I_{n\leq 3}^{ns}$, and T_{Σ_U} constrained by n (since $d_{\Sigma_U} + d_{\Sigma_R} \leq 3$) with $[\mathfrak{g}_{\Sigma_U}]$ then determined from compatible pairs $T_{\Sigma_U}, T_{\Sigma_R}$ via Table 11.

Note that an $\mathfrak{su}(2)$ flavor summand can also arise from Σ_M in $\mathfrak{so}(7)$ cases with $d_{\Sigma_U} + d_{\Sigma_R} \leq 1$. Non-trivial $[\mathfrak{g}_{\Sigma}]$ may also arise when $N \geq 10$ (and $[\mathfrak{g}_{\Sigma}] \subset \mathfrak{sp}(4)$), as can non-trivial $[\mathfrak{g}_{\Sigma_R}] \subset \mathfrak{su}(2)$ provided $T_{\Sigma_R} \sim I_3^{ns}$ and $\mathfrak{g}_{\Sigma_M}, \mathfrak{g}_{\Sigma} \sim \mathfrak{so}(7), \mathfrak{so}(9)$. For N = 13, the maximum for $[\mathfrak{g}_{\Sigma}]$ is $\mathfrak{sp}(4)$. For N = 12, this becomes $\mathfrak{sp}(3)$ for $T_{\Sigma_R} \sim I_2$ and $\mathfrak{sp}(2)$ for $T_{\Sigma_R} \sim I_3^{ns}$. For N = 11, these T_{Σ_R} cases instead yield $\mathfrak{su}(2) \oplus \mathfrak{sp}(2)$ and $\mathfrak{sp}(2)$, respectively; these become $\mathfrak{su}(2)$ and trivial summand, respectively, for N = 10.

Type on Σ	Compatible types on Σ'	GS summand maxima from Σ
III	I_0	$\mathfrak{su}(2) \oplus \mathfrak{so}(7)$
		$\mathfrak{sp}(3)$
I_3^{ns}	I_0	$\mathfrak{su}(3)^{\oplus 3}$
		$\mathfrak{so}(13)$
		$\mathfrak{su}(2) \oplus \mathfrak{su}(6)$
		$\mathfrak{su}(3) \oplus \mathfrak{su}(5)$
I_2	I_0	$\mathfrak{so}(12)$
		$\mathfrak{su}(2) \oplus \mathfrak{su}(3)^{\oplus 2}$
		$\mathfrak{su}(2) \oplus \mathfrak{su}(5)$
II	I_0	\mathfrak{g}_2
${ m I}_1$	$ m I_0/I_2$	$\mathfrak{so}(9)$
		$\mathfrak{su}(3)^{\oplus 2}$
		$\mathfrak{su}(3) \oplus \mathfrak{su}(2)^{\oplus 2}$
I_0	$ m I_0/I_2/I_3^{ns}$	$\mathfrak{so}(8)$

Table 11. -1 curve T-junction flavor symmetry contributions for $2\overset{1}{3}1_{\Sigma'}4$.

A similar case merits mention with those above, that for 1231, a left-attachment permitting link. The structure of enhancements and flavor symmetries here follows at once from our discussion since this is simply a rearrangement of the curves in the first case above obtained by swapping the outer -2 and -1 curves. Details are thus also captured by (5.13).

Having concluded discussion of the special cases involving T-junctions at a -3 curve, we now turn to the cases involving linear $\cdots 31$ terminations. We begin with a few cases meriting separate discussion as they have highly constrained enhancement structure.

• ··· 5131 : There are many links of this form permitting left node-attachment. Since the -5 curve requires a gaugeless neighbor and the \mathfrak{e}_8 gauging condition applies to the neighboring curve, the resulting configurations are highly limited. In fact, there are only two possible configurations for the inner curves and we can easily detail the resulting outer -1 curve flavor summand possibilities in each case as in Table 12. Note that an $\mathfrak{su}(2)$ flavor summand may arise from the -3 curve in precisely the cases when it has a pair of gaugeless neighbors and Kodaira type \mathfrak{I}_0^{*ns} .

Type on Σ_a	Type on Σ_b	Type on Σ_c	GS summand maxima from Σ_c
\mathcal{I}_0^{*ns}	II	IV^{ns}	$\mathfrak{g}_2\oplus\mathfrak{su}(3)$
			$\mathfrak{sp}(2)$
		I_3^{ns}	$\mathfrak{so}(13)$
		III	$\mathfrak{so}(7) \oplus \mathfrak{su}(2)$
			$\mathfrak{sp}(3)$
		I_2	$\mathfrak{so}(12)$
		II	\mathfrak{f}_4
		I_1	$\mathfrak{su}(4)$
		I_0	$\mathfrak{so}(8)$
IV^s	I_0	I_0	\mathfrak{e}_6

Table 12. -1 curve flavor symmetry contributions for $\cdots 51_{\Sigma_a} 3_{\Sigma_b} 1_{\Sigma_c}$.

- $\cdots 2_{\Sigma_a} 3_{\Sigma_b} 1_{\Sigma_c}$: Since the subquiver 23 again severely restricts assignments on $\alpha \sim 231$, we can easily list all configurations for links of this form along with $[\mathfrak{g}_{\Sigma}]$ (as shown in Table 13), these being all flavor summands from α except for $\mathfrak{su}(2)$ contributions from Σ_b when $T_{\Sigma_b} \sim I_0^{*ss}$ while $T_{\Sigma_c} \in \{I_0,I_1\}$. Note that left attachment of an $\mathfrak{e}_{\geq 6}$ node to 12231 allows only those configurations with Kodaira type assignments IV^{ns},I_0^{*ns} to the subquiver 23.
- $\mathfrak{g}131$: One can confirm via the comprehensive link listing appearing in Appendix D of [16] that the only remaining link allowing a left node to attach and $\cdots 31$ right termination is $\alpha \sim 131$ (as all remaining links feature terminations $\cdots 5131$ or $\cdots 231$). We now work through the permitted node attachments to α while noting that only nodes carrying $\mathfrak{so}(N)$ or \mathfrak{e}_6 are permitted by the \mathfrak{e}_8 gauging condition. The unique configuration when carrying \mathfrak{e}_6 is

$$\mathfrak{e}_6 \quad \underset{I_0}{\overset{\mathfrak{su}(3)}{1}} \quad \underset{IV^s}{\overset{\mathfrak{su}(3)}{3}} \quad 1 \quad [\mathfrak{e}_6] , \qquad (5.14)$$

and the unique flavor symmetry contribution from $n\alpha$ is also \mathfrak{e}_6 .

We abbreviate our discussion for $\mathfrak{so}(N)$ attachments since explicit listing for each of the finitely many allowed configurations of this type captures all relevant details and is available from the listing provided for 4131 via the accompanying workbook.

Type on Σ_a	Type on Σ_b	Type on Σ_c	GS summand maxima from Σ_c
III	I_0^{*ss}	I_3^{ns}	$\mathfrak{so}(13)$
		III	$\mathfrak{so}(7) \oplus \mathfrak{su}(2)$
			$\mathfrak{sp}(3)$
		I_2	$\mathfrak{so}(12)$
		II	$\mathfrak{sp}(3)^{'}$
			\mathfrak{g}_2
		${ m I}_1$	$\mathfrak{so}(9)$
			$\mathfrak{su}(3)^{\oplus 2}$
			$\mathfrak{su}(3) \oplus \mathfrak{su}(2)^{\oplus 2}$
		I_0	$\mathfrak{so}(8)$
$\mathrm{III}/\mathrm{IV}^{ns}$	I_0^{*ns}	II	\mathfrak{f}_4
	-	I_1	$\mathfrak{su}(4)$
		I_0	$\mathfrak{so}(8)$

Table 13. –1 curve flavor symmetry contributions for $\cdots 2_{\Sigma_a} 3_{\Sigma_b} 1_{\Sigma_c}$.

5.2.2.4 Outermost -1 curves in $\cdots 21$

The only curves permitting \mathfrak{e}_7 and \mathfrak{e}_8 global symmetry summands are of this form. We proceed through the forms for endings of such links.

• \cdots 3221: The unique flavor symmetry maximum arising from the outer -1 curve of such links is \mathfrak{e}_8 . The type assignments on these curves must appear as

• \cdots 2321: The unique flavor symmetry maximum arising from the outer -1 curve of any such link with a node attachment is \mathfrak{e}_7 . Configurations for these links simply appear as

- 1321_{Σ_R} . This link permits left attachment to a -4 curve Σ provided $\mathfrak{g}_{\Sigma} \cong \mathfrak{so}(8)$. All curves give trivial flavor summand except Σ_R which has $[\mathfrak{g}_{\Sigma_R}] \cong \mathfrak{e}_7$.
- · · · 51321: Links of this form permit various maximal global symmetry summands to arise from the outermost curve depending on the Kodaira types realizing the unique gauge assignment. All assignments are of the form

$$\cdots \quad \underset{\mathrm{IV}^{ns}}{5} \quad \underset{\mathrm{II}}{1} \quad \underset{I_0^{*ns}}{3} \quad \underset{T_2}{2} \quad \underset{T_1}{1} \quad [\mathfrak{g}] \ ,$$

where $[\mathfrak{g}]$ is determined from T_1, T_2 via Table 14.

• $\cdots 3_{\Sigma_a} 2_{\Sigma_b} 1_{\Sigma_c}$: Now that we have treated the special cases above with constrained gauge summands, we move to the general case which essentially merges the others. We

Type on Σ_2	Types on Σ_1	GS summand maxima from Σ
III	I_0	\mathfrak{e}_7
IV^{ns}	I_0	\mathfrak{e}_6
IV^{ns}	${ m I}_1$	$\mathfrak{su}(7)$
		$\mathfrak{su}(N) \oplus \mathfrak{su}(M), \ N+M=8, \ N\geq 2$
		$\mathfrak{so}(11)$
IV^{ns}	II	\mathfrak{f}_4
		$\mathfrak{sp}(2)^{\oplus}2$

Table 14. -1 curve flavor symmetry contributions for $\cdots 5132_{\Sigma_2}1_{\Sigma_1}$.

again read the three assignments for 32 from Table (4.1). Permitted $[\mathfrak{g}_{\Sigma_c}]$ appearing when $T_{\Sigma_b} \sim \mathrm{I}_0^{*ns}$ follow from Table 14. When instead $T_{\Sigma_b} \sim \mathrm{I}_0^{*ss}$, we follow the above discussion for $\cdots 2321$. Note that we have also now discussed all enhancements of the bare quiver 321. The remaining links not in the above special case groupings are (3)1321. These are quickly handled by short explicit workbook enabled listings.

5.3 Instanton-links with a node attachment

In this section we detail the flavor symmetry contributions which can arise from instanton-links joined to nodes. Since the attachments of instanton-links to a -4 curve are limited in longer bases other than (2)1414··· to have at most a single curve, we confine our analysis to $\mathfrak{e}_{\geq 6}$ nodes as Section 4.3 treats 41 and 412; this only 4122, which is treated by Sections 4.3,4.6 (in particular, by (4.12), (4.20), (4.21), (4.27), (4.29) and (4.30)). Such attachments cannot occur in bases with more than one node. Hence, their treatment does not affect our discussion of more elaborate bases. Note that instanton-link attachments to a -5 curve Σ must have length $l \leq 4$ with this becoming $l \leq 2$ for Σ an interior curve, the latter hence covered by Table 46 while we relegate $l \geq 3$ cases to workbook listings as these are structurally similar to the \mathfrak{e}_6 attachments treated explicitly here.

5.3.1 Gaugeless instanton links

We begin by discussing the flavor symmetry contributions from a gaugeless instanton-link $\alpha \sim \Sigma_1 \Sigma_2 \cdots$ attached to an \mathfrak{e} -type node $\Sigma_0 \leftrightarrow \mathfrak{g}_0$ with self-intersection $-m_0$. The permitted \mathcal{T}_{α} appear in Table 15.

The flavor summands $[\mathfrak{g}_i]$ which can arise depend on \mathcal{T}_{α} and \mathfrak{g}_0 . We will proceed by moving through each \mathfrak{g}_0 option. We first treat instanton-links having at least three curves before returning to discuss a few exceptions to the following rules for short instanton-links.

- $\mathfrak{g}_0 \cong \mathfrak{e}_8$: In this case, all flavor summands $[\mathfrak{g}_i]$ are trivial.
- $\mathfrak{g}_0 \cong \mathfrak{e}_7$: Only $[\mathfrak{g}_1]$ can be non-trivial. Assignments featuring type II curves give all $[\mathfrak{g}_i]$ trivial, while the others allow $[\mathfrak{g}_1] \cong \mathfrak{su}(2)$.
- $\mathfrak{g}_0 \cong \mathfrak{e}_6$: Again, only $[\mathfrak{g}_1]$ can be non-trivial. For the last type assignment form above, non-trivial $[\mathfrak{g}_1] \subset \mathfrak{su}(2)$ can arise. Those without type II curves each can allow $[\mathfrak{g}_1] \cong \mathfrak{su}(3)$.

$$m_0 \quad -1 \quad -2 \quad \cdots \quad -2$$

$$\mathfrak{g}_0 \quad I_0 \quad I_0 \quad \cdots \quad I_0$$

$$[\mathfrak{g}_1] \quad \cdots \quad [\mathfrak{g}_k]$$

$$\mathfrak{g}_0 \quad I_0 \quad I_1 \quad \cdots \quad I_1$$

$$[\mathfrak{g}_1] \quad \cdots \quad [\mathfrak{g}_k]$$

$$\mathfrak{g}_0 \quad I_0 \quad I_1 \quad \cdots \quad I_1$$

Table 15. All possible gaugeless instanton-link type assignments permitting attachment to an ε-type node for links with at least three curves.

 $|\mathfrak{g}_1|$

To treat the short instanton-links having length $l \leq 2$, we can simply extract these configurations from (4.4) and Table 46, the former directly treating l = 1. For l = 2 these simply obey the following.

- $\mathfrak{g}_0 \cong \mathfrak{e}_8$: In this case, $[\mathfrak{g}_2] \cong \mathfrak{su}(2)$ may arise for second and third type assignment forms above.
- $\mathfrak{g}_0 \cong \mathfrak{e}_7$: For the second type assignment form above, $[\mathfrak{g}_{i>0}] \cong \mathfrak{su}(2)$ may are yielding an $\mathfrak{su}(2)^{\oplus 2}$ flavor summand from α . The only non-trivial contribution which may arise for the third form above appears as $[\mathfrak{g}_2] \cong \mathfrak{su}(2)$.
- $\mathfrak{g}_0 \cong \mathfrak{e}_6$: The summands which can arise in the three cases for link type assignment forms are $[\mathfrak{su}(3), 0], [\mathfrak{su}(3), \mathfrak{su}(2)],$ and $[\mathfrak{su}(2), \mathfrak{su}(2)],$ respectively.

Note that for l=1, allowed values of $[\mathfrak{g}_1]$ are simply the maximal complementary Lie subalgebras of \mathfrak{g}_0 in \mathfrak{e}_8 .

5.3.2 Gauged instanton links

In this section we consider an \mathfrak{e}_q node attached to an instanton-link $\Sigma_1 \cdots \Sigma_k$ carrying any non-trivial gauge summand. We will break our discussion into two parts. The first concerns "classical enhancements" of the form

The second addresses enhancements involving any other Kodaira type, these being confined among types II, III, IV, and I_0^* .

5.3.2.1 Classical enhancements of an instanton link with node attachment

While we have already characterized flavor summands which can arise in subquivers of this form via characterizations for 12 and $22 \cdots 2$ in Section 4, we pause here to make a few comments. First note that \mathfrak{e} -node attachment requires $T_{\Sigma_0} \sim I_0$ and this imposes \mathfrak{g}_{Σ_1} is a

subalgebra of $\mathfrak{su}(3)$, $\mathfrak{su}(2)$, and n_0 in the cases for attachment to \mathfrak{e}_6 , \mathfrak{e}_7 , and \mathfrak{e}_8 , respectively. Strong restrictions \mathcal{T}_{α} follow via propagation of constraints along the link.

The possible $[\mathfrak{g}_{\alpha}]$ for various classical enhancements are subalgebras of those for a particular enhancement with $n_1 \leq n_2 \leq \cdots \leq n_k$. Convexity conditions for these enhancements as detailed in [16] follow from the rules of Section 4 and require that for these chains with increasing arguments of $\mathfrak{su}(n_i)$ algebras with k > 2 and i > 1 we have $n_{i+1} - n_i = m_q$, where $n_1 = m_q \leq 9 - q$.

The aforementioned maximal $[\mathfrak{g}_{\alpha}]$ yielding configuration among all enhancements of $\mathfrak{e}_q \alpha$ with q fixed has n_1 chosen to allow m_q and consequently n_k as large as possible. The resulting $[\mathfrak{g}_{\alpha}]$ appears as

$$\mathfrak{e}_{q} \stackrel{\mathbf{I}_{0}}{-1} \stackrel{\mathbf{I}_{n_{1}}^{s}}{-2} \stackrel{\mathbf{I}_{2n_{1}}^{s}}{-2} \cdots \stackrel{\mathbf{I}_{kn_{1}}^{s}}{-2} \cdots \stackrel{\mathbf{I}_{kn_{1}}^{s}}{-2} . \tag{5.16}$$

The remaining classical enhancements of the link are required via these convexity conditions for classical enhancements of chains of -2 curves to have n_i increasing to a maximal $n_{i_{\text{max}}}$ at some i_{max} and are non-increasing for $i > i_{\text{max}}$ with flavor summands appearing only from the curves immediately to the left of decreases and from the final -2 curve with ranks are governed by (4.26). Explicit workbook enabled listings of the permitted flavor summands for these remaining classical enhancements can be quickly procured.

5.3.2.2 Non-classical instanton-link enhancements with node attachment

In cases with any curve of the instanton-link having a Kodaira type other than I_n , every curve other than the -1 curve is prevented from having type I_n . These \mathcal{T}_{α} and \mathfrak{g}_i obey convexity conditions on d_i and $r_i \equiv \operatorname{rank}(\mathfrak{g}_i)$ reading

$$d_1 \le d_2 \le \dots \le d_m \ge d_{m+1} \ge d_{m+2} \ge \dots$$
 (5.17)

$$r_1 \le r_2 \le \dots \le r_m \ge r_{m+1} \ge r_{m+2} \ge \dots$$
 (5.18)

All possible forms for enhancements of instanton-links not of the form (5.16) with e-type node attachment appear in Table 16 with any flavor summands indicated. Intersection contribution tallying eliminates several possibilities which obey the required gauging and convexity conditions, e.g. \mathcal{T}_{α} beginning as II,III,IV. Trivial [\mathfrak{g}_1] results for $q \geq 7$ while q = 6 allows [\mathfrak{g}_1] $\cong \mathfrak{su}(2)$ provided T_{Σ_1} is gaugeless.

6 Gauging global symmetries

We now briefly discuss which flavor symmetries can be consistently gauged to yield a new SCFT, i.e., which 6D SCFT transitions result from promotion of a global symmetry subalgebra to a gauge summand. While room for additional gauging is permitted when we consider the theories coupled to gravity with a compact base (and furthermore that all continuous symmetries must then be gauged as argued for example in [26]), the permitted SCFT transitions resulting from global symmetry promotion are highly constrained and have not been

m_0 \mathfrak{g}_a	-1 I_0 $[\mathfrak{g}_b]$	-2 II	III	III			 III	$^{-2}$ II
\mathfrak{g}_a	I_0 $[\mathfrak{g}_b]$	II	IV^{ns}	IV^s			IV^s	${\rm IV}^{ns}/{\rm III}/{\rm II}$
\mathfrak{g}_a	I_0 $[\mathfrak{g}_b]$	II	III				III	$_{[\mathfrak{su}(2)]}^{\mathrm{III}}$
\mathfrak{g}_a	$\begin{bmatrix} \mathrm{I}_0 \\ [\mathfrak{g}_b] \end{bmatrix}$	II	IV^{ns}	IV^s			IV^s	IV^s $[\mathfrak{su}(3)]$
\mathfrak{g}_a	$[\mathfrak{g}_b]$	II	IV^{ns}	${\rm I}_0^{*ns}\\ [\mathfrak{sp}(2)]$	IV^{ns}	(II)		
\mathfrak{g}_a	$^{\mathrm{I}_{0}}_{[\mathfrak{g}_{b}]}$	II	IV^{ns}	$_{\left[\mathfrak{sp}(2)\right] }^{\mathrm{I}_{0}^{*ns}}$	$\mathrm{III}/\mathrm{IV}^{ns}$			
\mathfrak{g}_a	$^{\mathrm{I}_{0}}_{[\mathfrak{g}_{b}]}$	II	IV^{ns}	IV^s	IV^{ns}	(II)		
\mathfrak{g}_a	$^{\mathrm{I}_{0}}_{[\mathfrak{g}_{b}]}$	II	IV^{ns}	IV^{ns}	(II)			
\mathfrak{g}_a	$^{\mathrm{I}_{0}}_{[\mathfrak{g}_{b}]}$	II	IV^{ns}	${\rm I}_0^{*ns}\\ [\mathfrak{sp}(3)]$				
\mathfrak{g}_a	$^{\mathrm{I}_{0}}_{[\mathfrak{g}_{b}]}$	II	$IV^{ns} \\ [\mathfrak{su}(3)]$	II				
\mathfrak{g}_a	$^{\mathrm{I}_{0}}_{[\mathfrak{g}_{b}]}$	II	$[\mathfrak{g}_2]^{ns}$					
\mathfrak{g}_a	$[\mathfrak{g}_b]$	II	$_{\left[\mathfrak{su}(2)\right] }^{\mathrm{III}}$					
$\mathfrak{g}_a \cong \mathfrak{e}_{\leq 7}$:	Ι ₀	III	III				III	II
\mathfrak{g}_a	I_0	[su(2)] III	III				III	III
\mathfrak{g}_a	I_0	[su(2)] III	IV^s				IV^s	$[\mathfrak{su}(2)]$ IV^s
\mathfrak{g}_a	I_0	III	IV^s				IV^s	$[\mathfrak{su}(3)]$ III/IV^{ns}
\mathfrak{g}_a	I_0	III	${\rm I}_0^{*ns}\\ [\mathfrak{sp}(2)]$	$\mathrm{III}/\mathrm{IV}^{ns}$				
\mathfrak{g}_a	I_0	III	$ \begin{bmatrix} \mathfrak{sp}(2) \\ \mathfrak{I}_0^{*ss} \\ [\mathfrak{sp}(3)] \end{bmatrix} $	$\mathrm{III}/\mathrm{IV}^{ns}$				
\mathfrak{g}_a	I_0	III	$ \begin{bmatrix} \mathfrak{sp}(3) \\ I_0^{*ns} \\ [\mathfrak{sp}(3) \end{bmatrix} $					
\mathfrak{g}_a	I_0	III	$ \begin{bmatrix} \mathfrak{sp}(3) \\ \mathfrak{I}_0^{*ss} \\ \mathfrak{sp}(4) \end{bmatrix} $					
\mathfrak{g}_a	I_0	III	[sp(4)] II					
\mathfrak{g}_a	I_0	[su(2)] III	IV^{ns}					
$\mathfrak{g}_a\cong\mathfrak{e}_6$:								
$\mathfrak{g}_a = \mathfrak{t}_6.$	I_0	IV ^s [\$u(3)]	IVs				IVs	IV ^s [su(3)]
\mathfrak{g}_a	I_0	IV^{ns}	IV^s				IV^s	IV^s $[\mathfrak{su}(3)]$
\mathfrak{g}_a	I_0	$_{\left[\mathfrak{su}(3)\right] }^{\mathrm{IV}^{s}}$	IV^s				IV^s	IV ^{ns} (II) / II
\mathfrak{g}_a	I_0	IV^{ns}	IV^s				IV^s	${ m IV}^{ns}$ (II) / II
\mathfrak{g}_a	I_0	IV^{ns}	$_{[\mathfrak{sp}(2)]}^{\mathrm{I}_{0}^{*ns}}$	$\mathrm{III}/\mathrm{IV}^{ns}$				
\mathfrak{g}_a	I_0	IV^{ns}	IV^{ns}	(II)				

 ${\bf Table~16.~Non\text{-}classical~gauged~instanton\text{-}link~type~assignments~with~attachment~to~an~\mathfrak{e}\text{-}type~node}$ for links with at least three curves.

fully studied. In this section, we comment briefly on which of these transitions are visible within F-theory using a few tools we now have at our disposal.

As a first step, we will inspect the flavor symmetry maxima for single curve theories to examine when promoting global symmetry subalgebras to gauge summands carried on added neighboring curves results in at most reduced rank gaugings. Consider an SCFT base with a single compact component of the discriminant locus Σ with $\mathfrak{g}_{\Sigma} \equiv \mathfrak{g}_{M}$ along with a choice \mathfrak{g}_{GS} from among the geometrically realizable flavor symmetry maxima for such a theory. We now consider which other 6D SCFT bases with enhancement specified arise via promotion of a \mathfrak{g}_{GS} subalgebra to neighboring curve gauge summands yielding a configuration

this of course requiring that $\mathfrak{g}_L \oplus \mathfrak{g}_R \oplus \mathfrak{g}_U \subset \mathfrak{g}_{GS}$ (with terms omitted for absent neighboring curves in the first two cases). Note that the new base may have a different discrete U(2) subgroup Γ associated to it. We can of course study a variant of this approach by requiring Γ stays fixed or focus on the nature of permitted Γ transitions. We will instead focus on variants of the question whether $\widetilde{\mathfrak{g}}_{GS}$ can be made trivial while $\mathfrak{g}_L \oplus \mathfrak{g}_R \oplus \mathfrak{g}_U$ has smaller rank than \mathfrak{g}_{GS} , i.e., whether sub-maximal gauging can in fact occur. We will slightly refine this characterization since we often cannot gauge sufficiently many degrees of freedom via an SCFT transition to yield trivial $\widetilde{\mathfrak{g}}_{GS}$, as we now show.

6.1 Normal crossings constraints

As a preliminary step, we observe that the normal crossings condition barring three gauged neighbors from meeting a -1 curve provides many cases where all SCFT transitions fully gauging \mathfrak{g}_{GS} (or even any of its maximal subalgebras) away to neighboring curves is not possible. This includes all single curve enhancements of a -1 curve having global symmetry maxima with at least three summands since each neighboring curve can contribute at most one gauge summand. In particular, this restriction applies to the cases shown in Table 17 which we can read off from Table (6.1) of [21] with the further tightenings for type III and IV curves appearing above in Table 3.

Gauge algebra on Σ	Kodaira type	Flavor symmetry maxima
$\mathfrak{su}(2)$	III	$\mathfrak{so}(7) \oplus \mathfrak{so}(7) \oplus \mathfrak{su}(2)$
	IV^{ns}	$\mathfrak{g}_2\oplus\mathfrak{g}_2\oplus\mathfrak{su}(3)$
$\mathfrak{su}(3)$	IV^s	$\mathfrak{su}(3)^{\oplus 4}$
		$\mathfrak{su}(3)^{\oplus 2} \oplus \mathfrak{sp}(2)$
$\mathfrak{so}(8)$	I_0^{*s}	$\mathfrak{sp}(3) \oplus \mathfrak{sp}(3) \oplus \mathfrak{sp}(1)^{\oplus 3}$

Table 17. Selected single curve theories on a -1 curve permitting only sub-maximal gauging of flavor symmetry maxima to yield neighboring curve gauge summands for a valid SCFT base.

However, we note this restriction is not relevant in determining which theories can be eliminated for lack of a consistent gauging of global symmetries when considering compact bases and coupling to gravity. In that context, we may relax the positive definite adjacency

matrix condition to allow multiple -1 curves intersecting Σ , hence making full gauging of the flavor symmetries in these cases again plausible.

Having trimmed the types of restrictions we might seek to find more significant consequences, we move on and discard the above cases as a minor curiosity.

6.2 Global to gauge symmetry promotion and 6D SCFT transitions

As a next step towards addressing which flavor symmetries can be consistently gauged onto neighboring curves, we begin with an example where complete gauging is possible for a particular choice of resulting base, while other bases we can form result in a somewhat surprising loss of continuous degrees of freedom during gauging. Consider a -2 curve with gauge algebra $\mathfrak{so}(7)$. The unique flavor symmetry maximum for this single curve theory is $\mathfrak{g}_{GS} \cong \mathfrak{sp}(1) \oplus \mathfrak{sp}(4)$. While we are able to gauge the entire flavor symmetry and can even do so to yield an SCFT base, e.g. 221 with the configuration

$$\begin{array}{ccc} 2 & 2_{\Sigma} & 1 \\ (\mathrm{III},\mathfrak{su}(2)) & (\mathrm{I}_0^{*ss},\mathfrak{so}(7)) & (\mathrm{I}_8^{ns},\mathfrak{sp}(4)) \end{array},$$

we cannot do so for the base $\alpha \sim 22_{\Sigma}^2 2$, nor can we even gauge the neighboring curves in this base to obtain a maximal subalgebra of \mathfrak{g}_{GS} . Though a priori possible to give neighboring curves yielding a maximal Lie subalgebra of \mathfrak{g}_{GS} when comparing the number of neighbors and the collection of such subalgebras, an inspection of possible Kodaira type assignments to these curves reveals only sub-maximal gauging is permitted.

More surprisingly, the neighboring curve gauge summands together with the remaining global symmetries on Σ in the presence of these neighboring curves gives a sub-maximal sub-algebra $\mathfrak{g}_{GS} \oplus \mathfrak{su}(2)^{\oplus 3}$ of \mathfrak{g}_{GS} . In other words, the requiring gauging of \mathfrak{g}_{GS} to form this base gives a rank-reducing breaking of \mathfrak{g}_{GS} , as we now confirm. Consider that the neighboring -2 curves must have Kodaira type III for intersection with Σ . The resulting configuration appears as

$$(\text{III},\mathfrak{su}(2)) \\ 2 \\ (\text{III},\mathfrak{su}(2)) \\ (I_0^{*ss},\mathfrak{so}(7)) \\ [\widetilde{\mathfrak{g}}_{GS}]$$

and requires contributions to $(\tilde{a}, \tilde{b}, \tilde{d})_{\Sigma} \sim (\geq 4, \geq 6, 12)$ for the T-junction given by at least $(3, \geq 6, 9)$. As a result, the only symmetry bearing curve Kodaira types which can simultaneously intersect Σ are $I_{\leq 3}^{ns}$ and III. Further gauging of any remaining global symmetry is impossible due to adjacency matrix requirements on SCFT bases. The remaining global symmetry for the resulting base (which arises purely from Σ hence matching $\tilde{\mathfrak{g}}_{GS}$) together with the neighboring curve gauge summands form a sub-maximal algebra \mathfrak{g}_{max} of \mathfrak{g}_{GS} since

$$\widetilde{\mathfrak{g}}_{\mathrm{GS}} \oplus \mathfrak{su}(2)^{\oplus 3} \subset \mathfrak{su}(2)^{\oplus 4} \subset \mathfrak{su}(2)^{\oplus 5} \subset \mathfrak{g}_{\mathrm{GS}}.$$

We henceforth regard this phenomenon as our definition of sub-maximal gauging, i.e., when the sum of neighboring gauge and residual global symmetry algebras $\tilde{\mathfrak{g}}_{GS}$ along Σ are not maximal in \mathfrak{g}_{GS} . Observe that the discrete U(2) subgroup, Γ_2 associated to the original base with the single compact curve Σ is trivial, while that for the base in the above gauging, Γ_{α} is not. This suggests that the emergence of non-trivial discrete U(2) gauge fields may be an ingredient in determining permitted global symmetry gauging rules and hence a helpful tool in classifying 6D SCFT RG flows.

Considering this phenomenon more generally defines an interesting structure associating to each single curve flavor symmetry maximum the collection of relatively maximal algebras which can be gauged for given neighboring curves defining a base with discrete U(2) subgroup Γ . In other words, there is a distinguished class of Lie subalgebras for each of the flavor symmetry maxima with each member in this class of subalgebras associated to a discrete U(2) subgroup. Additional structure emerges since not all Γ associated permissible SCFT gauging transitions are shared for the distinct flavor maxima with fixed Kodaira type; furthermore, multiple Kodaira types in some cases may realize a given gauge algebra.

A broad survey of single curve gaugings appears in Table 18.

7 Conclusions and outlook

We have carried out a systematic investigation global symmetries for each 6D SCFT realizable in F-theory appearing in the classification of [16] and produced a tentative classification of the geometrically realizable global symmetries of these theories. The tools we have provided include an implementation of an algorithm enabling explicit listing of the Kodaira type realizations for each 6D SCFT gauge enhancement helping to complete the geometry to field theory "dictionary" for these theories. We have detailed the structure of global symmetries permitted via this algorithm in terms of the "atomic decomposition" of 6D SCFT bases from [16] and in terms of certain shorter chains which may occur enabling us to recast our findings via simple constraint equations for these symmetries in terms of the geometric realizations of each gauge theory, i.e., the Kodaira type assignments compatible with each gauge assignment.

This has eliminated certain CFTs detailed in the classification of [16] on geometric grounds and shown that the refined classification can be recast in purely geometric terms without appeal to anomaly cancellation. We have investigated the gauging of 6D SCFT global symmetries which yield transitions between SCFTs and found such gaugings can result in rank reductions. We have derived novel restrictions on Calabi-Yau threefold elliptic fibrations, carried out local analysis of nearly all permitted singular locus collisions, and found many local and global constraints on permitted collections of singular fiber degenerations for such fibrations. This provides steps towards a general analog of [38] by constraining singular fiber degenerations along chains of curves with arbitrary Kodaira types. Our approach strongly constrains the space of non-compact CY threefolds and makes explicit all potentially viable varieties of this type at finite distance in the moduli space meeting a transverse singular fiber collision hypothesis up to specification of non-compact singular fibers not associated to a non-abelian algebras (with this latter caveat easily removed by trivial adjustments in our algorithm).

g_{gauge} on Σ $m = 1$:	Туре	GS max.	Gaugable	Base(s)	Types	$\mathfrak{g}_{\mathrm{gauged}} \oplus [\widetilde{\mathfrak{g}}_{\mathrm{GS}_{\sum}}] \ \mathrm{max}(s)$	Sub-maximal
su(2)	I_2	$\mathfrak{so}(20)$	√	14	$(-)I_6^{*s}$		
			X	12	$ \begin{smallmatrix} [\mathrm{I}_3^s/\mathrm{IV}^s] \\ (-) & \mathrm{I}_3^{*ns} \end{smallmatrix} $	$\mathfrak{so}(13)^* \oplus \left[\mathfrak{su}(3)\right]^\dagger$	✓
					$\stackrel{[\mathrm{I}_3^{*s}]}{(-)\mathrm{IV}^s}$	$\mathfrak{su}(3) \oplus [\mathfrak{so}(14)]$	X
					$^{[\mathrm{I}_{7}^{s}]}_{(-)\mathrm{IV}^{s}}$	$\mathfrak{su}(3) \oplus [\mathfrak{su}(7)]^\dagger$	✓
					$ \stackrel{[\mathrm{I}_4^{*s}]}{(-)} \mathrm{III} $	$\mathfrak{su}(2) \oplus [\mathfrak{so}(16)]$	X
			X	12, 13	$\begin{matrix} [\mathbf{I}_N^{*s}] \\ (-) \mathbf{I}_M^{*s}, \\ N\!+\!M\!=\!2 \end{matrix}$	$\mathfrak{so}(2M+8) \oplus [\mathfrak{so}(2N+8)]$	X
					$ \begin{smallmatrix} [\mathbf{I}_N^{ns/ss}] \\ (-) & \mathbf{I}_M^{ns/ss}, \\ N+M=2 \end{smallmatrix},$	$\mathfrak{so}(2M+7) \oplus [\mathfrak{so}(2N+7)]$	✓
			X	312, 313	${\mathop{\rm I}\nolimits_N^{*s}(-)}{\mathop{\rm I}\nolimits_M^{*s},\atop N+M=2}$	$(\mathfrak{so}(2M+8)\oplus\mathfrak{so}(2N+8))^*$	X
	III	$\mathfrak{so}(7)^{\oplus 2} \oplus \mathfrak{su}(2)$	x!!	313, 213	$\mathbf{I}_0^{*ss}\overset{[\mathrm{III}/\mathrm{I}_2]}{(-)}\mathbf{I}_0^{*ss}$	$(\mathfrak{so}(7)^{\oplus 2})^* \oplus [\mathfrak{su}(2)]^{\ddagger}$	X
	IV^{ns}	$(\mathfrak{g}_2^{\oplus 2})^* \oplus \mathfrak{su}(3)$	x!!	313, 213	$\mathbf{I}_0^{*ns}\overset{[\mathbf{IV}^s/\mathbf{I}_3^s]}{(-)}\mathbf{I}_0^{*ns}$	$\mathfrak{g}_2^{\oplus 2} \oplus [\mathfrak{su}(3)]^{\ddagger}$	X
$\mathfrak{su}(3)$	IV^s	$\mathfrak{su}(3)^{\bigoplus 4}$	$X^{!!}$	12	$\stackrel{[3\mathrm{IV}^s]}{(-)}\mathrm{IV}^s$	$\mathfrak{su}(3)^* \oplus [\mathfrak{su}(3)^{\oplus 3}]^{\ddagger}$	X
		$\mathfrak{su}(3)^{\oplus 2} \oplus \mathfrak{sp}(2)$	x!!	12	$ \begin{array}{c} {}_{[\mathrm{I}_{3}^{s}/\mathrm{IV}^{s},\mathrm{I}_{4}^{ns}]} \\ {}_{(-)} \end{array} \mathrm{IV}^{s} $	$\mathfrak{su}(3)^* \oplus \left[\mathfrak{su}(3) \oplus \mathfrak{sp}(2)\right]^{\ddagger}$	X
$\mathfrak{so}(8)$	I_0^{*s}	$\mathfrak{sp}(3)^{\oplus 2} \oplus \mathfrak{sp}(1)^{\oplus 3}$	$\mathbf{x}^!$	12	$ \begin{array}{c} \left[2\mathbf{I}_{6}^{ns},\left(\mathbf{III/I_{2}/I_{3}^{ns}}\right)\right)\right] \\ (-) & \mathbf{III} \end{array} $	$\mathfrak{sp}(1)^* \oplus [\mathfrak{sp}(3)^{\bigoplus 2} \oplus \mathfrak{sp}(1)]^\dagger$	✓
$m = 2$: $\mathfrak{su}(3)$	IV^s	$\mathfrak{su}(3)^{\oplus 2}$	√	222	$IV^s(-)IV^s$		
4(0)		211(3)	· ✓	221	$IV^s(-)(I_3^s/IV^s)$		
		$\mathfrak{sp}(2)$	✓	21	$(-)I_4^s$		
			X	222	$(III/IV^{ns})(-)(III/IV^{ns})$	$\mathfrak{su}(2)\oplus\mathfrak{su}(2)$	X
$\mathfrak{su}(2)$	IV^{ns}	\mathfrak{g}_2	✓	23, 22, 21	$(-)I_0^{*ns}$		
				123	$(I_0/I_1/II)(-)I_0^{*ns}$		
				223, 222	$II(-)I_0^{*ns}$		
			X	222	$II(-)IV^s$	$\mathfrak{su}(3)$	✓
	III	so(7)	✓	23, 22, 21	$(-)I_0^{*ss}$		
	III	so(7)	✓	123, 122	$I_0(-)I_0^{*ss}$		
			X	222	$II(-)IV^s$	$\mathfrak{su}(3)^*$	✓
			X	222	$\mathrm{III}(-)\mathrm{III}$	$(\mathfrak{su}(2)^{\oplus 2})^*$	✓
$\mathfrak{so}(7)$	I_0^{*ss}	$\mathfrak{sp}(4) \oplus \mathfrak{sp}(1)$	✓	221	$III(-)I_8^{ns}$		
			X	222	$^{[\mathrm{I}_{6}^{ns}]}$ III $(-)$ III	$(\mathfrak{sp}(1)^{\oplus 2})^* \oplus [\mathfrak{sp}(3)]$	X
			X	$\begin{smallmatrix}2\\222\end{smallmatrix}$	$\underset{[\mathrm{III}/\mathrm{I}_{3}^{ns}]}{\overset{\mathrm{III}}{(-)}}\mathrm{III}$	$(\mathfrak{sp}(1)^{\oplus 3})^* \oplus [\mathfrak{sp}(1)]$	✓

Table 18. Selected gaugings of single curve SCFT GS maxima. Here '†' indicates that a GS factor is not gaugable onto any additional neighboring compact curve allowed in any SCFT base, '‡' the same due to the normal crossings condition, 'X!' that the GS (relative) maximum is not fully gaugable for any SCFT base, and 'X!!' the same due to the normal crossings condition. Here '*' indicates a relatively maximal gauging for the given base and '**' the same among all bases; unique gauging for a given base is indicated with an '*!' symbol.

We hope these tools prove useful in the classification of 6D RG flows and a complete classification of all 6D SCFTs. In particular, whether the multiple global geometrically

realizable global symmetry maxima which arise in many cases correspond to distinct theories (i.e., if there terms under which the global symmetries of F-theory models provide SCFT invariants) is a question we leave to future work. While the relations between gauge and global symmetries of 6D SCFTs with those of discrete U(2) gauge fields determining endpoints we have discussed are suggestive, we hope that additional investigation may help clarify the precise interplay between these ingredients determining the field content of these theories.

A Intersection contributions and forbidden pair intersections

In this appendix we extend the intersection contributions data collected in [21, 22] to include that for pairs of curves with A, B > 0 in which either curve may be compact. The lone exception to the latter concerns cases of non-compact transverse curves which carry no gauge-summand, namely those with Kodaira types I_0 , I_1 , or II. Such curves cannot contribute global symmetry summands and hence only require consideration in cases where the transverse curve can be compact component of the discriminant locus.

Before proceeding, we note that studying the contributions to curves with A>0 or B>0 from transverse gauged fibers was safely ignored in [21, 22] since for the theories treated in those works, the maximal flavor symmetry inducing configurations arise for a curve with fixed Kodaira type when A = B = 0. However, in treating flavor symmetries for more general SCFTs with a base consisting of more than a single compact curve, the minimal values of A, B along a given curve may be non-zero. For example the -1 curve in the base $(12)1_{\Sigma}2231513221(12)$ requires Σ here has type I_0 with $A_{\Sigma} \geq 4$. This minimum value of A_{Σ} along Σ depends significantly on the presence of non-neighboring curves, even those which do not affect the minimum gauging of the neighboring curves as illustrated in Table 19. This degree of "non-locality" is somewhat surprising: the quiver $(12)1_{\Sigma}22315$ requires the same minimum as $(12)1_{\Sigma}22315132$ given by $A_{\Sigma}=3$, while addition of the gaugeless type II curve of self-intersection -2 in the final position to yield $(12)1_{\Sigma}223151322$ raises this minimum to $A_{\Sigma} = 4$. By the same token, the only assignments of orders of vanishing along each curve of the quiver 1223151322 compatible with a left attachment of a non-compact II* fiber inducing the (unique) \mathfrak{e}_8 global symmetry maximum for this quiver have assignments to the -1 curve of the form $(A \ge 4, 0, 0)$.

Our approach stems in part from this subtlety that the minimal values of A, B are hence "global" in quiver position as illustrated by the above example. An exhaustive computer search approach to determining global symmetries beginning with assignment of orders of vanishing along each compact component of the discriminant locus followed by maximality checks of global symmetry subalgebras which may arise on transverse non-compact components thus naturally merits consideration of compact curves with A, B > 0 in addition to A = B = 0 cases. This in turn makes development of local models for all such intersections a natural first step.

We shall go somewhat further than required by developing the intersection contribution data from such local models for a somewhat broader class of intersections than actually arise in the minimal order assignments to SCFT bases. This approach has certain benefits. First, it allows us to be cavalier in assigning larger orders of vanishing and allowing automation to ensure we have not missed any global symmetry maxima inducing configurations which may require non-minimal A,B assignments. Furthermore, this allows us to more tightly constrain non-minimal A,B configurations which we hope may find application addressing codimension-two singularities and perhaps development of a framework which may come to bear on issues concerning the gauging of global symmetries beyond the scope addressed in this work.

Minimum value of A along Σ	Compatible subquiver(s)
0	(12)1
1	(12)12
2	(12)122
	(12)1223
	(12)12231
3	(12)122315
	(12)1223151
	(12)12231513
	(12)122315132
4	(12)1223151322
	(12)12231513221
	(12)12231513221(12)

Table 19. Minimum orders of vanishing of $f|_{\Sigma}$ for various subquivers of $(12)1_{\Sigma}2231513221(12)$ with compatible Kodaira type (and hence gauge) assignments given by truncations of the only viable assignment along this quiver, namely $II^*,I_0,II,IV^{ns},I_0^{*ns},II,IV^{*ns},II,I_0^{*ns},II,I_0^{*ns},II,I_0,II^*$.

Permitted A,B values in longer quivers are often highly constrained, sometimes allowing only a single globally consistent choice while locally in quiver position infinitely many cases are permitted. For example, the unique permitted values on the quiver 71231513221(12) are

while the subquiver 13221(12) permits infinitely choices of these values consistent with the Kodaira type assignments above.

In many cases, the allowed A, B values force particular gauge assignments. Consider for example the base 232. We can bypass anomaly cancellation machinery and more involved global analysis of the monodromy cover for I_0^* fibers by noting that the only orders of vanishing consistent with the naïve intersection contribution constraints of (2.11) leave the only configuration

$$\begin{array}{cccc} \text{(III,su(2))} & \text{($I_0^{*ss}, \mathfrak{so}(7)$)} & \text{(III,su(2)} \\ 2 & 3 & 2 \\ \text{($1,2+B_L,3$)} & \text{($2,3+B,6$)} & \text{($1,2+B_R,3$)} \end{array}, \tag{A.2}$$

where $B \geq 1$ requires that the I_0^* fiber is semi-split (as we can read from Table 25 along with the observation of A.6.2.1 that $\mathfrak{so}(8)$ would have required purely even \tilde{a} contributions), thus yielding an $\mathfrak{so}(7)$ gauge summand.

As an example yielding novel constraints, we consider the minimal left \mathfrak{f}_4 attachment compatible enhancement of the interior link 1321 with right \mathfrak{e}_7 -node attachment to a curve Σ with self-intersection -m having minimal orders of vanishing along each curve as indicated below.

Note that Σ_R must type I₀ since gaugeless curves with type other than I₀ lead to non-minimal intersection with a curve having III* fiber; $B_{\Sigma'} \geq 1$ follows immediately from the naïve residuals tallying requirements of (2.11). Provided that $5 \leq m_{\Sigma} \leq 7$, there is no inconsitency with $B_{\Sigma_R} = 1$. However, when m = 8, naïve intersection contributions of (2.11) from Σ_R to Σ rule out the configuration. Since additional orders of vanishing of \tilde{g}_{Σ_R} and \tilde{g}_{Σ} are coupled, i.e., $B_{\Sigma_R} \geq 1 + B_{\Sigma}$, any attempt to permit the required vanishings along Σ by raising B_{Σ} in turn raises B_{Σ_R} . However, this is not compatible with the indicated gauge assignment since it forces $B_{\Sigma_M} > 0$ and in turn $B_{\Sigma_L} > 0$, thus requiring an $\mathfrak{so}(7)$ gauge summand along Σ_M as we can read from Table 25. Further note that in these cases with $m_{\Sigma} = 8$, this further enhancement of Σ_L to $\mathfrak{so}(7)$ is unacceptable in the presence of a left \mathfrak{f}_4 attachment (which we can easily confirm via the \mathfrak{e}_8 gauging condition since $\mathfrak{so}(7) \oplus \mathfrak{f}_4 \not\subset \mathfrak{e}_8$).

We next consider the quiver 2231322 which minimally supports an assignment with Kodaira types leading to trivial contribution from the -1 curve (via "Persson's list" restrictions). When the Kodaira type on the -1 curve is raised to type II allowing the potential for a non-trivial flavor symmetry summand to appear there (which is a priori possible while maintaining the E_8 gauging condition since $\mathfrak{g}_2 \oplus \mathfrak{su}(2) \subset \mathfrak{f}_4$), we have the following assignment with the minimal orders along each curve required by (2.11) indicated below.

The only possible global symmetry can only occur from a type I_2 fiber. It hence is relevant in our analysis to determine the local models for intersections of curves with fibers of various Kodaira types having A, B > 0.

Before turning to a systematic analysis of all intersection contributions of potential relevance to constraining F-theory SCFT models, we begin with a simple example to demonstrate the method we follow to derive the intersection contribution data appearing in this section which in turn plays a key role in our algorithm to eliminate various gauge enhancements of quivers and possible global symmetry summand inducing non-compact transverse curve configurations. Additional examples confined to A = B = 0 cases following the same

approach can be found in [21, 22].

Since the A, B values which may appear in arbitrary configurations consisting of an SCFT base decorated with noncompact transverse curves are somewhat non-trivial to constrain $a\ priori$ and the results of a comprehensive analysis of intersection contributions for all permitted intersections of Kodaira fibers may find alternative uses in constraining elliptically fibered Calabi-Yau threefolds more generally, we shall tabulate intersection contributions for nearly all curve pairs (with the exceptions of -1, -1 intersections and gaugeless non-compact fibers which clearly do not arise in SCFT bases with non-compact global symmetry inducing fiber configurations), though many of the indicated intersections do not arise in minimal assignments for SCFT bases. These cases become relevant when we consider alternative settings allowing us to relax the positive definite adjacency matrix condition or the matter content dictated by which codimension two orders of vanishing may appear. Though we shall not carry out analysis of these features in this work, we hope that the tools devoloped here may facilitate their investigation.

A.1 Computing intersection contributions

We now detail an example illustrating the method underlying our approach to determining intersection contributions. Certain subtleties make some cases significantly more involved than illustrated in the following simple, but most relevant issues have been discussed at length in [21, 22]. A few further issues arise in treating compact pair intersections, as we shall discuss in various cases treated in this appendix.

As in the configuration above, we let Σ be a type II curve along $\{z=0\}$ with orders of vanishing given by (1+A,1,2)=(2,1,2) and Σ' a type I₂ curve along $\{\sigma=0\}$ (with orders of vanishing (0,0,2)). Let P denote the point of their intersection at $\sigma=z=0$. The general form for f,g,Δ of a type I₂ curve can be read from (A.8) of [21] as

$$f = -\frac{1}{48}\phi^{2} + f_{1}\sigma + f_{2}\sigma^{2} + O(\sigma^{3}) ,$$

$$g = \frac{1}{864}\phi^{3} - \frac{1}{12}\phi f_{1}\sigma + (\widetilde{g}_{2} - \frac{1}{12}\phi f_{2})\sigma^{2} + O(\sigma^{3}) ,$$

$$\Delta = \frac{1}{16}\left(\phi^{3}\widetilde{g}_{2} - \phi^{2}f_{1}^{2}\right)\sigma^{2} + O(\sigma^{3}) .$$
(A.5)

Imposing these divisibility conditions then yields

$$f = -\frac{1}{48}z^{2}\phi^{2} + z^{2}f_{1}\sigma + z^{2}f_{2}\sigma^{2} + O(z^{2}\sigma^{3}) ,$$

$$g = \frac{1}{864}z^{3}\phi^{3} - z^{3}\frac{1}{12}\phi f_{1}\sigma + (z\tilde{g}_{2} - z^{3}\frac{1}{12}\phi f_{2})\sigma^{2} + O(z\sigma^{3}) ,$$

$$\Delta = \frac{1}{16}z^{4} \left(\phi^{3}\tilde{g}_{2} - \phi^{2}f_{1}^{2}\right)\sigma^{2} + O(z\sigma^{3}) ,$$
(A.6)

where we have replaced ϕ/z , f_i/z^2 , \tilde{g}_2/z with ϕ , f_i , \tilde{g}_2 for simplicity of notation. We read the minimal orders of vanishing giving "intersection contributions" to Σ via the minimum σ -degrees of the lowest order terms in \tilde{f}_{Σ} , \tilde{g}_{Σ} , $\tilde{\Delta}_{\Sigma}$ (namely those of z-degrees 2, 1, 2, respectively, as required to match the z-orders along Σ) to obtain

$$(\tilde{a}_P, \tilde{b}_P, \tilde{d}_P)_{\Sigma} \ge (0, 2, 4). \tag{A.7}$$

Thus, the potential $\mathfrak{sp}(1)$ flavor symmetry summand appearing in (A.4) is impossible. Note this would have yielded a configuration with transverse curve algebras contained in the global symmetry maxima for a type II curve appearing in [22]. The contributions analysis therein does eliminate the configuration, but requires the above augmentation to produce the lowered \tilde{a}_P minimum indicated above.

A.2 Preliminaries

In the following sections, we let Σ be a curve at $\{z=0\}$ with $-\Sigma \cdot \Sigma = m$, having transverse intersections with curves Σ'_j located at $\{\sigma_j = 0\}$. Let the orders of vanishing along Σ be (a,b,d) and those along Σ'_j be given by (a'_j,b'_j,c'_j) .

A.3 Type II curve intersections

We introduce further constraints on collisions involving a Kodaira type II curve in A.7 for cases involving an I_n^* curve. Here we focus on the remaining non-trivial cases, those involving an I_n curve. Such collisions were studied at length in [22] when the I_n curve is non-compact and A = 0 along the type II curve. The tight restrictions we find in sections A.4,A.5 for type III and IV curves have only weaker analogues here. Underlying this distinction is that we are farther from non-minimality in II, I_n collisions and that as a consequence we are required to consider intersections where the most general form for the relevant local models of type I_n curves is unknown as these include the cases $7 \le n \le 9$.

We now proceed to make mild generalizations of the intersection contribution data first appearing in [22] that are required in the present work. Part of our work is dispatched by reading from Table 42 taken from [21] which states that $A \geq 3$ is not possible for intersections with I_n curves having $n \geq 4$, a bound we revise here since this only holds for non-compact I_n curves. The A = 0 results can be read directly from the contribution tables of [22]; in one case we find a small correction. This leaves us to determine the relevant contributions from compact I_n curves for all n, and non-compact curves only for $n \leq 4$. Since type II curves do not carry a non-abelian gauge algebra, we can safely ignore collisions of compact I_n curves with non-compact type II curves.

We collect intersection contributions for the remaining cases in Table 20. The '!' symbol there indicates disagreement with [22]. Entries marked with '†' are not permitted via the inductive form for I_n curves appearing as (A.25)-(A.28) in [21]. The '*' symbol indicates the contributions are only valid for a non-compact I_n curve, 'X.' that the intersection is valid only for non-compact I_n curve, and 'X..' that the intersection exceeds numbers of vanishings available for a type II curve even with m=1. Entries to the right of those indicated with an 'X', 'X.', 'X..' are similarly forbidden.

A.3.1 Intersection with an I_0^{*s} curve

The analysis for intersection of a type II curve with a transverse curve holding type I_0^{*s} in [22] bars such intersections but implicitly uses that B=0 along the I_0^{*s} curve, say Σ' , to obtain non-minimality of the intersection. Provided $B \geq 2$, such intersections are also non-minimal. However, in the special case that B=1 factorization of the monodromy is

$A = a - 1$ $n_{ns/s}$	0	1	2	3 ···		a-1
2	(1, 2, 4)		$\cdot (a \mod$	(2,2,4)(X. i)	$f A \ge 4) \cdots$	
3_{ns}	(1, 2, 4)	(0, 3, 6)	$(1,3,6)^*$	<i>Y</i>	$(a \mod 2, 3, 6)$	$(6)^*X.\cdots$
3_s	(2, 3, 6)	(2, 3, 6)	(2, 3, 6)	$\cdots (2(1 -$	$\delta_{4,a}$), 3, 6)(X	$A \geq 4$.
4_{ns}	(2, 4, 8)	(0, 4, 8)	$(2,4,8)^*\Sigma$	ζ. ··· (2	$2(a \mod 2), 4$	$(0,8)^*X.\cdots$
4_s	(2,4,8)!	(2,4,8)	$\cdots (2(1 -$	$\delta_{a,4}$), 4, 8)(2	$X. \text{ if } A \geq 4)^*$	
5_{ns}	(2,4,8)	$(0,5,10), (2,4,8)^*$	$(1,4,8)^*$	· · · (2	$(4,4,8)^*X$	
$(\geq 5)_s$	X					
6_{ns}	(2,4,8)	$(0,6,12), (2,4,8)^*$		$\cdots (2,4,8)$	*X	
7_{ns}	$(\le 3, \le 6, \le 12)$	X^{\dagger}				
8_{ns}	$(\le 4, \le 8, \le 16)^{\dagger} X^{\dagger}$					
9_{ns}	$(\le 4, \le 8, \le 16)^{\dagger} X^{\dagger}$					
$(n \ge 10)_{ns}$	$(\lfloor \frac{n}{2} \rfloor, 2\lfloor \frac{n}{2} \rfloor, 4\lfloor \frac{n}{2} \rfloor) X$					

Table 20. Intersection contributions to type II curve from a (non-compact*) I_n curve.

possible. We can read from (A.9) that intersection contributions to Σ are then given by $(2 + (a \mod 2), 4, 8)$ and contributions to I_0^{*s} curve are $(2\lceil a/2\rceil, 1, 4\lceil a/2\rceil)$.

A.4 Type III curve intersections

Let Σ be a curve with Kodaira type III and orders of vanishing (a, b, 3) = (1, 2 + B, 3). Suppose that Σ' has orders of vanishing (a', b', d'). Note Σ has odd type, making \tilde{d} contributions thrice those of \tilde{a} contributions. The only technical cases for such intersections concern transverse curves with type I_n or I_n^* . The latter are restricted for $n \geq 1$ due to non-minimality. We treat intersections with I_0^* curves in section A.6, focusing here on treating Σ' with type I_n in each case relevant to global symmetry computation, namely those involving at least one compact curve.

A.4.1 III, I_n intersections

A.4.1.1 Type III with $B \geq 0$ intersection with a non-compact type I_n curve

We now extend the contribution data for cases with B=0 analyzed in [21] to those with B>0. Reading from Tables A.1,A.2 of [21], we find values for the local intersection contributions to a III with B=0 and that the restriction that $B\geq 2$ requires $n\leq 3$ for non-minimality. We make a correction to this bound; the revisions appear in the appendices as Tables 42,41. First, we collect the results of contributions for intersections analyzed [21] and the remaining B>0 cases of contributions to a type III with m=1,2 from a non-compact transverse I_n curve in Table 21. Note that in the cases with $n\geq 7$, we compute contributions working from the inductive Tate forms for I_n curves from (A.25)-(A.28) of [21] that are potentially not the most general when $7\leq n\leq 9$. Here Σ has residuals given by (5,8+B,15) for m=1 and (2,4+2B,6) when m=2.

In Table 21, entries indicated with '*' are only valid for non-compact I_n curves and those with '†' are permitted only for I_n non-compact. Those entries with '!' correct Table A.2 of [21]. The symbol 'X' indicates a non-minimal intersection and entries to the right of an 'X' are also non-minimal. For m = 2, those entries with any contribution exceeding those allowed are forbidden; these are indicated with a subscript '1'.

B $n_{ns/s}$	0	1	2	3	•••	b-2
2_{ns}	(1, 1, 3)	(1, 0, 3)	(1, 1, 3)			$(1, b \mod 3, 3)$
3_{ns}	(2, 2, 6)	$(3,0,9)_1,(2,2,6)^*$	$(2,2,6)^*$	$(2,2,6)^{\dagger}$		$(2, 2, 6)^{\dagger}$
3_s	(2, 2, 6)	(2, 2, 6)	$(2,2,6)^{\dagger}$			$(2, 2, 6)^{\dagger}$
4_{ns}	(2,2,6)!	$(3,0,9)_1,(2,2,6)^*$	$(2,2,6)^{\dagger}$			$(2, 2, 6)^{\dagger}$
4_s	(2, 3, 6)	(2, 3, 6)	$(2,3,6)^{\dagger}$			$(2, 3, 6)^{\dagger}$
5_{ns}	$(3,3,9)_1$	$(3,0,9)_1$	X			
$(\geq 5)_s$	X					
6_{ns}	$(3,3,9)_1$	$(5,0,15)_1$	X			
$(10 \ge n \ge 7)_{ns}$	$(\lceil \frac{n}{2} \rceil, \lceil \frac{n}{2} \rceil, 3\lceil \frac{n}{2} \rceil)_1$	X	X			
$(\geq 11)_{ns}$	X					

Table 21. Intersection contributions to III from a (non-compact) I_n curve.

A.4.1.2 Type III with $B \ge 0$ and m = 2 intersection with a compact I_n curve with m = 1.

The only case of interest for III, I_n intersections with I_n compact arising in F-theory quivers involve a type III curve with m=2 since two -1 curves do not intersect in any valid base and m'=2 on Σ' with type I_n has $(\tilde{a},\tilde{b})=(0,0)$, thus preventing intersection with any type III curve. We collect the contributions for valid intersections in Table 22. For large n, it will be helpful in making our table succinct to define

$$q(n) = \begin{cases} 4 \text{ if } n \text{ is even} \\ 5 \text{ if } n \text{ is odd.} \end{cases}$$
 (A.8)

The table entries indicate the minimal intersection contributions to/from a Σ , a (compact unless marked with 'X') type III curve having orders (1,b,3) = (1,2+B,3) with m=2 transversely intersecting Σ' , a compact I_n curve with m'=1. Note the residuals on a (compact) type III curve with m=2 are (2,4+2B,6). Here, 'X'/'X.' indicate an intersection forbidden by the number of allowed vanishings along Σ/Σ' , respectively, and '-' a non-minimal intersection. Entries to the right of an '-', 'X', or 'X.' are similarly forbidden. Intersections corresponding to entries with an 'X' are permitted only for non-compact Σ .

B $n_{ns/s}$	0	1	2	3	4	≥ 5
1	(1,1,3)/(2,3,5)	(1,0,3)/(2,3,5)	$\dots (1, b \mod b)$		131'/	Χ.
2	(1,1,3)/(2,3,4)	(1,0,3)/(4,6,6),	(2,1,6)/(4,6,8)	(2,1,6)/(4,6,9)	(2,0,6)/(4,6,9)	X.
		(2,0,6)/(2,3,5)				
3_{ns}	(2,2,6)/(2,3,5)	X/(2,3,5)	X/X.			
3_s	(2,2,6)/(4,6,6)	(2,2,6)/(4,6,7)	_			
4_{ns}	(2,2,6)/(2,3,4)	X/(2,3,5)	X/X.			
4_s	(2,3,6)/(4,6,6)	(2,2,6)/(4,6,6)	_			
5ns	X/(2,3,5)	X/(2,3,5)	X/X.			
$(\geq 5)_s$	_					
6_{ns}	X/(2,3,4)	X/(2,3,5)	X/X.			
$(\geq 7)_{ns}$	X/(2,3,q(n))	X/(2,3,5)	X/X.			

Table 22. Intersection contributions for (compact m=2) type III, compact type I_n intersections.

A.4.1.3 Intersection contribution to a compact I_n curve with m=1 from a non-compact III with $B \geq 0$.

The remaining intersections of interest between type III and type I_n curves concern contributions to an I_n curve from a type III curve giving a global symmetry summand. The relevant contributions to the type I_n curves here are also given in Table 22, marked with an 'X' when we require the non-compactness (or m = 1 if we are not concerned with constructing an F-theory SCFT base but rather an F-theory base with gravity coupled) along the type III condition to hold.

A.5 Type IV curve intersections

Here we collect information about monodromy rules for type IV curves and intersection contributions involving transverse curves. The only subtle cases involve type I_n and I_0^* curves since I_n^* intersections with n > 0 results in non-minimality.

A.5.1 Preliminaries

Let Σ be a curve with type IV. Orders of vanishing are then given by (a, b, 4) = (2 + A, 2, 4). Note that Σ has even type. Reading from 2, we see the monodromy along Σ is determined by whether $\frac{g}{z^2}|_{\Sigma}$ is a square; the larger gauge algebra, $\mathfrak{su}(3)$, occurs if so.

A.5.2 Intersections of IV with I_n curves

A.5.2.1 IV with $A \ge 0$ meeting I_n curves for global symmetry or quiver intersections

This case is detailed in [21] when the transverse type I_n curves are non-compact and A = 0 along the type IV curve. These contributions appear with a minor correction for intersection with an I_3^{ns} fiber (which also holds for the compact pair case) in Table 41. We shall use these contributions for the compact pair case when A = 0 as then they remain unchanged for these type pairings; note that the actual minimal contributions must be modified from these table values (as they depend on monodromy along the IV curve) to give even \tilde{b} contributions to

the type IV in the IV^s case. From Table (6.1) of [21], we have that transverse I_n curves carry at most $\mathfrak{sp}(4)$ symmetry. Note that as indicated in Table 42, $n \leq 3$ is required when A > 0 for non-minimality. We collect the results of contributions to (and from when applicable) a type IV curve intersecting a type I_n curve for these remaining cases in Tables 23 and 24, separating the A = 0 case in which n > 3 is permitted.

$n_{(ns/s)}$ $A_{(ns/s)}$	2_{ns}	3_{ns}	3_s
1_{ns}	(1,2,4)//(4,6,8)	-/(1,3,6)	(1,3,6)/(1,2,4)//(4,6,8)
1_s	(1,2,4)//(4,6,8)	$-/(1,3,6)^*$	$(1,3,6)^*/(1,2,4)//(4,6,8)^*$
2_{ns}	(0,2,4)//(4,6,8)	-/(0,3,6),(1,2,4)	(0,3,6)/(1,2,4)//(4,6,8)
2_s	(0,2,4)//(4,6,8)	$-/(0,3,6)^*,(1,2,4)$	$(0,3,6)^*/(1,2,4)//(4,6,8)^*$
$A \ge 3_{ns}, \ 2 + A \in 4\mathbb{Z}$	-/ $(0,2,4)$	-/(0,3,6)/(1,2,4)	-/(0,3,6),(1,2,4)
$A \ge 3_{ns}, \ 2 + A \in 2\mathbb{Z} \setminus 4\mathbb{Z}$	-/ $(0,2,4)$	-/(0,3,6),(1,2,4)	-/(1,3,6),(1,2,4)
$A \geq 3_{ns}, A \notin 2\mathbb{Z}$	-/ $(1,2,4)$	-/(1,3,6)	-/(1,3,6),(1,2,4)
$A \ge 3_s, \ 2 + A \in 4\mathbb{Z}$	-/ $(0,2,4)$	$-/(0,3,6)^*/(1,2,4)$	$-/(0,3,6)^*, (1,2,4)$
$A \ge 3_s, \ 2 + A \in 2\mathbb{Z} \setminus 4\mathbb{Z}$	-/ $(0,2,4)$	$-/(0,3,6)^*/(1,2,4)$	$-/(1,3,6)^*,(1,2,4)$
$A \ge 3_s, A \notin 2\mathbb{Z}$	-/ $(1,2,4)$	$-/(1,3,6)^*$	$-/(1,3,6)^*,(1,2,4)$

Table 23. Intersection contributions to a (compact) IV^{ns/s} with A > 0 from//to a transverse compact/non-compact I_n curve (with 'to contributions' only when compact). An 'X' indicates the intersection is forbidden by non-minimality considerations and a '-' an intersection forbidden by residuals considerations. Here (*) indicates an intersection allowed only when m = 1 on IV via limitations of \tilde{b} on IV.

IV^{ns}/IV^s $n_{(ns/s)}$	$\mathfrak{su}(2)$	$\mathfrak{su}(3)$
2_{ns}	(0, 2, 4)	(0, 2, 4)
3_{ns}	(0,3,6),(1,2,4)	$(0,3,6)^*,(1,2,4)$
3_s	(1,3,6),(1,2,4)	$(1,3,6)^*,(1,2,4)$
$\geq 4_s$	X	X
4_{ns}	(0, 4, 8)	$(0,4,8)^*$
$9_{ns} > n \ge 5_{ns}$	$(0, n, 2n)^*$	$(0,2\left\lceil\frac{n}{2}\right\rceil,4\left\lceil\frac{n}{2}\right\rceil)^*$
$\geq 9_{ns}$	-	-

Table 24. Intersection contributions to $IV^{ns/s}$ with A=0 from a transverse non-compact I_n curve. An X indicates the intersection is forbidden by minimality considerations. Here (*) indicates a permitted intersection only when IV has m=1, and (-) an intersection \tilde{b} on IV forbids in all cases.

A.6 Type I_0^* curve intersections

Here we compile information about monodromy rules for I_0^* curves and intersection contributions to residuals counts involving transverse curves from an I_0^* curve.

A.6.1 Preliminaries

Let $\Sigma = \{\sigma = 0\}$ be a curve with type I_0^* and orders of vanishing (a,b,6) = (2+A,3+B,6). Suppose that $\Sigma' = \{z = 0\}$ is a transverse curve with orders of vanishing (a',b',d'). Recall that we refer to the cases with 2b' = 3a' as 'hybrid type', those with 2b' > 3a' as 'odd type' and those with 2b' < 3a' as 'even type'. The contributions to residual vanishings of Δ along Σ' from intersection with the transverse curve Σ are given by $3\tilde{a}$ and $2\tilde{b}$ in the odd and even type cases, respectively, where \tilde{a} and \tilde{b} are the residuals contributions to Σ' from a curve Σ for vanishings of f, g, respectively.

The monodromy along Σ is determined by whether $Q(\psi) = \psi^3 + (f/\sigma^2)|_{\{\sigma=0\}}\psi + (g/\sigma^3)|_{\{\sigma=0\}}$ is fully split (giving algebra $\mathfrak{so}(8)$), partially split (giving algebra $\mathfrak{so}(7)$), or irreducible (giving gauge algebra \mathfrak{g}_2).

A.6.1.1 Gauge algebra \mathfrak{g}_2 :

Here we can write the monodromy cover as $Q = \psi^3 + p\psi + q$, with Q irreducible.

A > **0**: In this case, Q becomes $\psi^3 + q$ with irreducibility implying that q is not a cube; otherwise, we could factor Q as $(\psi - \alpha)(\psi^2 + \alpha\psi + \alpha^2)$ with $q = -\alpha^3$. Since $q = (g/\sigma^3)|_{\sigma=0}$, we conclude that Σ cannot have intersections with curves Σ'_j with types $(-, 3b'_j, -)$ using all available g residuals along Σ . Said differently, $g = \sigma^3(\nu\phi^3 + g_4\sigma^4 + O(\sigma^5))$ with ν cube-free and deg $(\nu) > 0$.

 $\mathbf{B} > \mathbf{0}$: Here $Q = \psi(\psi^2 + p)$, and since this is not an irreducible cubic, this case is not possible.

A.6.1.2 Gauge algebra $\mathfrak{so}(7)$:

Since the cover is split in this case, $Q = (\psi - \alpha)(\psi^2 + \lambda \psi + \mu)$. Since the ψ^2 term vanishes, we have $\alpha = r$ and

$$Q = \psi^3 + (\mu - \lambda^2)\psi - \mu\lambda.$$

 $\mathbf{A} > \mathbf{0}$: This case requires $\mu = \lambda^2$, and hence $Q = \psi^3 - \lambda^3$. This means that Q is fully split since $\psi^2 + \lambda \psi + \mu = \psi^2 + \lambda \psi + \lambda^2$, which has discriminant $\lambda^2 - 4\lambda^2 = -3\lambda^2$, which indeed has a square root. We conclude this case is prohibited.

 $\mathbf{B} > \mathbf{0}$: In this case, $Q = \psi(\psi^2 + \mu)$, and that this is not fully split implies $\mu = (f/\sigma^2)|_{\sigma=0}$ is not a square. Hence, Σ cannot have intersections with curves of types $(2a'_j, -, -)$ using all f residuals along Σ and we conclude that Σ cannot receive purely even f intersection contributions using all f residual vanishings. Said another way, $f = \sigma^2(\mu\phi^2 + f_3\sigma + O(\sigma^2))$ with μ square-free and $\deg(\mu) > 0$. When m = 3, $\tilde{a} = 2$, but the form of f clearly bars even contributions to \tilde{a} since $\deg(\mu) > 0$. Hence, intersection with a type II curve with orders (2,1,2) is prohibited as are intersections with an I_0 with orders (2,0,0).

A.6.1.3 Gauge algebra $\mathfrak{so}(8)$:

The monodromy cover is fully split here and appears as $(\psi - \alpha)(\psi - \beta)(\psi - \gamma)$. To have the ψ^2 term vanish we have

$$Q = \psi^3 + (-\beta^2 - \alpha^2 - \alpha\beta)\psi - \alpha\beta(\alpha + \beta).$$

Now we note that for m=4, we have that for either A,B>0 this is the only possible gauge algebra. For A>0, m=4, we have $\tilde{b}=0$ and hence the monodromy cover after appropriate rescaling appears as ψ^3+1 and hence factors completely. For B>0, m=4 the cover appears as $\psi(\psi^2+1)$ after rescaling since here $\tilde{a}=0$, and hence the cover can be fully split.

 $\mathbf{A} > \mathbf{0}$: In this case, $-\beta^2 - \alpha^2 - \alpha\beta = 0$. Substituting for β^2 using this identity gives $(g/\sigma^3)_{\sigma=0} = -\alpha\beta(\alpha+\beta) = \alpha^3$. Thus $g = \sigma^3(\alpha^3 + g_4\sigma + O(\sigma^5))$. This implies that all contributions to the residuals in g come in multiples of 3. For example, we have larger than expected contributions to g residuals from intersections with curves of type II. As another consequence, we see that since A > 0, inspecting the case of an intersection with type III shows that we in fact have a (4,6,12) point as the remaining terms in g are of total order at least 6.

 $\mathbf{B} > \mathbf{0}$: Here we instead have that $\alpha\beta(\alpha + \beta) = 0$, giving three cases: $\alpha = 0, \beta = 0$, and $\alpha = -\beta$. In each, we have $Q = \psi^3 + (\alpha^2)\psi$ (renaming β as α as needed). Thus,

$$f = \sigma^2(-\alpha^2 + f_3\sigma + O(\sigma^2)). \tag{A.9}$$

We conclude that all \tilde{a} contributions must be even.

A.6.1.4 Summary of Restrictions

We collect the restricted monodromy assignments in Table 25.

	A > 0	B > 0
\mathfrak{g}_2	√	X
$\mathfrak{so}(7)$	X	\checkmark
$\mathfrak{so}(8)$	\checkmark	\checkmark

Table 25. Forbidden monodromy assignments on $I_0^* \sim (2 + A, 3 + B, 6)$.

A.6.2 Intersections contributions from I_0^*

Here we study the contributions to the residual vanishings along Σ' from a transverse intersection with Σ in each of the cases above.

A.6.2.1 Gauge algebra $\mathfrak{so}(8)$:

Using the above preliminaries, we have the following table of intersection contributions from Σ with $\mathfrak{so}(8)$ gauge algebra to Σ' . This depends on the orders of vanishing along Σ' , whether the order in g there is a multiple of three, and if Σ' is of even or odd type. Recall that Σ' with orders (a',b',d') is of even type if 3a>2b, odd type if 3a<2b, and hybrid type otherwise. We do not explore the latter case in Table 26. Note that I_0 can appear in any of the three types as orders of vanishing for I_0 are given by (a',b',0) with one of a' or b' necessarily zero.

A > 0	$b' \equiv 0 \mod 3$	$b' \not\equiv 0 \mod 3$
	(2+A,3,-)	(a, 4, -)
Even Type on Σ' :	(a, 3, 6)	(a, 4, 8)
Odd Type on Σ' :	(a, 3, 3a)	(a, 4, 3a)

Table 26. Intersection contributions from $I_0^{*s} \sim (a = 2 + A, b = 3 + B, 6)$.

A.6.2.2 Gauge algebra $\mathfrak{so}(7)$:

Here we only need to study the case B > 0. When Σ' has even type, we have minimal contributions to residuals along Σ' given by (2, b, 2b). In the odd type on Σ' case these are instead (2, b, 6).

A.6.2.3 Gauge algebra \mathfrak{g}_2 :

Only A > 0 is relevant here. We have contributions given by (a, 3, 6) in the even type case and by (a, 3, 3a) in the odd type case.

A.6.3 Restricted tuples

We now discuss some consequences of the above I_0^* restrictions. Residual vanishing counts along Σ before any intersections are (8-2m+2A,12-3m+3B,24-6m), where $m=\Sigma\cdot\Sigma$. We list forbidden collections of transverse curves simultaneously meeting Σ for various values of m and a given monodromy assignment in Table 27. An X indicates the monodromy assignment for specified values of A, B, m is forbidden. Separate forbidden collections are semicolon-separated. Note that we do not use all available vanishings with some collections. Rather, any collection containing a forbidden collection is also ruled out since the required vanishing conditions cannot be met with any of the indicated transverse subcollections. For example, in the case with data given by $\mathfrak{so}(8)$, A>0, m=3, the presence of two transverse curves with types (.,1,.) prevents $\widehat{g}=(g/\sigma^2)|_{\sigma=0}$ from being a cube (since these each require 2 additional vanishings of \widehat{g} at their intersections with Σ), but this contradicts $\widehat{b}=3$.

The form of the relevant restricted polynomials for $\mathfrak{so}(8)$ with A, B > 0 rule out a significant number of intersections that satisfy naive residuals tallying. Notable cases include

A > 0	m=4	m = 3	m = 2	m = 1
\mathfrak{g}_2	X	(.,3,.)	2(.,3,.);(.,6,.),	3(.,3,.);(.,6,.)(.,3,.);(.,9,.)
$\mathfrak{so}(7)$	X	X	X	X
$\mathfrak{so}(8)$		2(.,1,.);(.,2,.)(.,1,.)	3(.,1,.);2(.,2,.)(.,1,.);3(.,2,.);	4(.,1,.);4(.,2,.);2(.,3,.)2(.,1,.);
			(.,3,.)(.,2,.)(.,1,.)	(.,4,.)(.,2,.)(.,1,.);
			(.,3,.)2(.,1,.);(.,4,.)(.,1,.)	4(.,1,.);(.,2,.)3(.,1,.);
B > 0				
\mathfrak{g}_2	X	X	X	X
$\mathfrak{so}(7)$	X	(2,.,.)	2(2,.,.);(4,.,.)	3(2,.,.); (4,.,.)(2,.,.); (6,.,.)
so (8)		2(1,.,.)	(2,.,.)2(1,.,.);3(1.,.)	$4(1,.,.); (2,.,.)2(1,.,.); (2,.,.)3(1,.,.); (3,.,.)2(1,.,.); \cdots$

Table 27. Forbidden transverse curve collections meeting I_0^* with orders (a = 2 + A, b = 3 + B, 6).

 $\mathfrak{so}(8), B > 0$ intersection with a type III curve (with orders $(1, \geq 2, 3)$) since this hence induces non-minimality and $\mathfrak{so}(8), B > 1$ intersection with type II curves. Other non-trivial prohibitions include $\mathfrak{so}(8), A > 0$ intersections with any type IV curves or type III curves.

A.6.4 Intersection contributions to I_0^*

A.6.4.1 I_0^* with A > 0 meets multiple I_n curves:

Let Σ be a curve with type I_0^* at z=0 having orders of vanishing (2+A,3,6). Consider first A>0. Here Σ has even type and the contributions to residual vanishings of $\Delta|_{z=0}$ are induced precisely by those of $g|_{z=0}$.

In the case that $m = -\Sigma \cdot \Sigma = 3$, the residual vanishings along Σ are given by (-,3,6). Working from the general local form of an I_2 curve found in (A.2) of [21], we can place further restrictions to give the forms for I_n with n > 2. For an I_2 curve at $\sigma = 0$ to meet Σ , we have $z|\phi$. Since A>0, Σ has even type so each vanishing of Δ along Σ corresponds to a vanishing of g there, and hence for two I_2 curves at σ, σ' , (using the general form separately for each) restricting to $\sigma = 0$ and $\sigma' = 0$ and using that there is a \tilde{b} contribution at each intersection, we have $z^2|\phi$ in each expansion (rather than only the a priori requirement that $z|\phi$ needed for intersection with an arbitrary I_0^* curve). Since g goes at $\phi^3 + O(\sigma)$, we thus have a priori contribution to the residuals of the I_0^* given by $(-, \geq 1, \geq 2)$ at each I_2 intersection and contributions ($\geq 4, \geq 6, \geq 8$) to each I_2 curve. If compact, the I_2 curves must have self intersections given by -1 and they cannot meet other type I_n with $n \leq 4$ curves. Since $z^2|f_1$ and $z^2|\phi$ we can read from the form of g in (A.2) of [21] that there are larger residuals contributions to Σ given by $(-, \geq 2, \geq 4)$ from each intersection with an I_n when $n \geq 2$. Hence these triples are disallowed as they exceed the permitted number of vanishings along Σ . Note that results of this kind follow from intersection contribution tallying as read from the general forms of I_n unless A = B = 0 when special treatment is required.

⁶More generally, for $\Sigma' \sim I_n$ rather than I_2 with $\Sigma' \cdot \Sigma' = -1$, we cannot have intersection with curves other than I_p with $p \leq (n+12) - 2n$ when n is even and (n+12) - 3n when n is odd.

A.6.5 I_0^* restricted tuples with A = B = 0

We now briefly discuss certain forbidden configurations for a curve Σ of type I_0^* curves with orders of vanishing given precisely by (2,3,6). We will proceed by working through the cases for m_{Σ} . The restrictions we find are helpful in allowing us to eliminate the need for anomaly cancellation machinery while characterizing 6D SCFT gauge enhancement structure.

A.6.5.1 $\Sigma \cdot \Sigma = -3$:

Here $(\tilde{a}, \tilde{b}, \tilde{d})_{\Sigma} = (2, 3, 6)$. We shall inspect intersections of Σ lying along z = 0 with pairs of transverse singular curves Σ_1, Σ_2 having intersections at $\sigma = 0$ and $\sigma' = 0$, respectively, with these related by $\sigma = 1/\sigma'$. Let us denote the restrictions to Σ of $\tilde{f}, \tilde{g}, \tilde{\Delta}$ to Σ by $\hat{f}, \hat{g}, \hat{\Delta}$.

Result A.1. The configuration I_2 I_0^* I_2 requires at least a semi-split I_0^* curve Σ for $m_{\Sigma} = 3$.

<u>Proof:</u> Let the two I_2 fibers be denoted Σ_1, Σ_2 . Now Σ_i intersection with Σ requires that the forms of \widehat{f}, \widehat{g} are those giving the general form for I_2 of (A.5) modified such that the relevant coefficient functions are instead constant.

Proceeding in this fashion while imposing both I_2 intersections, we shall simply obtain a partial splitting of the monodromy cover polynomial $\psi^3 + \hat{f}\psi + \hat{g}$ via explicit factorization. The most general $\hat{f}, \hat{g}, \hat{\Delta}$ are given in the patch with coordinates z, σ by

$$\widehat{f} = -3\phi^2 + f_1\sigma - 3\Phi^2\sigma^2$$

$$\widehat{g} = 2\phi^3 - f_1\phi\sigma - f_1\Phi\sigma^2 + 2\Phi^3\sigma^3$$

where ϕ, Φ, f_1 are unspecified constants. One can then partially factor the monodromy cover as

$$\psi^{3} + \hat{f}\psi + \hat{g} = ((\phi + \Phi\sigma) - \psi)((2\phi^{2} - f_{1}\sigma - 2\phi\Phi\sigma + 2\Phi^{2}\sigma^{2}) - (\phi + \Phi\sigma)\psi - \psi^{2})$$

in this coordinate patch. Note that we can now also read off the factorization of the monodromy cover polynomial on the other patch. \Box

This implies the gauge assignment on the base 131 given by $\mathfrak{su}(2)$, \mathfrak{g}_2 , $\mathfrak{su}(2)$ is not viable. Similar methods forbid the triple I_2 I_0^{*ns} III and show that when the III here has orders (1,3,3), we can forbid that I_2 I_0^* III regardless of monodromy. Likewise, the triples I_2 I_0^* IV and I_4 I_0^* I_2 are also forbidden for all of monodromy choices.

Result A.2. If Σ is semi-split, intersection contributions to Σ' having type I_3^{ns} (even if non-compact) are at least (2,3,7). Contributions to Σ from Σ' are at least (0,0,4).

<u>Proof:</u> Since Σ is semi-split with A = B = 0, the monodromy cover appears as

$$\psi^{3} + (f/z^{2})|_{z=0} \cdot \psi + (g/z^{3})|_{z=0} = (\psi - \lambda)(\psi^{2} + \lambda\psi + \mu) . \tag{A.10}$$

and the residual discriminant $\widehat{\Delta}_{\Sigma} = (\Delta/z^6)|_{z=0}$ is

$$4(\mu - \lambda^2)^3 + 27\lambda^2\mu^2 = (4\mu - \lambda^2)(\mu + 2\lambda^2)^2 . \tag{A.11}$$

Since λ is a section of $-2K_B - \Sigma$ and μ is a section of $-4K_B - 2\Sigma$, m = 3 gives $\deg(\lambda) = 1$ and $\deg(\mu) = 2$. Define $\varphi \equiv 4\mu - \lambda^2$ and $\rho \equiv \mu + 2\lambda^2$, noting $\deg(\varphi) = \deg(\rho) = 2$. Let Σ' be an I_3^{ns} curve at $\{\sigma = 0\}$. Now φ and ρ cannot share any roots since this would require $\sigma|\mu,\sigma|\lambda$, in turn giving $\sigma|\widetilde{f}_{\Sigma}$ and forcing splitting of Σ' (as it yields $z^3|\widetilde{f}_{\Sigma'}$ and further consequences necessary in the non-compact case which are obtained by inspection of (A.10) together with (A.11) of [21]), contrary to hypothesis. Since φ and ρ cannot share any roots and we have $\sigma^3|\widehat{\Delta}_{\Sigma}$, we must have $\sigma^3|\rho^2$ and hence $\sigma^4|\rho^2$. Thus, $\sigma^4|\widehat{\Delta}_{\Sigma}$ and the discriminant expanded along $\{\sigma = 0\}$ reads

$$\Delta = z^7 \Delta_3 \sigma^3 + O(\sigma^4, z^6), \tag{A.12}$$

from which we conclude intersection contributions to Σ' are at least (2,3,7) and those from Σ' are at least (0,0,4).

This result prevents $\mathfrak{so}(13)$, $\mathfrak{sp}(1)$, $\mathfrak{so}(7)$ gauge assignments to m13 for $2 \leq m \leq 4$ upon consideration of other residual contribution considerations, thus reproducing a key anomaly cancellation result of [16] via geometric restrictions.

Since φ is the discriminant of the quadratic term in (A.10), this cannot be a square, as Σ would then be a fully split I_0^{*s} curve carrying $\mathfrak{so}(8)$ algebra. Using this fact allows extension of the above argument to eliminate several configurations including

II
$$\Sigma$$
 $I_{3 \leq l \leq 4}^{ns}$, I_2 Σ $I_{3 \leq l \leq 4}^{ns}$, $[I_2]$ Σ $I_{3 \leq l \leq 4}^{ns}$, (A.13)
II Σ I_2 , and II Σ II.

Similar argument easily eliminates Σ , I_5^{ns} . This is also key in matching anomaly cancellation restrictions.

A.6.5.2 $\Sigma \cdot \Sigma = -2$:

Additional constraints can be derived by extending the argument of Result A.2.

1. The configuration

$$II/III \quad 2_{\sum_{\substack{I_0^{*ss} \\ [\mathfrak{g}]}}} \quad III \tag{A.14}$$

has $[\mathfrak{g}] \cong [\mathfrak{sp}(2) \oplus \mathfrak{sp}(1)]$, as we now show. An $I_{\geq 4}^{ns}$ intersection requires A = B = 0 along Σ and $\deg(\varphi) = 4$ for m = 2. Let the type III intersections with Σ be at $\{\sigma_i = 0\}$. We have $\sigma_i|\rho$, $\sigma_i|\varphi$. Any I_n fiber at $\{\sigma = 0\}$ has $n \leq 4$ since we must have $\sigma^n|\varphi^2$. The latter holds since ρ and φ cannot share a root σ unless $\sigma|\lambda$ and $\sigma|\mu$, but this is impossible since $\deg(\lambda) = 2$ and $\sigma_1\sigma_2|\lambda$. An additional $\mathfrak{sp}(1)$ summand from an I_2 fiber at $\{\sigma' = 0\}$ giving $\sigma'^2|\rho$ exhausts all roots of $\tilde{\Delta}_{\Sigma}$. This applies to restrict global symmetries of 122 and 222 with the above assignment.

$$II/III \quad 2_{\sum \atop I_0^{*ss}} \quad [\mathfrak{g}] \tag{A.15}$$

has $[\mathfrak{g}] \cong [\mathfrak{sp}(3) \oplus \mathfrak{sp}(1)]$. Here we have $\sigma_1 | \varphi$, $\sigma_1 | \rho$. This leaves the maximal configuration for the remaining roots of φ and ρ occupied by I_6^{ns} and I_2^{ns} fibers, respectively, as two I_4^{ns} fibers can be eliminated. The latter requires three distinct shared roots of φ and ρ though $\deg(\lambda = 2)$. In particular, this applies to the bases 12 and 22 with type III required for 22.

A similar extension of the argument yields following holding for Σ with any m.

Result A.3. Let Σ be an I_0^{*ss} curve at $\{z=0\}$ and Σ' a type II with $(a,b,d)_{\Sigma'}=(1+A,1,2)$ curve at $\{\sigma=0\}$. Contributions to Σ are at least (1,2,3) for A=0 and (1+A,3,4) for A>0. Those to Σ' are at least (2,4,8).

A.6.5.3 Additional tools to match anomaly cancellation conditions from geometry

One of the few conditions for which we require further geometric insight (beyond those available via tracking contribution counts and single curve global symmetry maxima) in order to match known constraints derived via anomaly cancellation machinery is the following claim.

Result A.4. That the quiver 322 cannot have algebras $\mathfrak{so}(7)$, $\mathfrak{su}(2)$, - follows from geometric considerations.

This condition appears in [16] and is argued on partially on anomaly cancellation grounds. We now show this follows from geometry without field theory considerations. Along with the other geometric constraints derived here, in [21], and those in the appendices of [16], non-minimality and intersection contribution tallying more than suffice to match all 6D SCFT enhancements constraints on all links and hence on all bases to those one can reach while also employing anomaly cancellation considerations. Some enhancements are eliminated via the present considerations, as discussed in Section 3.

<u>Proof</u>: With residuals contribution tracking, we find that the only enhancements of 322 remaining are the options $\mathfrak{so}(7)$, $\mathfrak{su}(2)$ and \mathfrak{g}_2 , $\mathfrak{su}(2)$ on the 32 subquiver. To see that $\mathfrak{so}(7)$ is forbidden on the -3 curve Σ , we first note that in all the available type assignments on the link $3\Sigma^2$, Σ , Σ' have orders precisely (2,3,6),(2,2,4), respectively. It thus suffices to show that under the following conditions, the assignment $\mathfrak{so}(7)$ to Σ is not possible. In fact, this argument now follows directly from Appendix E.3 of [16]. Nonetheless, we shall give a pair of alternative arguments demonstrating the utility of various tools.

Our setup leaves only one possibility for the residuals on Σ : they are given by (0,1,2) and hence the form of \widehat{f}_{Σ} , \widehat{g}_{Σ} are given by $f \sim c_1 w^2$ and $g \sim c_2 z w^2$ where c_1, c_2 are nonzero constants and the IV lies at w = 0. Observe that $z \neq w$ (or we would have a codimension two (4,6,12) point along the I_0^* curve). The resulting monodromy cover is then irreducible.

We have the cover given by $P = \psi^3 + c_1 w^2 \psi + c_2 z w^2$ that cannot be semi-split, since as we saw above the ψ^2 term vanishing requires that

$$Q = (\psi - \alpha)(\psi^2 + \lambda\psi + \mu) = \psi^3 + (\mu - \lambda^2)\psi - \mu\lambda.$$

With self intersection -3, the residuals on are (2,3,6) for type I_0^* with orders (2,3,6). Hence $\deg(\mu-\lambda^2)=2$ and $\deg(s\lambda)=3$ with the degrees of μ,λ being 2,1 respectively. We can then identify $\mu\sim w^2$ and $\lambda\sim z$ where z gives the other vanishing of g along the I_0^* . We have $\widehat{g}=c_2\lambda\mu=(cw^2)(c'z)$ and $\widehat{f}=(\mu-\lambda^2)=(cw^2-c'^2z^2)$, where c,c' are nonzero constants. This means f has two distinct roots along the I_0^* , contradicting that we use both available vanishings at once in meeting the type IV curve.

Alternate proof: Suppose we have the $\mathfrak{so}(7)$ algebra on the -3 curve. We know that $\deg \mu = 2$ and $\deg \lambda = 1$ in the case with orders (2,3,6) along the I_0^* . Expanding each and imposing that $\mu - \lambda^2 = \hat{f} = f_2 w^2$ and $-\lambda \mu = \hat{g} = g_2 w^2 + g_3 w^3$ using the divisibility requirements from meeting a IV, where here $\hat{f} = (f/\sigma^2)|_{\sigma=0}$ and $\hat{g} = (g/\sigma^3)|_{\sigma=0}$, we have

$$\lambda = \lambda_0 + \lambda_1 \sigma$$

$$\mu = \mu_0 + \mu_1 \sigma + \mu_2 \sigma^2$$

$$\psi^3 + (\mu - \lambda^2) \psi - \mu \lambda = \psi^3 + \hat{f} \psi + \hat{g},$$

$$\implies \lambda_0 = \mu_0 = \mu_1 = 0.$$

This gives $\mu\lambda = O(\sigma^3)$, preventing matching the σ^2 term of \widehat{g} unless $g_2 = 0$. The latter induces non-minimality.

Result A.5. When Σ is a curve with m=3 and type I_0^{*ss} having orders (a,b,d)=(2,3,6), a type III curve Σ' with orders (1,3,3) at $\sigma=0$ contributes at least (2,3,6) to the allowed vanishings along Σ .

Proof: We proceed as above, here imposing the requirements that

$$\lambda = \lambda_0 + \lambda_1 \sigma$$

$$\mu = \mu_0 + \mu_1 \sigma + \mu_2 \sigma^2,$$

$$\psi^3 + (\mu - \lambda^2) \psi - \mu \lambda = \psi^3 + \widehat{f} \psi + \widehat{g}$$

$$\widehat{f} = f_1 \sigma + f_2 \sigma^2$$

$$\widehat{g} = g_3 \sigma^3.$$

Proceeding to match the terms of \hat{f} and $\mu - \lambda^2$ order by order and then those of g, we find

before completing the matching that

$$\lambda_0 = 0, \quad \mu_0 = 0,$$

$$\mu_1 = f_1, \quad \mu_2 = f_2 + \lambda_1^2,$$

$$\implies \mu - \lambda^2 = \widehat{f},$$

$$-\mu\lambda = -\lambda_1 f_1 \sigma^2 - \lambda_1 (\lambda_1^2 + f_2)^2 \sigma^3.$$

From the latter we see that one of λ_1 , f_1 must be zero since \tilde{g} is zero at order σ^2 . We rule out the first case as it induces infinite intersection contribution, leaving $f_1 = 0$. Intersection contributions to the I_0^{*ss} are then given by (2,3,6). (Note this forbids any additional intersections along Σ , even with an I_0 curve having $A \geq 1$.)

The above seemingly mild restriction plays an important role in determining which enhancement configurations are permitted and the degrees of freedom which remain to become global symmetry summands.

A.6.6 Contributions to I_0^* with A, B > 0 from I_n

We now investigate the details of intersection contributions in the few permitted values for n in for I_0^* intersections. When A, B > 0, the situation is even more restrictive. The maximal allowed n for I_n meeting I_0^* in each case of A, B > 0 is given in Table 41. So that we may refer to the general forms for I_n type curves, let's suppose our I_0^* here lies at z = 0.

A.6.6.1 A > 0, $\mathfrak{so}(8)$:

We will use the observation that since we have algebra $\mathfrak{so}(8)$, intersection contributions to \tilde{b} are multiples of 3. Those to \tilde{d} are then the doubles of those \tilde{b} contributions as A>0 is an even type I_0^* . From Table 42, we see that the maximal allowed intersection with I_n in this case with A>0 is for n=3.

I_n compact:

We will treat the three possible values of n separately when Σ' here is a Kodaira type I_n curve that is compact and has self-intersection -1. Note that we must have $A \leq 2$, since otherwise we exceed the 4 allowed f residual contributions to Σ' . Since A > 0, we must be without monodromy along Σ' in the one relevant case where n = 3. When n = 1, 2 we note that $z^2 | \phi$ with ϕ as in (A.4,A.8) of [21], respectively. Considering this fact together with the restriction that we have contributions in threes yields Table 28.

Table 28. Intersection contributions to I_0^{*s} with A > 0 from/to I_n . An 'X' indicates the intersection is forbidden by non-minimality.

Note that in the case when A = 1 and n = 1, we must have at least $z^4|g_1$ and $z^4|g_2$ in (A.4) of [21] via the above consideration that g intersection contributions must come in threes here. This has total order of f, g given by 4, 5 in both cases, falling barely short of non-minimality. The other cases n > 1 are barred by similar considerations.

Non-compact I_n curves for global symmetry:

We carry out a similar study here with the change that ϕ is allowed higher degree here, introducing the possibility of intersections with I₂ or I₃. Since we are concerned with global symmetry, we safely ignore n=1 (as I₁ curves carry the trivial algebra). However, intersections for n>1 are forbidden as a result of non-minimality following from the strong requirement that contributions to \tilde{b} are divisible by 3. This result is indicated in Table 29.

$$\begin{array}{c|cc}
 & n & 2 & \geq 3 \\
\hline
 & \geq 1 & X & X
\end{array}$$

Table 29. Intersection Contributions to I_0^{*s} with A > 0 from an I_n non-compact curve. An 'X' indicates the intersection is forbidden by non-minimality.

A.6.6.2 B > **0** $\mathfrak{so}(8)$:

This case has similar requirements to those above with the main difference being that the contributions to residuals in f are required to be even here as we saw in the preceding analysis. We collect results for this case in Table 30.

B	1	2
1	(2,1,6)/(4,6,10)	Χ
2	X	X
3	X	X

Table 30. Intersection Contributions to I_0^{*s} with B > 0 from/to I_n . An 'X' indicates the intersection is forbidden by non-minimality.

A.6.6.3 B > **0**, $\mathfrak{so}(7)$:

Again we consider intersections with a transverse type I_n curve, Σ' using restrictions from Table 42 which dictate that the maximum value of n here is 2. We will use that we have odd type on the I_0^* ; we will not need to use that intersection contributions to the I_0^* in this case are dictated by the lowest order z term in f, say $\mu_1 \gamma^2$ with μ_1 square-free and of nonzero degree (since in this case the relevant term cannot be a square, or equivalently, contributions to \tilde{a} along an I_0^{*ss} cannot have purely even f residual contributions).

I_n compact:

With these constraints, we produce Table 31 by reading from the general forms for I_n as they appear in [21] Appendix A. Note, we have $B \leq 3$, as the degree of ϕ (A.4) of [21] is 2 in the only relevant compact I_n intersections, those for a curve with self-intersection -1. For a non-compact I_n , we can raise the degree of ϕ to allow large values of B for example

B	1	2
1	(1,1,3)/(4,6,10)	(1,1,3)/(4,6,8)
2	(1,1,3)/(4,6,10)	X
3	(1,1,3)/(4,6,10) (1,1,3)/(4,6,10) (1,0,3)/(4,6,10)	X

Table 31. Intersection contributions with I_0^{*ss} with B > 0 from/to an I_n curve. An 'X' indicates the intersection is forbidden by minimality considerations.

when meeting I_2 . Such intersections are barred for Σ' compact. We have not used the condition that \tilde{a} contributions cannot be purely even, instead limitations being induced by minimality considerations. We collect our results in Table 31.

Non-compact I_n curves for global symmetry:

Our results here only concern $n \geq 2$ since n = 1 does not yield global symmetry. From Table 42, we cannot exceed n = 2. We have the identical result when B = 1. When $B \geq 2$, we can avoid non-minimality by raising the degree of ϕ . In this case, we only are interested in the intersection contributions to the I_0^* . We collect the relevant result in Table 32.

Table 32. Intersection Contributions to I_0^{*ss} with B > 0 from a transverse non-compact I_n curve. An 'X' indicates the intersection is forbidden by non-minimality considerations.

A.6.7 A > 0, \mathfrak{g}_2

The a priori restrictions in this case are similar to those for the $\mathfrak{so}(8)$ case with the exception that g contributions are not forced to be multiples of three. On the contrary, we are prevented from having contributions which consist entirely of multiples of three, though this is irrelevant in our analysis here. When n=3, we use that ϕ_0 rather than μ in (A.11) of [21] must carry all divisibility (we have $z|\phi_0$ and have thus used all available roots of ϕ_0) since we are considering the case of intersection with a compact I_n curve where the

f, g residuals are limited by 4,6, respectively. We find there is non-minimal intersection for $n \geq 3$ as this would require $z^2 | \psi_1$ with ψ_1 as in (A.11) of [21].

A n	1	2	3
1	(1,1,2)/(4,6,9)	(1,2,4)/(4,6,9)	Χ
2	(1,1,2)/(4,6,9) (0,1,2)/(4,6,9)	(0,2,4)/(4,6,9)	Χ

Table 33. Intersection contributions to I_0^{*ns} with A > 0 from/to I_n . An 'X' indicates the intersection is forbidden by non-minimality considerations.

A.7 Type I_n^* curve intersections

In this section we collect contributions to residual vanishings from an intersection with an I_n^* curve. The main focus is the case with transverse curve of type I_n .

A.7.1 Single I_n^* intersections with a type I_m curve

In this section, we find the minimal simultaneous contributions to the residual vanishings to each curve from an I_n^* , I_m intersection. The result is that there is a simple general pattern for these contributions which we expect to hold in all cases where intersection should be allowed via the *a priori* residual vanishings allowed on each curve. Some of the general forms of such intersections have been constructed for this analysis, but the most general form in the large n, m case for arbitrary n, m has not. Hence a portion of our results here for $7 \le m \le 9$ is conjectural. We expect these contributions to be a generalization of the cases we have compiled in the table below. The general form of the conjecture is then that we have contributions to the residual vanishings along the I_n^* and I_m curves given by (0,0,m) and (2,3,n), respectively in the case with or without monodromy along the I_n^* for even m; for m odd instead these contributions are given by (0,0,m) and (2,3,n) in the case with monodromy and (0,0,m+1), (2,3,n+1) in the case without monodromy, respectively. Note that the I_m is non-split (i.e., has monodromy) since we consider an intersection with I_n^* .

A.7.1.1 Intersection with type I_1^*

Meeting I_1 :

We begin by considering an intersection contributions to an I_1 curve from an I_1^* curve in cases with and without monodromy. This requires working several cases and looking for the minimum. The detailed calculations can be easily carried out with a computer algebra system but are somewhat cumbersome to treat by hand. We find that these minimal contributions to the I_1 are given by (2,3,7) and (2,3,8) from I_1^{*ns} and I_1^{*s} , respectively. Note the agreement with [22].

Meeting I_2 :

Here we find that values for the cases with and without monodromy have the same intersection contributions to the I_2 , namely (2,3,7) and those to the I_1^* are given by (0,0,2) regardless of monodromy.

Meeting I_3 :

Here we find that the monodromy again matters and the contributions to the I_3 are as in the I_1 case given by (2,3,7) and (2,3,8) from I_1^{*ns} and I_1^{*s} , respectively, before we consider the monodromy condition along the I_3 . Investigating monodromy involves detailed inspection, but again can be readily treated using a computer algebra system. We find that for $\mathfrak{su}(3)$ along I_3 , the intersection becomes a (4,6,12) point; this same result appears to hold for either monodromy along the I_1^* .

Note that since I_n^* is obtained by imposing further constraints on an I_1^* and we did not use the monodromy information from the I_1^* , this forbids the intersection of I_3^s with higher I_n^* curves as well. Likewise, moving to the cases $I_{n\geq 3}$ also simply imposes additional constraints on f, g, but the term determining monodromy along $\Sigma = I_n$ remains the same and its form simply becomes more constrained as we increase n. This method is then an alternative demonstration that I_n^* cannot intersect I_m^s for $(m \geq 3, n \geq 1)$.

Meeting I_4 :

In this case, the minimal contributions are (2,3,7) with or without monodromy along the I_1^* .

A.7.1.2 I_n^* with $n \ge 4$:

Here we implement the constraints for I_n^* beginning with the inductive form of I_m and vice versa (for large n using the inductive form along the I_n^* and imposing the constraints for I_1 , then I_2 , etc.) and concluding by imposing monodromy constraints for the I_n^* . This allows one to inspect the resulting form to determine the minimal simultaneous intersection contributions in each case. We find the general pattern for low n appears to continue, but proving this in full generality is beyond our reach. Those cases we have explicitly checked are found in Table 34.

A.7.2 Summary

We find the following minimal simultaneous intersection contributions to I_n from I_m^* curves and vice versa, respectively. While it is a priori possible that the minimal contributions could be realized for each with different intersections giving the minimal ones, this does not appear to be the case; it appears possible in all cases studied to simultaneously realize the minimal contributions to both the I_n^* and the I_n curve. Note that only intersections that do not give (4,6,12) points are considered here. Note there is one remaining possible (necessarily simultaneous) singularity of f,g since there are remaining residuals after the I_n^* intersection given by (2,3,-) (which can be located anywhere we choose other than at the original intersection) and there cannot be additional transverse curves over which the fibration is singular not meeting at this point along the I_n curve that are not of type I_p for some p. The transverse curves also must have $(a,b) \leq (2,3)$. In other words, any other

intersection with a curve of which the fibration is singular must give either contribution (2,3,-) (there can be at most one of these) or contributions (0,0,-).

	I_1^{*ns}	I_1^{*s}	I_2^{*ns}	I_2^{*s}	 I_4^{*ns}	I_4^{*s}
I_1	(2,3,7)/(0,0,1)	(2,3,8)/(0,0,2)	(2,3,8)/(0,0,1)	(2,3,9)/(0,0,2)	(2,3,10)/(0,0,1)	(2,3,11)/(0,0,2)
I_2	(2,3,7)/(0,0,2)	(2,3,7)/(0,0,2)	(2,3,8)/(0,0,2)	(2,3,8)/(0,0,2)	(2,3,10)/(0,0,2)	(2,3,10)/(0,0,2)
I_3	(2,3,7)/(0,0,3)	(2,3,8)/(0,0,4)	(2,3,8)/(0,0,3)	(2,3,9)/(0,0,4)		
I_4	(2,3,7)/(0,0,4)	(2,3,7)/(0,0,4)				
I_5	(2,3,7)/(0,0,5)	(2,3,8)/(0,0,6)				
I_6	(2,3,7)/(0,0,6)	(2,3,7)/(0,0,6)				
:						
I_8 (†)	(2,3,7)/(0,0,8)	(2,3,7)/(0,0,8)	(2,3,8)/(0,0,8)	(2,3,8)/(0,0,8)		
:						

Table 34. Minimal simultaneous intersection contributions in I_n, I_k^* collisions to I_n and I_k^* , respectively. (The '†' symbol indicates the less general inductive form is used for I_n).

A.7.3 Multiple I_n^* curves meeting a type I_m curve

In this case, we must have the self-intersection along the I_m curve, say Σ , with $\Sigma \cdot \Sigma = -1$ since for $-\Sigma \cdot \Sigma > 1$ we have no vanishings of f, g possible. The total residuals are (4, 6, 12 + m) along Σ , so at most two I_n^* curves can meet Σ , and such a pair leaves the no remaining residuals in f, g. Note that intersection with a pair of I_n^* curves requires that the I_m curve has monodromy.

A.7.4 Compact curve intersections for pairs with types II, I_n^*

We first observe that the only relevant case here is n=1, as a type II curve cannot meet an I_n^* curve with n>1; such intersections are non-minimal even when the I_n^* is non-compact. We consider here the case with both curves compact, thus introducing additional constraints not applicable to the situations considered in [21]. Along the I_n^* curve, $(\tilde{a}, \tilde{b}) = (2(4-m), 3(4-m))$ and II gives a non-trivial f, g contribution. Hence, m=4 does not need to be considered. We summarize the contributions for all remaining cases of such an intersection in Table 35. Since $I_{\geq 1}^{*s}$ and $I_{\geq 2}^{*ns}$ intersections with a type II curve are non-minimal, all relevant local contribution data for $II, I_{n\geq 1}^*$ intersections are captured in our table.

Note that Kodaira types beyond II other than I_n family types are banned from I_n^* intersection by non-minimality. Thus we have given here the set of possible intersection contributions for types other than I_0 , which we have recorded separately.

A.8 I_0, I_n^* curve intersections

We now find the intersection contributions to a curve Σ with type I_0 from an I_n^* curve, Σ' , which may be non-compact. Our computations rely on the general forms of I_n^* given in Appendix B of [21]. We impose divisibility conditions on these local models as required for intersection with a compact I_0 curve having specified properties and read of the intersection contributions to Σ in each case while recording which of these allow Σ' compact and tabulating intersection contributions to Σ' in such cases.

M	3	2	1
0	(2,3,4)/(3,4,8)		
1	(2,3,4)/(2,4,8)		
2	X	(4,6,7)/(3,4,8)	
3	X	(4,6,7)/(2,4,8)	
4	X	X	(6,9,10)/(3,4,8)
5	X	X	(6,9,10)/(2,4,8)
≥ 6	X	X	X

Table 35. Intersection contributions to/from a compact I_1^{*ns} with $\Sigma \cdot \Sigma = -m$ intersecting a II. An X indicates the intersection is non-minimal and an (X..)X, that the intersection is banned by (naive) residuals considerations. Entries to the right of an allowed entry have the same values.

Let the vanishings along Σ be given by (A, B, 0), noting that we must have one of A, B being zero. We consider Σ' along $\{\sigma=0\}$ whose form is given by one of the expansions from [21] (B.1)-(B.5). We compile the total order at the intersection point in 36, writing 'X' for non-minimal intersections. By inspecting the form of I_n^* , imposing the required divisibility conditions to have z^A dividing f or z^B dividing g, and then checking the monodromy condition for I_n^* , we arrive at the indicated minimal total orders at the intersection. We do not record the case A = B = 0 here since the minimal total order is always (2,3,n) in such cases and all intersections are allowed except when the Σ' has self intersection -4; for such curves, all A, B > 0 intersections are trivially banned by a priori residuals tracking. Terminal entries with A or B referenced indicate the general pattern holds for all A or B, applying also to the entries below such an entry. Note that we need only explore $n \leq 4$ since further intersections are forbidden via [38].

	I_1^{*ns}	I_1^{*s}	\mathcal{I}_2^{*ns}	I_2^{*s}	I_3^{*ns}	I_3^{*s}	I_4^*
A = 1	(4, 4, 8)	(4, 4, 8)	(4, 5, 10)	(4, 5, 10)	(3+A,5,10)	Χ	X
A = 2	(4, 4, 8)	(4, 4, 8)	(4, 5, 10)	(5, 5, 10)		X	X
A = 3	(2+2[A/2],4,8)	(2+2[A/2],4,8)	(6, 5, 10)	(6, 5, 10)		X	X
A = 4			(3+A, 5, 10)	(3+A,5,10)		Χ	Χ
B=1	(3, 5, 9)	(3, 5, 9)	(3,4+B,9)	(3,4+B,9)	X	Χ	X
B=2	(3, 6, 9)	(3, 6, 9)			X	X	X
B=3	(3, 6, 9)	(3, 7, 9)			X	X	X
B=4	(3, 7, 9)	(3, 7, 9)			X	X	Χ

Table 36. Minimal total order of I_0, I_n^* intersections

A.9 Compact I_0,I_n^* curve intersections

The residual vanishing counts along an I_n^* curve with negative self-intersection m are given by

$$\tilde{a} = -4(m-2) + 2m = 8 - 2m$$

$$\tilde{b} = -6(m-2) + 3m = 12 - 3m$$

$$\tilde{d} = -12(m-2) + (n+6)m = 24 + (n-6)m.$$

In particular, the constraints on \tilde{a} , \tilde{b} and the general forms of I_n^* together imply that u_1 in the general form has the number of roots indicated in Table 37. This data allows us

Table 37. Degree of u_1 for I_n^* with $\Sigma \cdot \Sigma = -m$.

to find the following rules for intersections with type $I_0 \sim (A, B, 0)$ singularities which are not necessarily compact nor transverse curves but simply singularities along the I_n^* locus. The latter implies that any remaining residuals in purely f or g have such intersection contributions, but we should note that there may in some cases indicated as non-minimal which may in fact be allowed point singularities in f, g to the corresponding order; that is, these tables are intending to track contributions from transverse curves but also give the contributions for point singularities when a transverse curve of the corresponding type is allowed. In other terms, only in cases where the intersections are indicated as allowed rather than non-minimal do we track the data, as our priority is to treat transverse curves rather than simply singular points (but some information for point singularities does result). The contributions to the I_0 are also noted for use in the case that the singularity is an intersection with a it compact transverse I_0 curve. Note that for m=4, we cannot have intersection with a curve of type $I_0 \sim (A, B, 0)$ with either of A > 0 or B > 0. This fact and other restrictions of this form are already accounted for via simple residuals tracking without modification from what follows below. For A = B = 0, it is easy to see the intersection contributions in both monodromy cases are simply (2,3,6+n), the naïve estimate. We collect the relevant results in Table 38.

A.9.1 m = 3

Residuals along the I_n^* here are given by (2,3,6+3n). We find intersection contributions and non-minimal intersections appearing in Table 38.

A.9.2 m = 2

Here residual vanishings along the I_n^* are given by (4,6,12+2n). Hence, A,B are capped for I_0 at 4,6. The relevant contribution data is recorded in Table 39.

	I_1^{*ns}	I_1^{*s}	I_2^{*ns}	I_2^{*s}	$I_{\geq 3}^*$
A = 1	(3,4,8)/(2,3,3)	(3,4,8)/(2,3,3)	(3,5,10)/(2,3,3)	X.	Χ.
A = 2	(2,4,8)/(2,3,3)	(2,4,8)/(2,3,3)	(2,5,10)/(2,3,3)	X.	Χ.
$A \ge 3$	-	-	-	-	-
B=1	(3,4,9)/(2,3,4)	(3,4,9)/(2,3,5)	(3,4,9)/(2,3,2)	(3,4,9)/(2,3,2)	Χ
B=2	(3,4,9)/(2,3,4)	X.	X.	X.	X
B=3	(3,3,9)/(2,3,4)	X.	X.	X.	X
$B \ge 4$	-	-	-	-	-

Table 38. Intersection Contributions to $I_0 \sim (A, B, 0)$ and I_n^* with m = 3, respectively. 'X' indicates non-minimal intersection and '-' indicates exceeding allowed residuals. 'X.' indicates that the intersection is non-minimal here while in the non-compact case it is was not yet forbidden via the previous analysis in the non-compact case.

	I_1^{*ns}	I_1^{*s}	I_2^{*ns}	I_2^{*s}	I_3^{*ns}	$I_{\geq 3}^{*s}$	$I_{\geq 4}^{*ns}$
A = 1	(3,4,8)/(2,3,3)	(3,4,8)/(2,3,3)	(3,5,10)/(2,3,3)	(3,5,10)/(4,6,6)	Χ.	Χ	X
A = 2	(2,4,8)/(2,3,3)	(2,4,8)/(2,3,3)	(2,5,10)/(2,3,3)	(3,5,10)/(4,6,6)	Χ.	X	X
A = 3	(3,4,8)/(4,6,6)	(3,4,8)/(4,6,6)	(3,5,10)/(4,6,6)	(3,5,10)/(4,6,6)	Χ.	X	X
A = 4	(2,4,8)/(4,6,6)	(2,4,8)/(4,6,6)	(2,5,10)/(4,6,6)	(2,5,10)/(4,6,6)	Χ.	X	X
$A \ge 5$	-	-	-	-	-	-	-
B=1	(3,4,9)/(2,3,4)	(3,4,9)/(2,3,5)	(3,4,9)/(2,3,2)	(3,4,9)/(2,3,2)	Χ	Χ	X
B=2	(3,4,9)/(2,3,4)	(3,4,9)/(4,6,8)	(3,4,9)/(4,6,4)	(3,4,9)/(4,6,4)	X	X	X
B=3	(3,3,9)/(2,3,4)	(3,4,9)/(4,6,8)	Χ.	X.	X	X	X
B=4	(3,4,9)/(4,6,8)	(3,4,9)/(4,6,8)	X.	X.	X	X	X
B=5	(3,4,9)/(4,6,8)	(3,4,9)/(4,6,8)	Χ.	X.	X	X	X
B = 6	(3,3,9)/(4,6,8)	(3,3,9)/(4,6,8)	X.	X.	X	X	X
$B \ge 7$	-	-	-	-	-	-	-

Table 39. Intersection contributions to $I_0 \sim (A, B, 0)$ and I_n^* with m = 2, respectively. 'X' indicates non-minimal intersection or not allowed to have a particular I_n^* on a curve of this self intersection and '-' indicates exceeding allowed residuals. 'X.' indicates that the intersection is non-minimal here while in the non-compact case it is was not yet forbidden via the previous analysis in the non-compact case.

A.9.3 m = 1

In this case, the residual vanishings along the I_n^* are instead given by (6, 9, 18 + n). Hence A, B for I_0 are at most 6, 9, respectively. Contribution data for these intersections appears in Table 40.

A.10 Type I_n intersections with A = B = 0 curves

In Table 41 we show intersection contributions from type I_n curves to those of every other possible gauged Kodaira type having minimal orders of vanishing on the transverse curve, i.e., curves with A = B = 0. Up to a couple of minor corrections indicated here with a superscript '!' symbol, this contribution data is taken from [21]. Note that in the other subsections in this work we have treated the remaining A > 0 and B > 0 cases as needed to since quiver with more than a single curve in many cases require nonzero A, B values giving larger contributions. In the following table taken from [21] which we reproduce here for ease of reference, we collect the largest values of n permitted for I_n intersection with a non-compact curve having any of the various other Kodaira types with the exception of I_n^*

	I_1^{*ns}	I_1^{*s}	${ m I}_2^{*ns}$	${ m I}_2^{*s}$	I_3^{*ns}	$I_{\geq 3}^{*s}$	$I_{\geq 4}^{*ns}$
A = 1	(3,4,8)/(2,3,3)	(3,4,8)/(2,3,3)	(3,5,10)/(2,3,3)	(3,5,10)/(4,6,6)	Χ.	Χ	X
A = 2	(2,4,8)/(2,3,3)	(2,4,8)/(2,3,3)	(2,5,10)/(2,3,3)	(3,5,10)/(4,6,6)	Χ.	X	X
A = 3	(3,4,8)/(4,6,6)	(3,4,8)/(4,6,6)	(3,5,10)/(4,6,6)	(3,5,10)/(4,6,6)	Χ.	X	X
A = 4	(2,4,8)/(4,6,6)	(2,4,8)/(4,6,6)	(2,5,10)/(4,6,6)	(2,5,10)/(4,6,6)	Χ.	X	X
A = 5	(3,4,8)/(6,9,9)	(3,4,8)/(6,9,9)X	(3,5,10)/(6,9,9)	X.	Χ.	X	X
A = 6	(2,4,8)/(6,9,9)	(2,4,8)/(6,9,9)X	(2,5,10)/(6,9,9)	X.	Χ.	X	X
$A \geq 7$	-	-	-	-	-	-	-
B=1	(3,4,9)/(2,3,4)	(3,4,9)/(2,3,5)	(3,4,9)/(2,3,2)	(3,4,9)/(2,3,2)	Χ	Χ	X
B=2	(3,4,9)/(2,3,4)	(3,4,9)/(4,6,8)	(3,4,9)/(4,6,4)	(3,4,9)/(4,6,4)	X	X	X
B=3	(3,3,9)/(2,3,4)	(3,4,9)/(4,6,8)	(3,4,9)/(6,9,6)	(3,4,9)/(6,9,6)	X	X	X
B=4	(3,4,9)/(4,6,8)	(3,4,9)/(4,6,8)	X.	Χ.	X	X	X
B=5	(3,4,9)/(4,6,8)	(3,4,9)/(4,6,8)	X.	Χ.	X	X	X
B=6	(3,3,9)/(4,6,8)	(3,3,9)/(4,6,8)	X.	Χ.	X	X	X
B = 7	(3,4,9)/(6,9,12)	X.	X.	X.	X	X	X
B = 8	(3,4,9)/(6,9,12)	X.	X.	X.	X	X	X
B=9	(3,3,9)/(6,9,12)	X.	X.	X.	X	X	X
$B \ge 10$	-	-	-	-	-	-	-

Table 40. Intersection contributions to $I_0 \sim (A, B, 0)$ and I_n^* with m = 1, respectively. 'X' indicates non-minimal intersection or not allowed to have a particular I_n^* on a curve of this self intersection and '-' indicates exceeding allowed residuals. 'X.' indicates that the intersection is non-minimal here while in the non-compact case it is was not yet forbidden via the previous analysis in the non-compact case.

	n	gauge algebra	\tilde{a}	$ ilde{b}$	$ ilde{d}$
I_0^*	≥ 2	$\mathfrak{sp}([n/2])$	0	0	$n^!$
IV	2	$\mathfrak{su}(2)$	0	2	4
IV	3	$\mathfrak{su}(2)$	0	3	6
IV	3	$\mathfrak{su}(3)^!$	1	2	4
IV	4	$\mathfrak{sp}(2)$	0	4	8
IV	5	$\mathfrak{sp}(2)$	0	5	10
IV	6	$\mathfrak{sp}(3)$	0	6	12
IV	≥ 7	$\mathfrak{sp}([n/2])$	0	n	2n
III	2	$\mathfrak{su}(2)$	1	1	3
III	3	b.p.	2	2	6
III	4	$\mathfrak{sp}(2)$	2	2!	6
III	4	$\mathfrak{su}(4)$	2	3	6
III	5	$\mathfrak{sp}(2)$	3	3	9
III	6	$\mathfrak{sp}(3)$	3	3	9
III	≥ 7	$\mathfrak{sp}([n/2])$	$\lceil n/2 \rceil$	$\lceil n/2 \rceil$	$3\lceil n/2\rceil$

Table 41. Local contributions from non-compact type \mathbf{I}_n curves.

which we have analyzed separately. Note that the maximal values of A, B permitted for such intersections are indicated.

	A = B = 0	A = 1	$A \ge 2$	B = 1	$B \ge 2$
II*	0	0	0	-	-
III^*	0	-	-	0	0
IV^*	1	1	1	-	-
I_0^*	∞	3	3	2	2
IV	∞	3	3	-	-
III	∞	-	-	∞	5!
II	∞	∞	4	-	-

Table 42. Allowed intersections for non-compact type I_n curves. Here a '!' superscript denotes a correction to the corresponding data in [21].

A.11 I_0, I_0^* curve intersections

Here we suppose that a curve Σ of type I_0 with vanishings (A, B, 0) at $\{z = 0\}$ meets a curve Σ' of type $I_0^* = \{\sigma = 0\} := \Sigma'$ and we investigate the restrictions on monodromy on Σ' for various values of A, B, the additional orders of vanishing of f, g along Σ , as above. We let A_0, B_0 give the orders of vanishing along Σ' as $(2 + A_0, 3 + B_0, 6)$. Here we have the monodromy cover given by $\psi^3 + (f/\sigma^2)|_{\{\sigma=0\}} + (g/\sigma^3)|_{\{\sigma=0\}}$ and in the case where this splits as $(\psi - \alpha)(\psi - \beta)(\psi - \gamma)$, it is given by

$$\psi^3 + \psi(-\beta^2 - \alpha^2 - \alpha\beta) - \alpha\beta(\alpha + \beta).$$

In the case that the I_0^* curve Σ' has $B_0 \geq 4$ so that we have orders of vanishing $(2, \geq 6, 6)$, we are near non-minimality. In fact, we find that if the I_0 has orders (1, 0, 0) or beyond in f, non-minimality forbids such an intersection.

To clarify, in this case $\alpha\beta(\alpha+\beta)$ must vanish. Hence one of α, β , or $\alpha+\beta$ must vanish. Suppose $\alpha=-\beta$. Then

$$\alpha^2 + \beta^2 + \alpha\beta = \alpha^2.$$

For z|f, we then have $z^2|(f/\sigma^2)|_{\{\sigma=0\}}$, giving a (4,6,12) point. To see this, we note that our requirements result in

$$f = \sigma^2(zg_2(z) + zg_3(z)\sigma + zg_4(z)\sigma^2 + \dots)$$

with $(f/\sigma^2)|_{\sigma=0}$ a square, making $zg_2(z)$ is a square. Hence, orders (3,6,9) are boosted, with non-minimality resulting after considering monodromy. The other cases are similar. When B>0 along the I_0 , there is no analogous result.

In the case that we have $A_0 > 0$, the coefficient on ψ vanishes and hence $(g/\sigma^3)|_{\sigma=0} = (\alpha^2 + \beta^2)(\alpha + \beta)$. The utility of this condition in considering $z^k|g$ to study B > 0 is not immediately obvious and we shall proceed without making use of it.

Given $\mathfrak{so}(7)$ algebra on I_0^* , the monodromy cover splits partially. We can write it as

$$\psi^3 + (\mu - \lambda^2)\psi - \lambda\mu.$$

When $A_0 > 0$, this becomes $\psi^3 - \lambda^3$. Since $\lambda^3 = (g/\sigma^3)|_{\sigma=0}$, we see that z divisibility of g along the I_0 becomes z^3 divisibility. In the case that $A_0 \ge 2$, the order in f is already 4 before intersection with the I_0 . This results in a (4,6,12) point as the (4,4,8) point at the intersection is boosted by the monodromy condition. In terms of expanding g, this reads

$$g = \sigma^3(zg_3(z) + zg_4(z)\sigma + zg_5(z)\sigma^2 + \dots)$$

with $zg_3(z)$ a cube. The latter requires that z^3 divides $g|_{\sigma=0}$. Hence, $A_0 \geq 2$ and $B \geq 1$ is forbidden for I_0^{*ss} . When we have \mathfrak{g}_2 algebra, the monodromy cover is irreducible, and

Table 43. Forbidden intersections and type restrictions

appears as $\psi^3 + q\psi + p$. If this had a root, it would appear as $\psi^3 + \psi(\mu - \lambda^2) - \lambda\mu$. In the case with $A_0 > 0$, irreducibility implies that $p \neq \lambda\mu$ where $\mu = \lambda^2$, i.e., $(g/\sigma^3)|_{\sigma=0}$ is not a cube. In particular, this prevents $(g/\sigma^3)|_{\sigma=0}$ from being constant, hence barring the case with no residual vanishings along the I_0^* after accounting for any other intersections. Here, $g = \sigma^3(g_3 + \sigma g_4 + \sigma^2 g_5 + \dots)$, and the above is simply to say g_3 is not a cube. This result applies in all configurations involving an I_0^* with \mathfrak{g}_2 algebra; there is nothing used about an intersection with I_0 . To phrase this differently, if we have an I_0^* with \mathfrak{g}_2 algebra and $A_0 > 0$, the other vanishings of g along this curve cannot all appear as cubes. Among other restrictions this imposes, we see that when $\Sigma' \cdot \Sigma' = -m$, with m given by 1, 2, 3, the residual vanishings of g before considering other intersections read g, g, g, respectively in these cases, implying for example that a g gauged g with g ocannot meet g, g other type III curves each having types g in the respective cases.

Similarly, for $B_0 > 0$ we have monodromy cover given by $\psi^3 + q\psi$. This is not irreducible, thus ruling out the case with \mathfrak{g}_2 algebra.

A few of these results are summarized in Table 43.

B Notes for using the computer algebra workbook

The arXiv submission of this work is accompanied by 'gsFunctions.nb,' computer algebra workbook for Mathematica enabling explicit listing of gauge enhancements and global symmetry maxima for nearly all 6D SCFTs. This notebook can be downloaded via the "Download:" link in the arXiv webpage featuring the submission history and abstract. Click on the "Other format" link and then on "Download source." After unzipping this file, all contents should be moved to a single folder. The 'gsFunctions.nb' workbook contains function definitions and the entire notebook should be evaluated to initialize them. At the bottom of this workbook are a series of examples with comments detailing instructions to initiate computation of gauge and global symmetries for an arbitrary at-most-trivalent base given as user input. Results can be written to a LaTex file in the workbook directory which can be compiled to view results condensed to the format of tables appearing

in Appendix C. Instructions for in-workbook use of several additional functions appear in comments detailing further examples.

C Tables of flavor symmetries for miscellaneous quivers

In this appendix we provide configuration data for a few miscellaneous bases. For each \mathcal{T} , summands of \mathfrak{g}_{global} appear under each curve with \mathfrak{g}_{global} totals shown in the rightmost column. Note that in listings for αm , permitted \mathcal{T} compatible with m are constrained via the permitted gauging rules discussed at the start of Section 4.

C.1 321m:

Configuration data for the bases $321m_{\Sigma}$ with $m \in \{3, 5, 6, 7, 8\}$ appear in Table 44; note that only some \mathcal{T} are compatible with the permitted gauging rules for m > 3.

3	2	1	m	GS Total:	:	:	:	:	:
$(I_0^{*ns},\mathfrak{g}_2)$	$(III,\mathfrak{su}(2))$	(I_0,n_0)	$(IV^{*s}, \mathfrak{e}_6)$	0	$(I_0^{*ns}, \mathfrak{g}_2)$	(III,su(2))	(I_0,n_0)	$(I_0^{*s},\mathfrak{so}(8))$	
$(I_0^{*ns}, \mathfrak{q}_2)$	$(IV^{ns}, \mathfrak{su}(2))$	(I_0, n_0)	(IV^{*s}, e_6)	U	0	0	A_1	A_1^3	A_1^4
		(0 / 0 /	, , ,	0	$(1_0^{\pi n 3}, \mathfrak{g}_2)$	$^{(\mathrm{IV}^{ns},\mathfrak{su}(2))}_{0}$	$(1_0, n_0)$ 0	$(I_0^{*s}, \mathfrak{so}(8)) = A_1^3$	A_1^3
$(I_0^{*ns}, \mathfrak{g}_2)$	$(III,\mathfrak{su}(2))$	(I_0,n_0)	(III^*, e_7)	Ď.		$(IV^{ns}, \mathfrak{su}(2))$		$(I_0^{*s},\mathfrak{so}(8))$	
$(I_0^{*ns}, \mathfrak{g}_2)$	$(III,\mathfrak{su}(2))$	(I_0, n_0)	$(IV^{*ns}, \mathfrak{f}_4)$	0	0	0	0	A_1^2	A_{1}^{2}
				0	(\mathfrak{g}_2)	$(\mathfrak{su}(2))$	(n ₀)	(so(8))	₄ 4
$(I_0^{*ns}, \mathfrak{g}_2)$	$(\mathrm{IV}^{ns},\mathfrak{su}(2))$	(II,n_0)	$(IV^{*ns}, \mathfrak{f}_4)$		$(I_0^{*ns}, \mathfrak{g}_2)$	0 (III,su(2))	A_1 (I_0, n_0)	$A_1^3 $ $(I_1^* {}^{ns}, \mathfrak{so}(9))$	A_1^4
(T*ns _)	$(IV^{ns}, \mathfrak{su}(2))$	/T \	$(IV^{*ns}, \mathfrak{f}_4)$	0	0	0	A_1	C_2	$A_1 \oplus C_2$
$(1_0^{\ldots},\mathfrak{g}_2)$	$(1V^{***},\mathfrak{su}(2))$	$(1_0, n_0)$	(10, , , , ,)	0	$(I_0^{*ns}, \mathfrak{g}_2)$	$(\mathrm{IV}^{ns},\mathfrak{su}(2))$		$(I_1^{*ns},\mathfrak{so}(9))$	
(I_0^{*ns}, g_2)	$(IV^{ns}, \mathfrak{su}(2))$	(II,n_0)	$(I_0^{*s}, \mathfrak{so}(8))$		0	0	0	C_2	C_2
				0	$(1_0^{110}, \mathfrak{g}_2)$	$_{0}^{(\mathrm{IV}^{ns},\mathfrak{su}(2))}$	(11,n ₀)	$(I_1^{*ns},\mathfrak{so}(9))$ C_2	C_2
$(I_0^{*ns}, \mathfrak{g}_2)$	$(III,\mathfrak{su}(2))$	(I_0,n_0)	$(I_0^{*ns},\mathfrak{g}_2)$. 2		$(IV^{ns},\mathfrak{su}(2))$	-	$(I_1^* ns, \mathfrak{so}(9))$	02
(I*ns no)	0 $(IV^{ns},\mathfrak{su}(2))$	A_1	A_1 $(I_0^* n^s, \mathfrak{g}_2)$	A_1^2	0	0	0	C_2	C_2
0	0	0	A_1	A_1	(\mathfrak{g}_2)	$(\mathfrak{su}(2))$	(n ₀)	(so(9))	
(I_0^{*ns}, g_2)	$(IV^{ns}, \mathfrak{su}(2))$	(II,n_0)	$(I_0^{*ns}, \mathfrak{g}_2)$		$(I_0^{*ns}, \mathfrak{g}_2)$	0	A_1	C_2	$A_1 \oplus C_2$
0	0	A_1	A_1	A_1^2	$(1_0, \mathfrak{g}_2)$	$(III,\mathfrak{su}(2))$ 0	(I_0,n_0) A_3	$(IV^s, \mathfrak{su}(3))$ 0	A_3
(\mathfrak{g}_2)	$(\mathfrak{su}(2))$	(n ₀)	(\mathfrak{g}_2)	. 2	0	0	$A_1 \oplus A_2$		$A_1 \oplus A_2$
$(I_0^{*ns}, \mathfrak{g}_2)$	0	A_1	A_1	A_1^2	(I_0^{*ns}, g_2)	$(\mathrm{IV}^{ns},\mathfrak{su}(2))$	(I_0, n_0)	$(IV^s, \mathfrak{su}(3))$	
(1 ₀ , y ₂)	$(III,\mathfrak{su}(2))$ 0	(I_0,n_0) A_1	$(I_1^{*s},\mathfrak{so}(10))$ C_3	$A_1 \oplus C_3$	0	0	A_1^2	0	A_1^2
$(I_0^* \overset{\circ}{n} \overset{\circ}{s}, \mathfrak{g}_2)$			$(I_1^{*s}, \mathfrak{so}(10))$	111 U U3	(\mathfrak{g}_2)	$(\mathfrak{su}(2))$	(n_0)	(su(3))	4
0	0	0	C_3	C_3	0	0	A_3 $A_1 \oplus A_2$	0	A_3 $A_1 \oplus A_2$
$(I_0^{*ns}, \mathfrak{g}_2)$			$(I_1^{*s},\mathfrak{so}(10))$		$(I_0^{*ss},\mathfrak{so}(7))$		(I_0,n_0)	(IV*s,e6)	$A_1 \oplus A_2$
0	0	0	C_3	C_3	A_1	0	0	0	A_1
(g ₂) 0	(su(2)) 0	$\binom{n_0}{A_1}$	$(\mathfrak{so}(10))$ C_3	$A_1 \oplus C_3$	$(I_0^{*ss},\mathfrak{so}(7))$		$(\mathrm{I}_0,\mathrm{n}_0)$	$(\mathrm{III}^*,\mathfrak{e}_7)$	
$(I_0^{*ns}, \mathfrak{g}_2)$	$(III,\mathfrak{su}(2))$		$(I_2^{*ns},\mathfrak{so}(11))$	111 U U3	A ₁	0	0	0	A_1
0	0	0	C_4	C_4	$(I_0^{*ss},\mathfrak{so}(7))$ A_1	(111,su(2)) 0	(I_0, n_0)	$(IV^*^{ns}, \mathfrak{f}_4)$ 0	A_1
$(I_0^{*ns}, \mathfrak{g}_2)$			$(I_2^{*ns},\mathfrak{so}(11))$		$(I_0^{*ss},\mathfrak{so}(7))$		(I_0, n_0)	$(I_0^{*ns}, \mathfrak{g}_2)$	Λ1
0	0	0	C_4	C_4	A_1	0	A_1	A_1	A_1^3
(g ₂)	(su(2)) 0	$\binom{n_0}{0}$	$(\mathfrak{so}(11))$ C_4	C_4	$(I_0^{*ss},\mathfrak{so}(7))$		$\left(\mathrm{I}_{0},\mathrm{n}_{0}\right)$	$(I_1^{*s},\mathfrak{so}(10))$	
$(I_0^{*ns}, \mathfrak{g}_2)$	$(III,\mathfrak{su}(2))$	(I_0, n_0)	$(I_2^{*s}, \mathfrak{so}(12))$	-4	A ₁	0	A_1	C_3	$A_1^2 \oplus C_3$
0	0	0	C_5	C_5	$(I_0^{*ss}, \mathfrak{so}(7))$ A_1	(111,su(2)) 0	(I_0, n_0) 0	$_{C_4}^{(\mathrm{I}_2^{*ns},\mathfrak{so}(11))}$	$A_1 \oplus C_4$
$(I_0^{*ns}, \mathfrak{g}_2)$	$(III,\mathfrak{su}(2))$	(I_0,n_0)	$(I_0^{*ss},\mathfrak{so}(7))$		$(I_0^{*ss},\mathfrak{so}(7))$		(I_0, n_0)	$(I_2^{*s}, \mathfrak{so}(12))$	A1 + 04
(I*ns a-)	$(IV^{ns}, \mathfrak{su}(2))$	A_1	C_2 $(I_0^{*ss},\mathfrak{so}(7))$	$A_1 \oplus C_2$	A_1	0	0	C_5	$A_1 \oplus C_5$
0	0	0	C_2	C_2	$(I_0^{*ss},\mathfrak{so}(7))$		(I_0,n_0)	$(I_0^{*ss},\mathfrak{so}(7))$	0
	$(IV^{ns},\mathfrak{su}(2))$		$(I_0^{*ss},\mathfrak{so}(7))$	- 2	A ₁	0	A_1	C_2	$A_1^2 \oplus C_2$
0	0	0	C_2	C_2	$(I_0^{*ss}, \mathfrak{so}(7))$ A_1	(111,su(2)) 0	(I_0, n_0) A_1	$(I_0^{*s}, \mathfrak{so}(8)) \\ A_1^3$	A_1^5
$(I_0^{*ns}, \mathfrak{g}_2)$			$(I_0^{*ss},\mathfrak{so}(7))$	4 0 0	$(I_0^{*ss},\mathfrak{so}(7))$		(I_0, n_0)	$(I_1^* \overset{A_1}{{}^{ns}}, \mathfrak{so}(9))$	A1
0 (ga)	0 (su(2))	A_1 (n_0)	C_2 $(\mathfrak{so}(7))$	$A_1 \oplus C_2$	A_1	0	A_1	C_2	$A_1^2 \oplus C_2$
(g_2)	(511(2))	A_1	C_2	$A_1 \oplus C_2$	$(I_0^{*ss},\mathfrak{so}(7))$		$\left(\mathrm{I}_{0},\!\mathrm{n}_{0}\right)$	$(\mathrm{IV}^s,\mathfrak{su}(3))$	-
					A_1	0	A_3	0	$A_1 \oplus A_3$
:	:	:	:	:	A_1	0	$A_1 \oplus A_2$	0	$A_1^2 \oplus A_2$

Table 44: All configurations for $321m,\;m\in\{3,5,6,7,8\}.$

C.2 31:

3	1	GS Total:	:	:	:	:	:	:
$(IV^{*s}, \mathfrak{e}_6)$	(I_0, n_0)		$(I_2^{*ns}, \mathfrak{so}(11))$	$(I_4^{ns},\mathfrak{sp}(2))$		$(I_0^{*ss}, \mathfrak{so}(7))$	(I_1, n_0)	
0	A_2	A_2	C_2	D_6	$C_2 \oplus D_6$	C_2	A_2^2	$A_2^2 \oplus C_2$
(III^*, \mathfrak{e}_7)	(I_0, n_0)		$(I_2^{*ns}, \mathfrak{so}(11))$		-2 U - 0	C_2	B_4	$B_4 \oplus C_2$
0	A_1	A_1	C_2	B ₆	$B_6 \oplus C_2$	C_2	$A_1^2 \oplus A_2$	
$(IV^{*ns}, \mathfrak{f}_4)$	(I_0,n_0)		(so(11))	$(\mathfrak{sp}(2))$	26 ⊕ 02	(so(7))	(n_0)	111 0 112 0 0
0	A_2	A_2	C_2	B_6	$B_6 \oplus C_2$	C_2	A_2^2	$A_2^2 \oplus C_2$
$(IV^{*ns}, \mathfrak{f}_4)$	(II,n_0)		$(I_2^{*ns}, \mathfrak{so}(11))$		$D_6 \oplus C_2$	C_2	B_4	$B_4 \oplus C_2$
0	\mathfrak{g}_2	\mathfrak{g}_2	A_1	D_8	$A_1 \oplus D_8$	C_2	$A_1^2 \oplus A_2$	
$(IV^{*ns}, \mathfrak{f}_4)$	(I_1,n_0)		$(I_2^{*ns}, \mathfrak{so}(11))$		$A_1 \oplus D_8$	$(I_0^{*ss}, \mathfrak{so}(7))$		$A_1 \oplus A_2 \oplus C$
0	A_2	A_2		•	$A_1 \oplus B_8$	0	D_8	
(\mathfrak{f}_4)	(n_0)		A_1	B_8 $(\mathfrak{sp}(3))$	$A_1 \oplus B_8$	$(I_0^{*ss}, \mathfrak{so}(7))$		D_8
0	\mathfrak{g}_2	\mathfrak{g}_2	(so(11))		4			42 A B
$(I_0^{*ns}, \mathfrak{g}_2)$	(I_0, n_0)		A_1	B_8	$A_1 \oplus B_8$	A_1	$A_1 \oplus B_3$	$A_1^2 \oplus B_3$
A_1	D_4	$A_1 \oplus D_4$	$(I_2^{*ns}, \mathfrak{so}(11))$	0	D	A ₁	C_3	$A_1 \oplus C_3$
$(I_0^{*ns}, \mathfrak{g}_2)$	(II,n_0)		0	D_{10}	D_{10}	$(I_0^{*ss}, \mathfrak{so}(7))$	$(I_2, \mathfrak{su}(2))$	4 - 5
A_1	f4	$A_1 \oplus \mathfrak{f}_4$	$(I_2^{*ns}, \mathfrak{so}(11))$		_	A ₁	D_6	$A_1 \oplus D_6$
$(I_0^{*ns}, \mathfrak{g}_2)$	(I_1, n_0)	1 0 /4	0	B_{10}	B_{10}	$(I_0^{*ss}, \mathfrak{so}(7))$		
A_1	A_3	$A_1 \oplus A_3$	$(\mathfrak{so}(11))$	$(\mathfrak{sp}(4))$		A_1	B_6	$A_1 \oplus B_6$
(\mathfrak{g}_2)	(n ₀)	1 03	0	B_{10}	B_{10}	$(\mathfrak{so}(7))$	$(\mathfrak{su}(2))$	
A_1	f4	$A_1 \oplus \mathfrak{f}_4$	$(\mathrm{I}_2^{*ns},\mathfrak{so}(11))$			A_1	B_6	$A_1 \oplus B_6$
$(I_0^{*ns}, \mathfrak{g}_2)$	$(III, \mathfrak{su}(2))$	1 ⊕ /4	C_3	D_4	$C_3 \oplus D_4$	$(I_0^{*s}, \mathfrak{so}(8))$	(I_0, n_0)	
0	$A_1 \oplus B_3$	$A_1 \oplus B_3$	$(I_2^{*ns}, \mathfrak{so}(11))$	$(I_3^{ns}, \mathfrak{su}(2))$		A_1^3	D_4	$A_1^3 \oplus D_4$
0	C_3	C_3	C_3	B_4	$B_4 \oplus C_3$	$(I_0^{*s}, \mathfrak{so}(8))$	(I_1, n_0)	0 0
$(I_0^{*ns}, \mathfrak{g}_2)$	$(IV^{ns}, \mathfrak{su}(2))$		$(\mathfrak{so}(11))$	$(\mathfrak{su}(2))$		A_{1}^{2}	A_2^2	$A_{1}^{2}\oplus A_{2}^{2}$
0	$A_2 \oplus \mathfrak{g}_2$	$A_2\oplus \mathfrak{g}_2$	C_3	B_4	$B_4 \oplus C_3$	$A_1^{ar{2}}$	B_3	$A_1^2 \oplus B_3$
0			$(I_2^{*s}, \mathfrak{so}(12))$	(I_0, n_0)		$(I_0^{*s}, \mathfrak{so}(8))$	(II,n_0)	
	C_2	C_2	C_5	A_1^2	$A_1^2 \oplus C_5$	0	g 2	\mathfrak{g}_2
$(I_0^{*ns}, \mathfrak{g}_2)$	$(I_2, \mathfrak{su}(2))$	D	$(I_2^{*s}, \mathfrak{so}(12))$	(I_1, n_0)		$(\mathfrak{so}(8))$	(n_0)	
0 (************************************	D_6	D_6	C_5	0	C_5	A_{1}^{3}	D_4	$A_1^3 \oplus D_4$
$(I_0^{*ns}, \mathfrak{g}_2)$	$(I_3^{ns}, \mathfrak{su}(2))$	D.	$(\mathfrak{so}(12))$	(n_0)		$A_1^{\tilde{2}}$	A_2^2	$A_1^2 \oplus A_2^2$
0	B_6	B_6	C_5	A_{1}^{2}	$A_1^2 \oplus C_5$	$(I_0^{*s}, \mathfrak{so}(8))$	$(I_2, \mathfrak{su}(2))$	
(\mathfrak{g}_2)	(su(2))	-	$(I_2^{*s}, \mathfrak{so}(12))$	$(I_4^{ns}, \mathfrak{sp}(2))$		A_1^2	D_6	$A_1^2 \oplus D_6$
0	B_6	B_6	C_3	D_6	$C_3 \oplus D_6$	$(I_0^{*s}, \mathfrak{so}(8))$	$(I_3^{ns}, \mathfrak{su}(2))$	
$(I_1^{*s}, \mathfrak{so}(10))$			$(\operatorname{I}_2^{*s},\mathfrak{so}(12))$			A_1	B_5	$A_1 \oplus B_5$
C_3	A_3	$A_3 \oplus C_3$	C_3	B_5	$B_5 \oplus C_3$	(so(8))	(su(2))	
C_3		$A_1 \oplus A_2 \oplus C_3$	(so(12))	$(\mathfrak{sp}(2))$		A_1^2	D_6	$A_1^2 \oplus D_6$
$(I_1^{*s}, \mathfrak{so}(10))$.2	C_3	D_6	$C_3 \oplus D_6$	$(I_1^* \overset{ns}{\underset{\circ}{,}} \mathfrak{so}(9))$	(I_0, n_0)	1
C_3	A_{1}^{2}	$A_1^2 \oplus C_3$	$(I_2^{*s}, \mathfrak{so}(12))$			C_2	A_3	$A_3 \oplus C_2$
$(\mathfrak{so}(10))$	(n_0)		C_2	D_8	$C_2 \oplus D_8$	C_2	$A_1 \oplus A_2$	$A_1 \oplus A_2 \oplus C$
C_3	A_3	$A_3 \oplus C_3$	$(I_2^{*s}, \mathfrak{so}(12))$	$(I_{\pi}^{ns},\mathfrak{sp}(3))$	-200	$(I_1^{*ns}, \mathfrak{so}(9))$	(II,n_0)	1 0 2 0 -
C_3	$A_1 \oplus A_2$	$A_1 \oplus A_2 \oplus C_3$	C_2	B_7	$B_7 \oplus C_2$	C_2	\mathfrak{g}_2	$C_2 \oplus \mathfrak{g}_2$
$(I_1^{*s}, \mathfrak{so}(10))$	$(\mathrm{I}_4^{ns},\mathfrak{s}\mathfrak{p}(2))$		(so(12))	$(\mathfrak{sp}(3))$	27 0 02	$(I_1^{*ns}, \mathfrak{so}(9))$	(I_1, n_0)	02 0 52
A_1	D_7	$A_1 \oplus D_7$	C_2	D_8	$C_2 \oplus D_8$	C_2	B_3	$B_3 \oplus C_2$
$(I_1^{*s}, \mathfrak{so}(10))$	$(I_5^{ns}, \mathfrak{sp}(2))$		$(I_2^{*s}, \mathfrak{so}(12))$		-2 · -8	(so(9))	(n_0)	$23 \oplus 22$
A_1	B_6	$A_1 \oplus B_6$	A_1	D_{10}	$A_1 \oplus D_{10}$	C_2	B_3	$B_3 \oplus C_2$
$(\mathfrak{so}(10))$	$(\mathfrak{sp}(2))$		$(I_2^{*s}, \mathfrak{so}(12))$		11 U D 10	C_2		$A_1 \oplus A_2 \oplus C_2$
A_1	D_7	$A_1 \oplus D_7$	A_1	B_9	$A_1 \oplus B_9$	$(I_1^{*ns}, \mathfrak{so}(9))$	(Ins en(2))	U A2 TC
$(I_1^{*s}, \mathfrak{so}(10))$	$(I_6^{ns}, \mathfrak{sp}(3))$		$(\mathfrak{so}(12))$	$(\mathfrak{sp}(4))$	11 T D9	0		D_7
0	D_9	D_9			A D	$(I_1^{*ns}, \mathfrak{so}(9))$	D_7 $(\mathbf{I}^{ns} \mathfrak{sn}(2))$	
$(I_1^{*s}, \mathfrak{so}(10))$	$(I_2, \mathfrak{su}(2))$		A_1	D_{10}	$A_1 \oplus D_{10}$			
C_2	D_5	$C_2 \oplus D_5$	$(I_2^{*s}, \mathfrak{so}(12))$		D	0	B_7	B_7
$(I_1^{*s}, \mathfrak{so}(10))$	$(\mathrm{I}_3^{ns},\mathfrak{su}(2))$	-	0 (I*S = (19))	D_{12}	D_{12}	(so(9))	$(\mathfrak{sp}(2))$	D
C_2	B_4	$B_4 \oplus C_2$	$(I_2^{*s}, \mathfrak{so}(12))$		$C \cap D$	0 (I*ns (0))	(I + (2))	B_7
(so(10))	(su(2))		C_4	D_4	$C_4 \oplus D_4$	$(I_1^* {}^{ns}, \mathfrak{so}(9))$		4
C_2	D_5	$C_2 \oplus D_5$	$(I_2^{*s}, \mathfrak{so}(12))$	-	D 6 6	A_1	D_5	$A_1 \oplus D_5$
$(I_2^{*ns}, \mathfrak{so}(11))$		2 - 0	C_4	B_3	$B_3 \oplus C_4$	$(I_1^{*ns}, \mathfrak{so}(9))$	-	
C_4	A_1^2	$A_1^2 \oplus C_4$	(so(12))	(su(2))		A_1	B_5	$A_1 \oplus B_5$
$(I_2^{*ns}, \mathfrak{so}(11))$		1 0 04	C_4	D_4	$C_4 \oplus D_4$	(so(9))	(su(2))	
C_4	A_1	$A_1 \oplus C_4$	$(\mathrm{I}_0^{*ss},\mathfrak{so}(7))$	(I_0, n_0)		A_1	B_5	$A_1 \oplus B_5$
(so(11))	(n_0)	111 W U4	C_2	D_4	$C_2 \oplus D_4$	$(\mathrm{IV}^s, \mathfrak{su}(3))$	(I_0, n_0)	
C_4	A_1^2	$A_1^2 \oplus C_4$	$(\mathrm{I}_0^{*ss},\mathfrak{so}(7))$	(II,n_0)		0	\mathfrak{e}_6	e 6
C4	A1	$A_1 \oplus C_4$	C_2	\mathfrak{g}_2	$C_2 \oplus \mathfrak{g}_2$			
:	:	:		:				
							onfiguration	

C.3 m12:

5	1	2	GS Total:	: : : : :
$(IV^{*s}, \mathfrak{e}_6)$	(I_0, n_0)	(I_0, n_0)		$(\mathrm{IV}^{*ns},\mathfrak{f}_4)$ $(\mathrm{II},\mathrm{n}_0)$ $(\mathrm{I}_0^{*ns},\mathfrak{g}_2)$
0	A_2	0	A_2	$ \begin{array}{cccccccccccccccccccccccccccccccccccc$
$(\mathrm{IV}^{*s}, \mathfrak{e}_6)$	(I_0, n_0)	(II,n_0)		
0	A_1	A_1	A_1^2	
(IV^{*s}, e_6)	(I_0, n_0)	(I_1, n_0)	-	2 2
0	A_2	A_1	$A_1 \oplus A_2$	
(\mathfrak{e}_6)	(n_0)	(n_0)		
0	A_2	A_1	$A_1 \oplus A_2$	$(IV^{*ns}, \mathfrak{f}_4) (I_0, n_0) \qquad (I_1, n_0)$
(IV^{*s}, e_6)	(I_0, n_0)	$(III,\mathfrak{su}(2))$		$0 \qquad A_2 \qquad A_1 \qquad A_1 \oplus A_2$
0	0	B_3	B_3	(IV^{*ns}, f_4) (II, n_0) (II, n_0)
$(IV^{*s}, \mathfrak{e}_6)$	(I_0, n_0)	$(I_2,\mathfrak{su}(2))$	Ü	$0 \qquad A_1 \qquad 0 \qquad A_1$
0	0	A_3	A_3	(IV^{*ns}, f_4) (I_1, n_0) (I_1, n_0)
$(IV^{*s}, \mathfrak{e}_6)$	(I_0, n_0)	$(IV^{ns}, \mathfrak{su}(2))$	Ü	$0 A_1 0 A_1$
0	0	$A_1 \oplus A_2$	$A_1 \oplus A_2$	(\mathfrak{f}_4) (\mathfrak{n}_0) (\mathfrak{n}_0)
0	0	\mathfrak{g}_2	g ₂	$0 \qquad A_2 \qquad A_1 \qquad A_1 \oplus A_2$
(e ₆)	(n ₀)	(su(2))		$(\mathrm{IV}^{*ns},\mathfrak{f}_4)$ $(\mathrm{I}_0,\mathrm{n}_0)$ $(\mathrm{III},\mathfrak{su}(2))$
0	0	B_3	B_3	$0 0 B_3 B_3$
0	0	$A_1 \oplus A_2$	$A_1 \oplus A_2$	$(\mathrm{IV}^{*ns},\mathfrak{f}_4)$ $(\mathrm{I}_0,\mathrm{n}_0)$ $(\mathrm{I}_2,\mathfrak{su}(2))$
$(IV^{*s}, \mathfrak{e}_6)$	(I_0, n_0)		1 \psi2	$0 0 A_3 A_3$
0	0	A_5	A_5	(IV^*ns,\mathfrak{f}_4) (II,n_0) $(III,\mathfrak{su}(2))$
$(IV^{*s}, \mathfrak{e}_6)$	(I_0, n_0)	$(IV^s, \mathfrak{su}(3))$	5	$0 0 A_1 A_1$
0	0	A_2^2	A_2^2	(IV^*n^s,\mathfrak{f}_4) (II,n_0) $(IV^{ns},\mathfrak{su}(2))$
0	0	C_2	C_2	$0 \qquad 0 \qquad \mathfrak{g}_2 \qquad \mathfrak{g}_2$
(e ₆)	(n ₀)	(su(3))	02	$(\mathrm{IV}^{*ns},\mathfrak{f}_4) (\mathrm{I}_1,\mathrm{n}_0) \qquad (\mathrm{I}_2,\mathfrak{su}(2))$
0	0	A_5	A_5	0 0 A_2 A_2
(III^*, e_7)	(I_0, n_0)	(I_0, n_0)	Α5	$(\mathrm{IV}^{*ns},\mathfrak{f}_4)$ $(\mathrm{I}_0,\mathrm{n}_0)$ $(\mathrm{IV}^{ns},\mathfrak{su}(2))$
0	A_1	0	A_1	$0 0 A_1 \oplus A_2 A_1 \oplus A_2$
(III^*, e_7)	(I_0, n_0)	(II,n ₀)	А	$0 0 \mathfrak{g}_2 \mathfrak{g}_2$
0	0	A_1	A_1	(\mathfrak{f}_4) (\mathfrak{n}_0) $(\mathfrak{su}(2))$
(III^*, e_7)	(I_0, n_0)	(I_1, n_0)	Al	0 0 B_3 B_3
0	A_1	A_1	A_{1}^{2}	$0 0 A_1 \oplus A_2 A_1 \oplus A_2$
	(n_0)	(n_0)	A1	$(\mathrm{IV}^{*ns},\mathfrak{f}_4)$ $(\mathrm{I}_0,\mathrm{n}_0)$ $(\mathrm{I}_3^s,\mathfrak{su}(3))$
(e ₇)	A_1	A_1	A_1^2	0 0 A_5 A_5
(III^*, e_7)	_	$(I_2,\mathfrak{su}(2))$	A1	$(\mathrm{IV}^{*ns},\mathfrak{f}_4)$ $(\mathrm{I}_1,\mathrm{n}_0)$ $(\mathrm{I}_3^s,\mathfrak{su}(3))$
0	(I_0,n_0)	A_3	4	0 0 A_4 A_4
(III^*, \mathfrak{e}_7)		$(III,\mathfrak{su}(2))$	A_3	$(\mathrm{IV}^{*ns},\mathfrak{f}_4)$ $(\mathrm{I}_0,\mathrm{n}_0)$ $(\mathrm{IV}^s,\mathfrak{su}(3))$
$(111^+, \mathfrak{e}_7)$	(I_0,n_0)		D	0 0 A_2^2 A_2^2
		B_3	B_3	0 0 C_2 C_2
(e ₇)	$\binom{n_0}{0}$	(su(2))	D	(\mathfrak{f}_4) (\mathfrak{n}_0) $(\mathfrak{su}(3))$
U	U	B_3	B_3	0 0 A_5 A_5
:	:	:	:	
		•		Table 46: All configurations for the base 512.

References

- [1] Edward Witten. Some comments on string dynamics. In Future perspectives in string theory. Proceedings, Conference, Strings'95, Los Angeles, USA, March 13-18, 1995, pages 501–523, 1995.
- [2] Nathan Seiberg and Edward Witten. Comments on string dynamics in six-dimensions. Nucl. Phys., B471:121–134, 1996.
- [3] Nathan Seiberg. Nontrivial fixed points of the renormalization group in six-dimensions. *Phys. Lett.*, B390:169–171, 1997.
- [4] Werner Nahm. Supersymmetries and their Representations. Nucl. Phys., B135:149, 1978.
- [5] Vijay Kumar and Washington Taylor. A bound on 6D $\mathcal{N}=1$ supergravities. Journal of High Energy Physics, 2009(12):050, 2009.
- [6] Vijay Kumar, David R. Morrison, and Washington Taylor. Mapping 6D $\mathcal{N}=1$ supergravities to F-theory. *Journal of High Energy Physics*, 2010(2):99, 2010.
- [7] Vijay Kumar, David R. Morrison, and Washington Taylor. Global aspects of the space of 6D $\mathcal{N}=1$ supergravities. Journal of High Energy Physics, 2010(11):118, 2010.

- [8] Vijay Kumar and Washington Taylor. String universality in six dimensions. Advances in Theoretical and Mathematical Physics, 15(2):325–353, 2011.
- [9] Sheldon Katz, David R. Morrison, Sakura Schafer-Nameki, and James Sully. Tate's algorithm and F-theory. *Journal of High Energy Physics*, 08:094, 2011.
- [10] Thomas W. Grimm and Washington Taylor. Structure in 6D and 4D $\mathcal{N}=1$ supergravity theories from F-theory. Journal of High Energy Physics, 2012(10):105, 2012.
- [11] David R. Morrison and Washington Taylor. Toric bases for 6D F-theory models. Fortschritte der Physik, 60(11-12):1187–1216, 2012.
- [12] David R. Morrison and Daniel S. Park. F-theory and the Mordell-Weil group of elliptically-fibered Calabi-Yau threefolds. *Journal of High Energy Physics*, 2012(10):128, 2012.
- [13] David R. Morrison and Washington Taylor. Classifying bases for 6D F-theory models. *Open Physics*, 10(5):1072–1088, 2012.
- [14] Jonathan J. Heckman. More on the matter of 6D SCFTs. Physics Letters B, 747:73–75, 2015.
- [15] Michele Del Zotto, Jonathan J. Heckman, Alessandro Tomasiello, and Cumrun Vafa. 6D conformal matter. *Journal of High Energy Physics*, 1502:054, 2015.
- [16] Jonathan J. Heckman, and David R. Morrison, Tom Rudelius, and Cumrun Vafa. Atomic Classification of 6D SCFTs. Fortsch. Phys., 63:468–530, 2015.
- [17] Jonathan J. Heckman and David R. Morrison, and Cumrun Vafa. On the Classification of 6D SCFTs and Generalized ADE Orbifolds. *Journal of High Energy Physics*, 05:028, 2014. [Erratum: JHEP06,017(2015)].
- [18] Jonathan J. Heckman, David R. Morrison, Tom Rudelius, and Cumrun Vafa. Geometry of 6D RG Flows. *Journal of High Energy Physics*, 09:052, 2015.
- [19] Jonathan J. Heckman, Tom Rudelius, and Alessandro Tomasiello. 6D RG flows and nilpotent hierarchies. *Journal of High Energy Physics*, 2016(7):1–44, 2016.
- [20] David R. Morrison and Cumrun Vafa. F-theory and $\mathcal{N}=1$ SCFTs in four dimensions. Journal of High Energy Physics, 08:070, 2016.
- [21] Marco Bertolini, Peter R. Merkx, and David R. Morrison. On the global symmetries of 6D superconformal field theories. *Journal of High Energy Physics*, 07:005, 2016.
- [22] David R. Morrison and Tom Rudelius. F-theory and Unpaired Tensors in 6D SCFTs and LSTs. Fortsch. Phys., 64:645–656, 2016.
- [23] David R. Morrison and Cumrun Vafa. Compactifications of F-theory on Calabi-Yau threefolds (I). Nucl. Phys., B473:74–92, 1996.
- [24] Edward Witten. Phase Transitions in M-Theory and F-Theory. Nuclear Phys. B, 471:195-216, 1996.
- [25] David R. Morrison and Cumrun Vafa. Compactifications of F-theory on Calabi-Yau threefolds (II). *Nuclear Physics B*, 476(3):437–469, 1996.
- [26] Tom Banks and Nathan Seiberg. Symmetries and strings in field theory and gravity. Physical Review D, 83(8):084019, 2011.
- [27] Kantaro Ohmori, Hiroyuki Shimizu, Yuji Tachikawa, and Kazuya Yonekura. 6D $\mathcal{N} = (1, 0)$ theories on S^1/T^2 and class S theories: part II. Journal of High Energy Physics, 12:131, 2015.

- [28] Kunihiko Kodaira. On compact analytic surfaces: II. Annals of Mathematics, pages 563–626, 1963.
- [29] Kunihiko Kodaira. On compact analytic surfaces, III. Annals of Mathematics, pages 1–40, 1963.
- [30] André Néron. Modeles minimaux des variétés abéliennes sur les corps locaux et globaux. Publications mathématiques de l'IHÉS, 21(1):5–125, 1964.
- [31] Michael Bershadsky, Kenneth A. Intriligator, Shamit Kachru, David R. Morrison, Vladimir Sadov, and Cumrun Vafa. Geometric singularities and enhanced gauge symmetries. *Nucl. Phys.*, B481:215–252, 1996.
- [32] Shing-Tung Yau. Calabi's Conjecture and Some New Results in Algebraic Geometry. Proceedings of the National Academy of Sciences of the United States of America, 74(5):1798–1799, 1977.
- [33] David R. Morrison and Washington Taylor. Matter and singularities. *Journal of High Energy Physics*, 2012(1):1–55, 2012.
- [34] Gang Tian. Smoothness of the universal deformation space of compact Calabi-Yau manifolds and its Peterson-Weil metric. In *Mathematical aspects of string theory*, pages 629–646. World Scientific, 1987.
- [35] Andrey N. Todorov. The Weil-Petersson geometry of the moduli space of $SU(n \ge 3)$ Calabi-Yau manifolds I. Communications in mathematical physics, 126(2):325–346, 1989.
- [36] Yoshiko Hayakawa. Degeneration of Calabi-Yau Manifold with Weil-Petersson Metric. arXiv preprint alg-geom/9507016, 118, 1995.
- [37] Chin-Lung Wang. On the incompleteness of the Weil-Petersson metric along degenerations of Calabi-Yau manifolds. *Mathematical Research Letters*, 4:157–172, 1997.
- [38] Ulf Persson. Configurations of Kodaira fibers on rational elliptic surfaces. *Mathematische Zeitschrift*, 205(1):1–47, 1990.
- [39] Evgenii B. Dynkin. Semisimple subalgebras of semisimple Lie algebras. *Matematicheskii Sbornik*, 72(2):349–462, 1952.